

Dissertation zur Erlangung des Doktorgrades
der Naturwissenschaften an der Fakultät für Biologie
der Ludwig-Maximilians-Universität München



PROTEOMICS OF NEWLY ASSEMBLED CHROMATIN

vorgelegt von
Miriam Caroline Pusch
aus Christchurch

Dissertation eingereicht am: 12. Dezember 2013

Mündliche Prüfung am: 25. Februar 2014

1. Gutachter: Prof. Dr. Peter Becker

2. Gutachter: Prof. Dr. Dirk Eick

3. Gutachter: Prof. Dr. Thomas Cremer

4. Gutachter: Prof. Dr. Michael Boshart

Eidesstattliche Erklärung

Ich versichere hiermit an Eides statt, dass die vorgelegte Dissertation von mir selbständig und ohne unerlaubte Hilfe angefertigt ist.

München, den

Miriam Pusch

TABLE OF CONTENTS

SUMMARY	9
ZUSAMMENFASSUNG	10
1. INTRODUCTION	11
1.1 Chromatin.....	12
1.1.1 Histones.....	12
Methylation and acetylation.....	13
Canonical histones and histone variants	14
1.1.2 Non-coding RNAs and chromatin regulation	15
<i>Trans</i> -acting non-coding RNAs.....	15
<i>Cis</i> -acting non-coding RNAs.....	15
Allele-specific RNAs	15
RNAs with activating or inhibiting function	16
RNAs as structural component of chromatin.....	17
1.2 Chromatin organisation and compaction	17
1.2.1 Chromatin domains and territories.....	19
1.3 Chromatin dynamics	21
1.3.1 Polymerases.....	21
1.3.2. Histone chaperones	21
Replication-coupled nucleosome assembly	21
Replication-independent nucleosome assembly	23
1.3.3 Chromatin remodellers	25
1.4 <i>In vitro</i> assembly systems	26
1.5 Aims of the thesis	28
2. MATERIALS & METHODS	31
2.1 Materials.....	32
2.2 Methods	34
2.2.1 Microbiology Methods.....	34
2.2.2 Nucleic Acid Methods.....	35
2.2.3 Tissue Culture Methods	37
2.2.4 Protein Methods	38
2.2.5 Chromatin Methods.....	41
2.2.6 Mass Spectrometry Methods.....	44
2.2.7 Immunohistochemical Methods	46

3. RESULTS	49
3.1 <i>In vitro</i> chromatin assembly	50
3.2 Analysis of chromatin-bound proteins	52
3.3 Proteomic data interpretation	54
Chromatin-associated proteins are highly interconnected	55
3.4 Early and late chromatin binding profiles differ in their protein composition	57
Chromatin complexes show distinct binding behaviour during assembly	58
3.5 RNA is a structural component of chromatin in <i>Drosophila melanogaster</i>	60
3.6 <i>In vitro</i> reconstituted chromatin recapitulates the RNA-dependent accessibility of chromatin ..	61
3.7 Chromatin accessibility is regulated by snoRNAs	62
3.8 Decondensation factor 31 is involved in chromatin opening	63
3.9 Df31 is a chromatin and RNA-binding protein	65
3.10 Df31 and snoRNA both act on euchromatic regions <i>in vivo</i>	66
3.11 Df31 interactome	67
4. DISCUSSION	71
4.1 Towards a detailed temporal proteomic analysis of chromatin assembly	72
4.2 Reproducibility of the system and future improvements	72
4.3 Ubiquitination in chromatin assembly and regulation	76
4.4 Chromatin-associated proteins and their interactions	77
4.5 Chromatin proteins and complexes show distinct kinetics	78
4.6 RNA is involved in structural properties of chromatin	79
4.7 Chromatin compaction can be reversed by specific subtypes of RNA	80
4.8 Chromatin structure is regulated by a ribonucleoprotein complex	80
4.9 SnoRNP complexes and their mode of action	81
4.10 Mechanisms of snoRNP-dependent chromatin opening	82
4.11 Df31 and its interactome	84
ABBREVIATIONS	87
REFERENCES	91
APPENDIX	103
ACKNOWLEDGEMENT	121
CURRICULUM VITAE	123

SUMMARY

DNA, histone and non-histone proteins are composed in a structure called chromatin. Chromatin has evolved as a dynamic structure able to compact when space is limited and decondense when access is needed. Especially in processes such as transcription, replication and repair chromatin is extensively disassembled and reassembled. In all those cases the assembly process follows a regulated order of events.

This study was aimed to investigate protein binding kinetics during chromatin assembly and to study their inter-dependency. An *in vitro* assembly system, which recapitulates key aspect of chromatin assembly *in vivo*, was used to investigate protein binding. Subsequent mass spectrometry was employed to identify and quantify chromatin-bound proteins in a time resolved manner.

Using this new established method it was found that during chromatin assembly a complex protein network is associated to chromatin. Also, protein binding differs between early and late assembly. Whereas most proteins bind during the onset of chromatin assembly, only few proteins show a clear tendency towards matured chromatin. Most interestingly, proteins that belong to the 26S proteasome, were strongly associated to chromatin suggesting that ubiquitination and proteolysis play a functional role during assembly.

Furthermore, RNA-dependent binding of proteins was investigated using the same chromatin reconstitution system. In this experiment, a protein called Decondensation factor 31 (Df31), was identified whose binding to chromatin is weakened upon RNA depletion and which is strongly required for an open chromatin structure. It forms a ribonucleoprotein (RNP) with snoRNAs as main ribonucleic acid component. Whereas Df31 seems to regulate specific domains within the nucleus, RNAs have a more global effect on chromatin structure suggesting that other RNPs exist that function likewise in other genomic regions.

The results in this thesis contribute to a better understanding of chromatin assembly and structural maintenance of chromatin and provide a starting point for new investigations in this direction.

ZUSAMMENFASSUNG

DNA, Histone und Nicht-Histon-Proteine bilden zusammen Chromatin, die Chromosomenstruktur aller eukaryotischen Lebewesen. Chromatin zeichnet sich besonders durch seine Dynamik aus. Das Genom wird so kompaktiert, dass es zum einen in den Zellkern passt, zum anderen regulatorischen Proteinen weiterhin Zugang zur DNA ermöglicht. Dies führt dazu, dass Chromatin während der Transkription, Replikation und DNA Reparatur ständigen strukturellen Veränderungen unterliegt. Diese Vorgänge folgen jedes Mal einer genau regulierten Abfolge von Ereignissen.

Ziel dieser Arbeit war die Untersuchung von Proteinbindungskinetiken während der Chromatinassemblierung und die Analyse ihres Bindungsverhaltens in Abhängigkeit von Histonmodifikationen und der Bindung weiterer Chromatin-bindender Proteine. Es wurde auf ein *in vitro* Rekonstitutionssystem zurückgegriffen, welches wesentliche Aspekte der *in vivo* Chromatinassemblierung rekapituliert. In Kombination mit massenspektrometrischer Proteinidentifizierung und -quantifizierung konnte ein zeitaufgelöstes Bild der Proteinbindung während der Chromatinassemblierung erzeugt werden. Es konnte gezeigt werden, dass ein Netzwerk von Proteinen während des Assemblierungsprozesses präsent ist. Die Mehrzahl der Proteine befinden sich während der frühen Assemblierungsphase am Chromatin und nur eine Untergruppe von Proteinen bindet spezifisch zu späteren Zeitpunkten. Besonders spannend ist die deutliche Anreicherung von Proteinen an das Chromatin, die für den proteosomalen Abbau anderer Proteine zuständig sind. Dies deutet darauf hin, dass Ubiquitinierung und Proteolyse eine wichtige funktionelle Rolle während der Chromatinassemblierung spielen.

Weiterhin wurde die neu-etablierte Methode verwendet, um die RNA-abhängige Bindung von Proteinen an das Chromatin zu beschreiben. Dabei wurde das Protein Decondensation factor 31 (Df31) identifiziert, dessen Binding an das Chromatin durch RNA gefördert wird und der für die Kompaktierung von Chromatin eine wichtige Rolle spielt. Df31 bildet zusammen mit snoRNAs einen Ribonucleoproteinkomplex (RNP). Während der Effekt der RNA auf die gesamte Chromatinstruktur gezeigt werden konnte, scheint Df31 nur in einzelnen, spezifischen Regionen eine strukturelle Funktion auszuüben. Es ist daher wahrscheinlich, dass weitere RNPs in anderen Bereichen des Genoms eine ganz ähnliche Aufgabe erfüllen.

Die Ergebnisse dieser Arbeit liefern einen Beitrag zum besseren Verständnis der Assemblierung von Chromatin und dessen strukturellen Komponenten. Darüber hinaus ergeben sich aus dieser Arbeit viele Ansatzpunkte für weitergehende Experimente.

1. INTRODUCTION

1. INTRODUCTION

1.1 Chromatin

Chromatin is the structure in which every eukaryotic genome is organised consisting of DNA, RNA, histone and non-histone proteins. Every diploid cell contains a genome of approximately 2 m in length, which needs to be fitted into a nucleus of just 10 μm in diameter. Therefore DNA needs to be packaged and organised in a manner that also ensures sufficient access for all DNA-dependent processes (Felsenfeld and Groudine, 2003). This unique task is mastered by the organisation of DNA into chromatin, a highly dynamic nucleoprotein structure (MacAlpine and Almouzni, 2013). The basic unit of this structure is the nucleosome, consisting of 147 bp of DNA wrapped ~ 1.7 times in a left-handed, superhelical turn around an octamer of four core histones (Luger et al., 1997). Histones are small, positively charged proteins, which exist in different numbers dependent on the organism. There are the core histones termed H2A, H2B, H3 and H4, the linker histone H1 and various histone variants that carry out specific functions (Van Holde, 1989; Annunziato 2008). Due to the phosphate groups in its phosphate-sugar backbone, DNA is negatively charged, explaining the tight binding between DNA and histones. When studied by electron microscopy chromatin appeared similar to beads on a string, which provided an early clue for the existence of nucleosomes (Olins and Olins, 1974; Woodcock et al., 1976). Cross-linking experiments could also demonstrate that H2A, H2B, H3 and H4 form a discrete protein octamer (Thomas and Kornberg, 1975).

1.1.1 Histones

Histones harbour a relatively unstructured N-terminal domain (NTD), a C-terminal and a globular domain. The latter consist of three α helices connected by two flexible loops and is referred to as the histone fold domain (Luger et al., 1997). This special structure allows histones to form dimers in a handshake manner (Arents and Moudrianakis, 1995). The relatively unstructured histone tails are easily accessible as they are protruding out the nucleosome (Luger and Richmond, 1998). This feature makes them a common target for a variety of posttranslational modifications (Fischle et al., 2003; Barth and Imhof, 2010). Histone modifications are involved in the regulation and establishment of gene expression patterns and can be added on newly synthesized histones as well as on histones that are already deposited (Jenuwein, 2001). The most frequent types of modifications are acetylation of lysines, methylation of arginines and lysines and phosphorylation of serines and threonines. Another group of modifications include ubiquitination and SUMOylation of lysines and ADP-ribosylation of glutamic acid (Fischle et al., 2003; Barth and Imhof, 2010). Recently, the modification of lysines by crotonic acid was identified via a mass spectrometry-based approach (Tan et al., 2011). Crotonylation is enriched on sex chromosomes and seems to specifically mark testis-specific genes. Histone modifications have in common that they can influence the state of chromatin. They can either act alone or in combination with other histone combinations. It has been suggested that the combination

of certain histone modification creates a “histone code” which specifies the transcriptional level of genomic regions (Jenuwein, 2001; Turner, 2002).

Methylation and acetylation

Methylation of lysine H3K4 and H3K36 is generally found in transcriptional active regions whereas methylation of lysine K9 and K27 on histone H3 is highly abundant in repressive chromatin. Methylation is the only posttranslational modification, which can be added as mono-, di- and trimethyl mark and asymmetrically in case of arginines (Wang et al., 2004). Multiple histone methyltransferases have been reported, including G9a, SUV39h1, SUV39h2, and ESET for lysine methylation and PRMT1 and CARM1 for arginine methylation (Strahl et al., 2001; Wang et al., 2001; Bauer et al., 2002; Lachner, 2003). Figure 1.1 shows the most common modification sites of histone H3 and H4 and the enzymes that set and remove the corresponding modification.

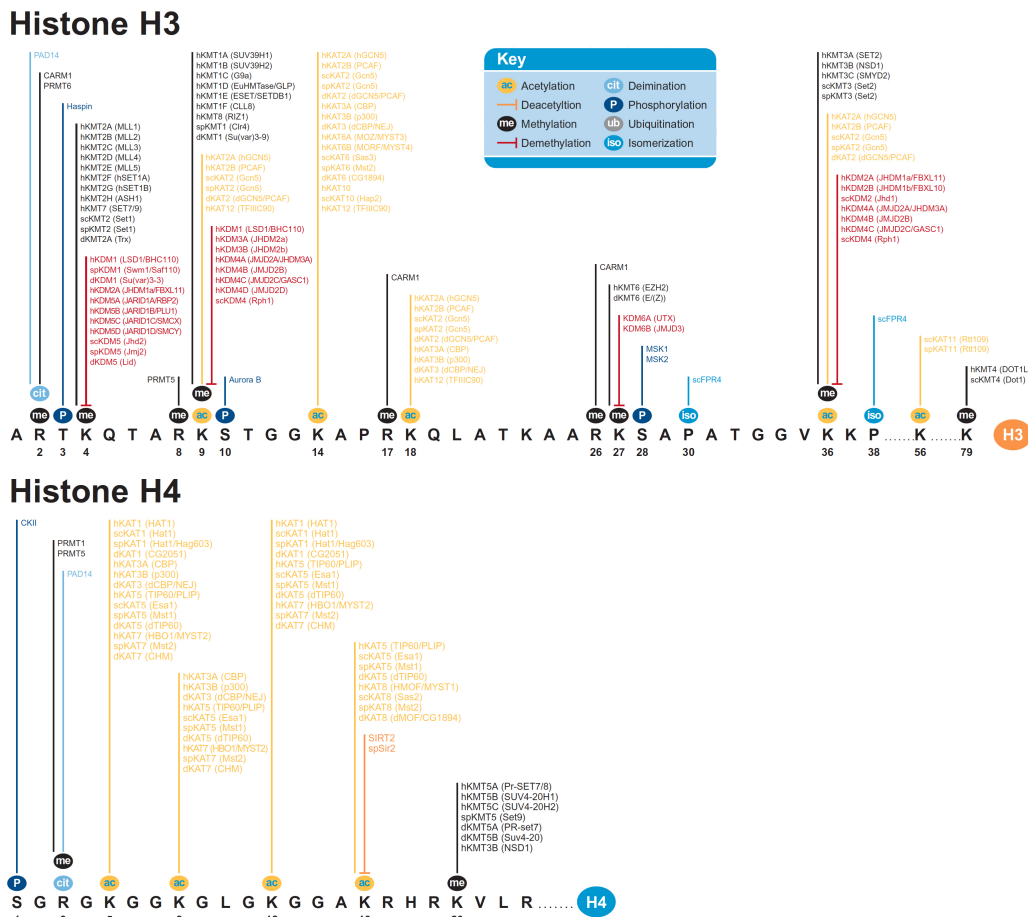


Figure 1.1: Histone modification map of H3 and H4.

Depicted are the most common sites of modification on histone H3 and H4 and their corresponding enzymes (from Abcam).

1. INTRODUCTION

Acetylation of histones correlates with a more open chromatin structure. Histone acetyltransferases (HATs) and histone deacetylases (HDACs) regulate the steady state of this modification (Strahl and Allis, 2000). Two acetylation marks on newly synthesized histones are conserved among species: Lysine 5 and Lysine 12 on histone H4 (Sobel et al., 1995; Benson, 2005). The responsible histone acetyltransferase HAT1 forms a complex with the H3-H4 dimer, CAF-1 and ASF1 before deposition (Tagami et al., 2004; Loyola et al., 2006). Both modifications are not required for CAF-1 binding and therefore seem to serve as a transient mark of newly synthesized histones (Ma et al., 1998).

Enzymes that set and remove histone modifications are also referred to as “writers” and “eraser”. Most posttranslational modifications are found on the histone amino termini and are recognized by chromatin-binding proteins. Those so-called “readers” bind to specific histone modifications via specialized domains and translate the information into a specific chromatin structure. A classic example is Heterochromatin protein 1 (HP1) which harbours a chromodomain that binds to methylated H3K9, a modification set by SUV39 (Lachner et al., 2001; Grewal and Jia, 2007). However, not only modifications on the histone tail can influence the chromatin state. An increasing number of histone modifications outside the N-terminal tail are now reported to play a role in chromatin-based processes (Mersfelder, 2006; Tropberger and Schneider, 2010; Tropberger et al., 2013).

Canonical histones and histone variants

In metazoans, the five histone genes are clustered into repeated units and their expression is restricted to S-phase when new histones are required in abundance. This tight regulation is achieved by cell-cycle regulated activation of transcription, a dynamic control of mRNA stability and a unique processing mechanism (White et al., 2007; Marzluff et al., 2008). A recent study could further show that whereas the core histones are only transcribed in a short pulse during early S-phase, H1 is transcribed throughout the whole S-phase (Guglielmi et al., 2013). Most metazoans own replication-dependent histones and histone variants, which can also be synthesized and deposited outside of S-phase. In humans, two proteins, H3.1 and H3.2, represent the canonical, replication-dependent histone whereas *Drosophila* only has one replication-dependent histone H3 (Ahmad and Henikoff, 2002; Tagami et al., 2004). H3 further exists as centromeric variant CenP A in human and Cid in *Drosophila*. Histone variants differ in their primary sequence and in contrast to canonical histones their mRNA is polyadenylated and can contain introns (Bönisch and Hake, 2012). H2A variants include macroH2A and H2ABbd, which are found in distinct chromatic regions. MacroH2A is strongly enriched on the inactive X chromosome and some autosomal regions and mainly linked to repressive chromatin (Costanzi and Pehrson, 1998; Bönisch and Hake, 2012). In contrast, H2ABbd is excluded from the inactive X and is distributed in transcriptionally active regions with high level of H4 acetylation (Chadwick and Willard, 2001).

1.1.2 Non-coding RNAs and chromatin regulation

There is increasing evidence that short (<200 nt) as well as long (>200 nt) non-coding RNAs can contribute to chromatin organisation. Non-coding RNAs (ncRNA) were shown to participate in epigenetic regulation by targeting the chromatin modulating machineries to their site of action (Figure 1.2). The mechanistic details of many of those processes are still poorly understood. However, one can differentiate between five main types of RNA involvement in chromatin regulation:

Trans-acting non-coding RNAs

Probably the best-known example of a *trans* acting non-coding RNA is HOTAIR. The 2.2 kb long ncRNA falls into the group of long intergenic non-coding RNA (lincRNA). It is derived from the mammalian HOXC cluster and was originally observed to repress transcription in *trans* at the *HOXD* locus on a different chromosome (Rinn et al., 2007). HOTAIR interacts with Polycomb Repressive Complex 2 (PRC2) and leads to H3K27 methylation at the *HOXD* locus. It further acts as a molecular scaffold via its binding to the lysine-specific histone demethylase 1 (LSD1) specific for H3K4, structurally bridging both chromatin modifying complexes (Tsai et al., 2010).

Cis-acting non-coding RNAs

Many ncRNAs transcribed from antisense strands of developmental and pluripotency loci are involved in the regulation of chromatin structure in *cis*. One example is the lincRNA HOTTIP (HOXA distal transcript antisense RNA) whose knockdown in human primary fibroblasts causes partial loss of the active H3K4 me2/me3 marks in genomic proximity of the HOTTIP gene (Wang et al., 2012). HOTTIP probably exerts its function via a direct interaction with the WDR5/MLL complex (the vertebrate homolog of Trithorax).

Allele-specific RNAs

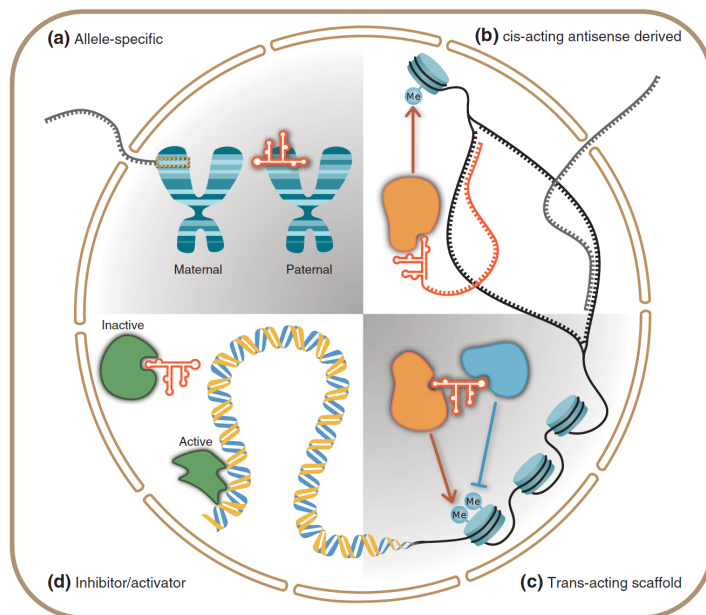
Although based on completely different mechanisms, non-coding RNAs are also implicated in dosage compensation in both, mammals and flies. In mammals, X chromosome inactivation is controlled by a multi-layered pathway, which involves a pair of ncRNAs. Those RNAs differentially recruit the epigenetic machinery to establish chromatin asymmetries (Kanduri et al., 2009). The Xist RNA (X-inactive specific transcript) is transcribed from the RepA locus and acts in *cis* on the chromosome from which it is expressed. Its interaction with the PRC2 complex and DNA methyltransferase 3a (DNMT3A) promotes propagation of H3K27 methylation and enhances hypermethylation (Sado, 2004; Zhao et al., 2008; Kanduri et al., 2009). Tsix expression from the future active chromosome epigenetically silences the Xist promoter, thereby blocking the Xist-mediated inactivation (Kanduri et al., 2009).

1. INTRODUCTION

In *Drosophila*, two essential but mutually redundant ncRNA, roX1 and roX2, are incorporated into the dosage compensation complex (DCC). Binding of the DCC to specific sites on the male X chromosome results in elevated levels of H4K16 acetylation and hence up-regulated expression of X-linked genes in male flies (Straub and Becker, 2011).

Another regulatory mechanism happening allele-specific is genomic imprinting. 15% of imprinted genes are regulated by ncRNAs (Reik and Walter, 2001). Examples are the antisense RNAs Air and Kcnq1ot1, which act in *cis* and involve silencing of the target region by methylation of histones (Nagano et al., 2008; Nahkuri and Paro, 2012).

Figure 1.2: Major functions of non-coding RNAs in the regulation of metazoan chromatin.



a) The ncRNA Xist and roX are involved in dosage compensation. Air and Kcnq1ot1 are required for imprinting and originate in introns of the sense genes. **b)** *Cis*-acting transcripts such as HOTTIP are derived from the opposite strand of the locus they are targeted to. Regulation involves action of Polycomb Group- or Trithorax Group-complexes. **c)** ncRNAs such as HOTAIR operate as structural scaffolds by bridging chromatin complexes with synergistic enzymatic functionalities. **d)** Some RNAs act as inhibitor or activator. The 7SK RNA is a cofactors of key chromatin components (from Nahkuri and Paro, 2012).

RNAs with activating or inhibiting function

Among the best-studied ncRNAs involved in pretranscriptional regulation is the 7SK RNA, an evolutionary highly conserved RNA found in vertebrates and higher invertebrates, such as *Drosophila melanogaster* (Gürsoy et al., 2000; Gruber et al., 2008). The 7SK RNA negatively regulates the positive transcription elongation factor b (P-TEFb) by inhibiting the phosphorylation of the C-terminal domain of RNA Polymerase II (Nguyen et al., 2001; Yang et al., 2001). While loops 1, 3 and 4 of the 7SK RNA are involved in P-TEFb interaction, loop 2 can specifically bind to the A/T hook of the architectural transcription factor and chromatin regulator HMGA1 (Eilebrecht et al., 2011b). It thereby competes with DNA binding to the same domain, modulates the function of HMGA1 and changes the expression of over 1500 genes (Eilebrecht et al., 2011a).

RNAs as structural component of chromatin

Beside the above-described roles of RNA in chromatin regulation a fifth category of non-coding RNA is emerging – that is the role as architectural component in chromatin higher order formation. More than four decades ago, co-fractionations of chromatin with stable associated RNA molecules led to the assumption that RNA is involved in the organisation of chromatin structure. In different organisms such as pea, calf, chicken and fruit fly, up to 2-10% of the total nucleic acid found in chromatin were shown to be RNAs (Huang and Bonner, 1965; Bonner and Widholm, 1967; Heyden and Zachau, 1971; Bynum and Volkin, 1980; Holoubek et al., 1983). Further research almost relegated these finding as contaminants from the isolation procedure or RNAs still being tethered to chromatin via RNA polymerase (Artman and Roth, 1971; Bonner, 1971). However, also recent studies now proof that RNA can be an integral component of chromatin (Rodríguez-Campos and Azorín, 2007; Mondal et al., 2010). Foci of heterochromatin 1 (HP1) are sensitive to treatment of RNase A and are recovered upon restoration of RNA, proposing a role of RNA in the formation of higher order structures in heterochromatin (Maison et al., 2002). Furthermore, there is experimental evidence that RNA associates with the mitotic spindle and plays a direct, translation-independent role in spindle assembly (Blower et al., 2005). Ribonucleoproteins, complexes of RNA and protein, have also been involved in the formation of chromosome territories (discussed below). RNA depletion causes the disruption and break down of higher order chromosome territory architectures (Ma et al., 1999). In addition, the decrease of cellular RNA by RNase A treatment results in compaction of cellular chromatin with slightly more resistant pericentromeric heterochromatin and can be connected to a class of coding RNAs. Although controversially discussed, several other studies argue for a role of RNA in chromatin structure. However, the exact mechanisms of RNA and its role in chromatin folding still need to be addressed.

1.2 Chromatin organisation and compaction

Histones and RNAs are structural and functional components of chromatin. Especially the role of histones in the formation of the nucleosome and higher order structures was studied extensively. H3 and H4 N-terminal tails mainly interact intranucleosomal whereas H2A and H2B N-terminal tails were described to interact with neighbouring nucleosomes (Fletcher and Hansen, 1995; Zheng, 2003; Luger, 2006). The basic H4 tail sequence was further shown to bind to the acidic surface of H2A-H2B dimers (Luger, 2006). In addition, there is increasing evidence for an involvement of the NTD of H3 and H4 in interarray formation (Kan et al., 2007; 2008).

The addition of one H1 protein to the nucleosome leads to the formation of the chromatosome, which occupies two full turns of DNA (Figure 1.3; Annunziato, 2008). H1 is able to bind to the linker DNA that separates the nucleosomes and that can vary in length of 10 to 80 base pairs dependent on species

1. INTRODUCTION

and cell type (Van Holde, 1989). Whereas the core histones have sizes between 11 and 17 kDa, H1 is usually larger with a size of around 22 kDa in human and 26 kDa in *Drosophila*. Among all histones, H1 is less conserved across species. It can also participate in nucleosome positioning and formation of higher-order chromatin structure (Widom, 1998; Thomas, 1999; Maier et al., 2008).

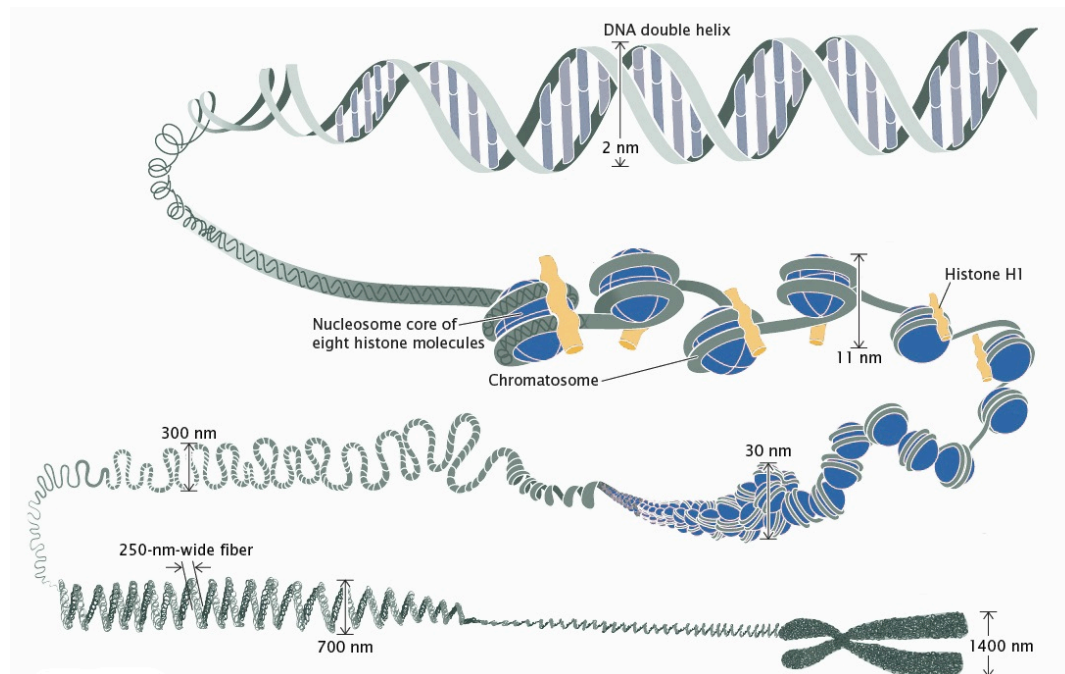


Figure 1.3: Packaging of chromatin happens on several levels of compaction.

DNA, a double-stranded helical structure, is assembled with histones to form nucleosomes. Each nucleosome consists of DNA wrapped 1.7 times around an octamer of histone proteins. Nucleosomes are the basic repetitive unit of chromatin. Via the formation of loops, arrays of nucleosomes can fold into higher order chromatin structures. These structures are further coiled and folded to form chromosomes (adapted from Annunziato, 2008).

Packaging of DNA into nucleosomes results in an 11 nm fibre which is referred to as “beads on a string” and which contributes to a 6-fold level of compaction. Still, a significantly higher degree of folding is needed to account for the condensation observed in mitotic chromosomes (Fussner et al., 2011). In 1997, Aaron Klug proposed that chromatin fibres form higher order structures with regular periodicity and that a mechanism for DNA compaction and gene silencing based on chromatin structure exists (Finch and Klug, 1976; Levy and Noll, 1981). Since then several different models have been suggested to describe the detailed higher order organisation of chromatin that forms the 30 nm fibre.

Two of those models gained widespread acceptance: the “one-start” and the “two-start” model (Figure 1.4). In the “one-start” model, proposed by Aaron Klug and others the 30 nm fibre resembles a solenoid with 6-8 nucleosomes per turn in which the linker DNA is bent in a continuously supercoiled

fashion between nucleosomes (Finch and Klug, 1976; Thoma et al., 1979; McGhee et al., 1983). The “two-start” model describes a twisted ribbon with a straight linker DNA that is oriented at angles varying from 0° to 50° to the fibre axis (Worcel et al., 1981; Woodcock et al., 1984).

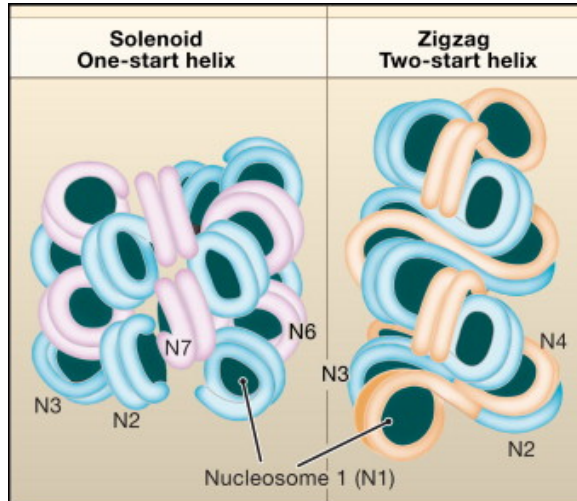


Figure 1.4: Models of the 30 nm fibre.

The “one-start” model describes a solenoid in which nucleosomes are spooled around a central axis, causing the linker DNA to bend. In the “two-start” model, nucleosomes position in a zig-zag formation with criss-crossing linker DNA between adjacent rows of nucleosomes (After Tremethick, 2007).

Although more than 30 years of work have passed since the discovery of the 30 nm fibre, the fundamental structure of eukaryotic chromatin remains controversial. The use of new techniques such as small angle X-ray scattering (SAXS), which allows the determination of periodic structures in biological samples, and cryo-electron microscopy led to the conclusion that the 30 nm fibre does not exist in human mitotic chromosomes (Nishino et al., 2012). Arrays of nucleosomes in solution adopt a 30 nm fibre, however chromatin obtained from nuclei seems to be mainly composed of irregularly folded nucleosomes. Those irregularities are a result of variations in linker length, occupancy of histone H1, post-translational modifications of histones, and the presence of histone variants (Bednar et al., 1998; Grigoryev and Woodcock, 2012). Other EM studies further suggest that with increasing chromatin concentrations, chromatin structure *in vitro* and *in vivo* is arranged as a “molten globule” arising from the interdigitation of over-crowded and irregularly folded nucleosomal arrays (Luger et al., 2012). Depending on the chromosome a packing ratio of 10.000 fold can be reached during metaphase. Looping and coiling of fibres also allows *cis* and *trans* interactions between distant genomic regions (Dekker, 2002) (Figure 1.5).

1.2.1 Chromatin domains and territories

Chromatin is found in at least two types of characteristic structures: euchromatin and heterochromatin. Already in 1935, Emil Heitz observed morphological differences between distinct chromatin regions during the cell cycle (Heitz, 1935). Many years later, those structures were described in more detail by light-microscopy studies (Elgin, 1996). The two chromatin forms can be distinguished cytologically by their staining behaviour during interphase of the cell cycle. Whereas euchromatin stains in a

1. INTRODUCTION

moderate fashion, heterochromatin stains intensely due to a high packing degree. Moreover, euchromatin is replicated early during S-phase and stays decondensed after mitosis; in contrast heterochromatin is replicated during middle to late S-phase and stays condensed after cell division (Grewal and Elgin, 2002; Elgin and Grewal, 2003). Heterochromatin is further characterised by low gene activity and genetically inactive satellite sequences (Lohe et al., 1993). It can be subdivided into constitutive heterochromatin, found on telomers and centromers, and facultative heterochromatin such as the silenced female X chromosome (Richards and Elgin, 2002). Constitutive heterochromatin remains condensed during the entire lifecycle of a cell whereas facultative heterochromatin can potentially reverse between heterochromatin and euchromatin (Craig, 2005).

During interphase chromosomes adopt highly organised structures and occupy discrete territories in the nucleus with preferential positions for the two different types of chromatin (Lanctôt et al., 2007; Cremer and Cremer, 2010). Heterochromatin is usually localised at the periphery of the nucleus, euchromatin preferentially within the centre of the nucleus (Shopland et al., 2006). Hi-C studies, which enable to capture the conformation of genomes, revealed that the nucleus is partitioned into well-demarcated physical regions, in which multiple genes (10-500 kb) build chromosomal domains whose boundaries are defined by so-called insulator proteins. Active domains can form intra- and interchromosomal contacts with each other and reach out of the territory whereas inactive domains strongly confine to their chromosomal territory (Belton et al., 2012; Sexton et al., 2012) (Figure 1.5).

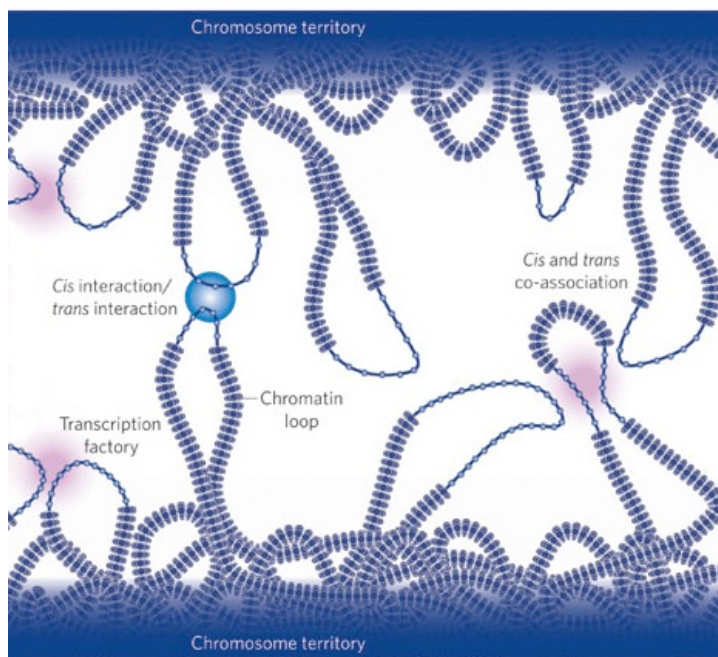


Figure 1.5: Nuclear organisation of the genome.

Loops of decondensed chromatin result in *cis* and *trans* interactions between chromosomes. Interactions can also occur between regulatory elements and/or gene loci and lead to coregulation. RNA FISH and 3C (Chromosome conformation capture) studies confirm colocalisation of active alleles of genes in *cis* and *trans* (adapted from Fraser and Bickmore, 2007).

1.3 Chromatin dynamics

Despite its sophisticated organisation within the nucleus, chromatin has to be highly dynamic during all phases of the cell cycle. This structural flexibility is accomplished by the concerted action of several factors.

1.3.1 Polymerases

Polymerases are involved in processes such as replication and repair in case of DNA polymerases and transcription in case of RNA polymerases. All protein-coding genes as well as small non-coding RNAs such as snRNA and snoRNAs are transcribed by RNA Pol II (Heidemann et al., 2013). RNA Pol II and SP6 polymerases were shown to be able to transcribe with the nucleosome being associated to DNA (Kireeva et al., 2002). Still, during other processes, nucleosomes impose a strong barrier and have to be removed to open up the chromatin fibre temporarily to allow the respective factors to proceed. The process of this transient histone eviction is referred to as chromatin disassembly and the redeposition as assembly. Mechanisms by which chromatin accessibility is changed involve histone modifications, histone variants and the displacement of histones by histone remodellers (Fischle et al., 2005; Smith and Peterson, 2005).

1.3.2. Histone chaperones

A variety of proteins interact with the four core histones. They function in their transfer from the cytoplasm to the nucleus and in the assembly of macromolecular structures and are therefore referred to as chaperones (Figure 1.6) (Laskey et al., 1978). The majority of those factors have a preference towards either H3-H4 dimers or H2A-H2B dimers. Histone chaperones have no sequence similarities in common suggesting that they have evolved independently into histone-binding proteins (Haushalter and Kadonaga, 2003; Elsässer and D'Arcy, 2012). Chaperones assemble nucleosomes in an ATP-independent manner. Until now a couple of histone chaperones could be identified that are conserved among different species. NAP1 and ASF1 bind to cytosolic H2A-H2B and H3-H4 dimers, respectively (Mosammaparast et al., 2002; Elsässer and D'Arcy, 2012). Both chaperones are responsible for the transfer of histone dimers into the nucleus, where the histones are channelled into distinct DNA-associated pathways. These events are typically divided into DNA replication-dependent or -independent nucleosome assembly.

Replication-coupled nucleosome assembly

During S-phase, the progressing replication machinery leads to an unwinding of the two DNA strands, resulting in the eviction of parental histones. The hexameric MCM2-7 helicase complex facilitates this process through the disruption of existing nucleosomes. H2A-H2B dimers are evicted first and get

1. INTRODUCTION

bound to the heterodimeric chaperone FACT, which interacts with the subunit MCM4 (Gambus et al., 2006). However, the exact molecular mechanism of parental histone recycling, especially in the case of H3-H4 dimers, remains unclear (Burgess and Zhang, 2013). Although there is experimental proof that H3-H4 tetramers do not seem to separate, structural studies show that ASF1 can physically block the formation of H3-H4 tetramers, suggesting splitting of H3-H4 tetramers into dimers (English et al., 2006; Natsume et al., 2007; Xu et al., 2010). Thus, ASF1 can act as a histone donor for other chaperones thereby creating a chaperone “assembly line” at the replication fork (Corpet et al., 2011).

How newly synthesized histones are assembled is relatively well understood. In S-Phase distinct cytosolic and nuclear H3-H4-ASF1 complexes exist, which show ubiquitous acetylation on H4K5 and K12 and heterogeneous H3 marks, including H3K18me1, H3K27ac, H3K27me1 and H3K79ac (Jasencakova et al., 2010). ASF1 imports H3-H4 dimers into the nucleus where it forms a complex with MCM2-7 and is needed for replication fork progression (Groth et al., 2007). In addition, H3-H4 dimers are transferred to CAF-1 for tetramer formation.

Assembly factor	Functional roles	Binding interactions
CAF1	Histone chaperone Replication-coupled chromatin assembly DNA repair Silencing Cell-cycle progression	H3-H4 PCNA Asf1
Asf1	Histone chaperone Replication-coupled chromatin assembly DNA repair Silencing Cell-cycle progression	H3-H4 CAF1 Brahma TAF ₂₅₀ /CCG1 RAD53 SAS-1 Hir1, Hir2
NAP1	Histone chaperone Nuclear import of histones	H2A-H2B H3-H4 Kap114 p300
HIR	Histone gene regulation Histone chaperone Replication-independent chromatin assembly Silencing	H2A-H2B H3-H4 Asf1
Nucleoplasmin	Maternal storage of histones in oocytes Histone chaperone during rapid rounds of replication in early embryo	H2A-H2B H3-H4
N1/N2	Maternal storage of histones in oocytes Histone chaperone during rapid rounds of replication in early embryo	H3-H4
Spt6	Histone-transfer vehicle Transcription-elongation factor	H3-H4 H2A-H2B
DF31	Histone-transfer vehicle Chromatin structural protein	
Nucleophosmin/ B23	Histone transfer vehicle Ribosome biogenesis Replication stimulatory factor	H3 RNA
ACF	DNA-translocating motor Chromatin assembly factor (requires chaperone) Chromatin remodelling factor	
RSF	Stimulates transcription <i>in vitro</i> Chromatin assembly factor (does not require chaperone) Chromatin remodelling factor	

Figure 1.6: Chromatin assembly factors.

Table showing histone chaperones and their preferred substrate. Some chaperones, e.g. NAP1 and Nucleoplasmin bind with higher affinities to H2A-H2B than H3-H4 or vice versa such as Spt6 (adapted from Haushalter and Kadonaga, 2003).

The chaperone CAF-1 was initially discovered through a DNA-replication-coupled chromatin assembly assay (Smith and Stillman, 1989). The trimeric complex (Caf1, Caf1-105 and Caf1-180 in *Drosophila*) is targeted to the replication fork via its binding to PCNA (proliferating cell nuclear antigen), a ring-shaped homotrimeric protein that serves as processivity factor of the DNA polymerase (Shibahara and Stillman, 1999; Moggs et al., 2000). Caf1-180 null mutant strains of *Drosophila* are hemizygous lethal and loss-of-function experiments in other species could also show the importance of CAF-1 for proper S-phase progression and viability *in vivo* (Quivy et al., 2001; Hoek and Stillman, 2003; Houlard et al., 2006; Song et al., 2007). The deposition of H3-H4 by CAF-1 is followed by the subsequent addition of H2A-H2B by the NAP1 chaperone, which completes the formation of new nucleosome (Zlatanova et al., 2007) (Figure 1.7). Just recently, the interaction of NAP1 and the H2A-H2B dimer was analysed by hydrogen-deuterium exchange coupled to mass spectrometry (D'Arcy et al., 2013). H2A-H2B dimers bound to NAP1 can form tetramers, which are mediated by multiple copies of H2B. Those interactions are similar to intranucleosomal interactions. NAP1 competes with histone-DNA and interhistone interactions thereby regulating the availability of H2A-H2B for chromatin assembly (D'Arcy et al., 2013). Whereas mixing events between H3-H4 dimers are not observed during replication, parental and newly synthesized H2A-H2B dimers were shown to be present in the very same nucleosome (Xu et al., 2010).

Replication-independent nucleosome assembly

Chaperones are also responsible for histone deposition in DNA repair and transcription, both involving disruption and restoration of the chromatin structure. The role of histone chaperones ASF1 and CAF-1 in chromatin restoration after DNA repair is described in detail (Soria et al., 2012). The “Access-Repair-Restore” model by Smerdon et al. is a well-accepted model of DNA repair (Smerdon, 1991). It describes the basic aspects of chromatin reorganisation during DNA repair: Nucleosomes are first disassembled to allow the repair machinery access to the site of damage. Once the actual repair is done, chromatin structure is restored to its original state. The extent of disassembly correlates with the severity of damage and the method of repair. DNA double strand breaks (DSB) trigger the phosphorylation of the H2A variant, H2AX (H2Av in *Drosophila*) around the break (Rogakou and Sekeri-Pataryas, 1999; Shroff et al., 2004; Iacovoni et al., 2010). Other histone modifications, such as H4 acetylation and methylation, can also contribute to the recruitment of checkpoint and repair factors (Deem et al., 2012). Restoration of chromatin largely involves chaperones and chromatin remodelers such as the Tip60 complex in *Drosophila* which specifically acetylates phosphoH2Av and exchanges it with unmodified H2Av (Kusch, 2004). This unique H2A variant seems to be maintained in the chromatin until repair is completed.

1. INTRODUCTION

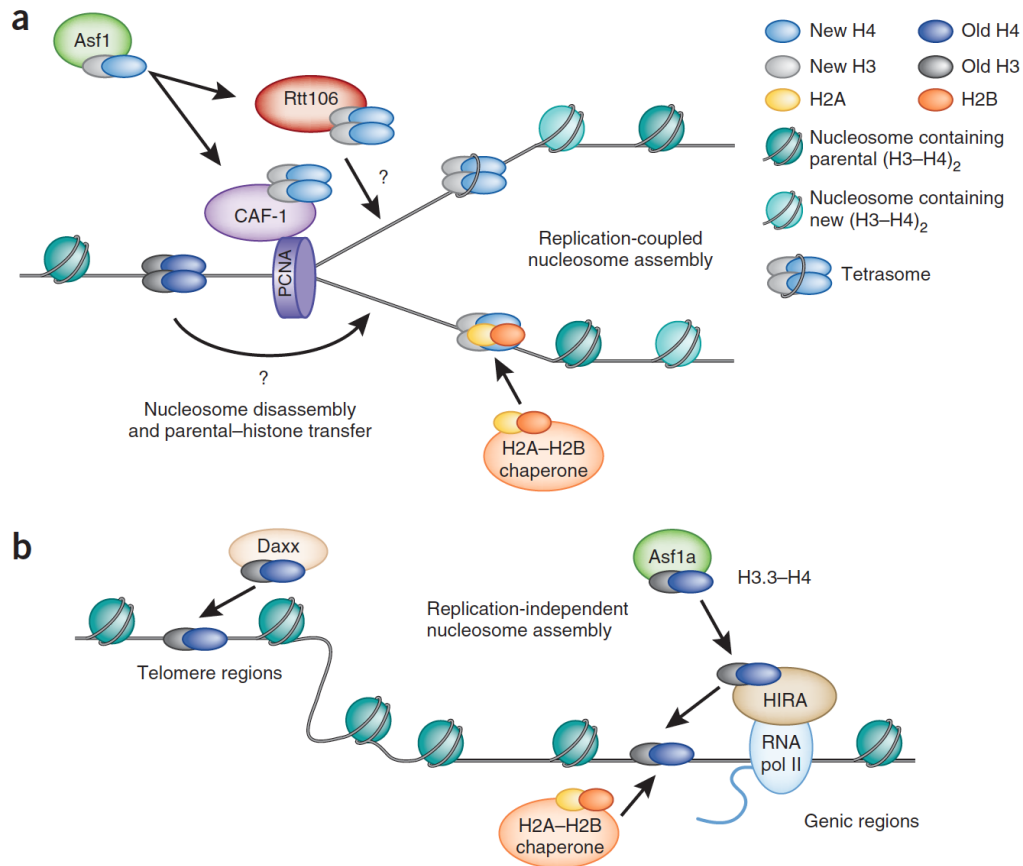


Figure 1.7: Histone dynamics at the replication fork.

a) Replication-coupled nucleosome assembly: Newly synthesized histone H3.1-H4 is imported into the nucleus by ASF1 and transferred to CAF-1. Deposition onto replicated DNA depends on the interaction between CAF-1 and PCNA. Parental histones are also transferred to the newly replicated DNA in a mechanism, which is not resolved yet. **b)** Replication-independent nucleosome assembly: HIRA and DAXX mediate deposition of H3.3-H4. HIRA is responsible for histones at genic regions, possibly through interactions with RNA polymerase II and double-stranded DNA. DAXX facilitates deposition of H3.3-H4 at telomere regions and regulatory elements (adapted from Burgess and Zhang, 2013).

ASF1 seems to be dispensable during the disassembly flanking a DSB, still it is required for the subsequent reassembly of nucleosomes (Chen et al., 2008). Studies in yeast could show that the ability of cells to progress in their cell cycle in presence of an unrepaired DSB is not impaired upon loss of ASF1 or CAF-1. However, the absence of either chaperone results in permanent activation of the DNA damage checkpoint (Kim and Haber, 2009). Additionally, CAF-1 has been reported to play a role in nucleotide excision repair (NER). On sites of DNA lesions, such as those induced by UV, CAF-1 and PCNA are recruited in an ATP-dependent manner (Moggs et al., 2000). CAF-1 is responsible for post-repair deposition of new histones and monoubiquitination of H2A. The exact function of this modification is however not deciphered yet (Polo et al., 2006; Zhu et al., 2009).

During transcription histone chaperones remove histones that occlude the promoter sequences and impede the formation of the preinitiation complex. This task is fulfilled through cooperation with histone modifiers and chromatin remodellers (Avvakumov et al., 2011). After transcription initiation the RNA polymerase II (RNA Pol II) progresses along the genes' coding regions, thereby creating positive super-coils that might destabilize nucleosomes sufficiently to allow direct disassembly (Elsässer and D'Arcy, 2012). Histone chaperones such as CAF-1, ASF1 and NAP1 bind to evicted histones and mediate their recycling behind the progressing RNA Pol II.

Even besides the events discussed above, chromatin is exposed to a constant exchange of histones. The H3 variant H3.3 is deposited throughout the whole cell cycle. The assembly of histone variant H3.3 along with H4 is mediated by multiple chaperones depending on their genomic localisation (MacAlpine and Almouzni, 2013). The chaperone HIRA is required for the assembly and exchange of H3.3 at genic regions. DAXX and ATRX on the opposite control H3.3 deposition at telomers and regulatory elements (Tagami et al., 2004; Goldberg et al., 2010) (Figure 1.7). Whereas nucleosomal H3-H4 multimers are relatively stable, H2A-H2B dimers undergo considerable exchange with free H2A-H2B, outside as well as during S-phase (Kimura and Cook, 2001; Jamai et al., 2007; Xu et al., 2010).

1.3.3 Chromatin remodellers

A different mechanism that leads to template accessibility is achieved by the action of chromatin remodellers. They use energy from ATP hydrolysis to perturb intrinsic histone-DNA interactions and thereby destabilize the nucleosomal particle. This in turn enables sliding or disassembly of histone octamers (Becker and Hörz, 2002). Chromatin remodellers act independently or in concert with histone chaperones to facilitate nucleosome assembly and are further needed to establish regularly spaced arrays of nucleosomes.

In *Drosophila*, the first remodelling complexes were identified by biochemical fractionation of crude extracts. This led to the identification of three remodelling complexes that share the same catalytic subunit ISWI (Tsukiyama and Wu, 1995; Ito et al., 1997; Varga-Weisz et al., 1997; Ito et al., 1999; Eberharter et al., 2001). The complexes NURF (nucleosomes remodelling factor), CHRAC and ACF (ATP-utilizing chromatin assembly and remodelling complex) are multisubunit complexes and have distinct functions in regulating chromatin structure. Whereas NURF is mainly involved in transcriptional regulation and affects higher-order chromatin structures, CHRAC and ACF can also function during chromatin assembly (Ito et al., 1997; Eberharter et al., 2001; Bao and Shen, 2007). CHRAC can further promote replication initiation (Alexiadis et al., 1998). Their catalytic subunit, the ATPase ISWI, is able to slide nucleosomes along DNA *in vitro*. However, accessory and regulatory

1. INTRODUCTION

domains seem to be needed for affinity and specificity for nucleosomes (Mueller-Planitz et al., 2012; Torigoe et al., 2013). This accounts not only for complexes belonging to the ISWI subfamily of remodellers but also for the other remodeller subfamilies SWI/SNF, Mi2/CHD and INO80.

1.4 *In vitro* assembly systems

Chromatin assembly is a stepwise process, which is highly regulated. Although many findings over the recent years have helped to understand those processes, the mechanisms that coordinate the individual steps are still insufficiently described. The analysis of functionally important aspects of chromatin formation are particularly difficult to accomplish *in vivo* as their depletion in many cases has severe impact on cell division and viability. Structural analyses of histone-chaperone complexes have provided mechanistic clues of the histone transfer between chaperone and DNA but the timing of those events remains elusive (Namboodiri et al., 2003; English et al., 2006; Elsässer and D'Arcy, 2012). Thus, key aspects of chromatin assembly can be better studied in an *in vitro* reconstitution system as it allows the dissection of the entire system and in this way helps in the description of important steps during assembly. Understanding the properties of individual chromatin components provides essential information to assess their behaviour in the living cell.

In the past, two approaches have been taken to study chromatin formation *in vitro* (Dilworth and Dingwall, 1988):

Fractionation of *Xenopus* extracts led to the identification of the first putative nucleosome assembly factor, nucleoplasmin (Laskey et al., 1978). Further experiments could show that nucleoplasmin, a highly acidic protein, can bind to free histones *in vitro* but not to DNA or chromatin. At physiological ionic strength it facilitates the formation of nucleosome core particles (Earnshaw et al., 1980). Those findings suggested that nucleoplasmin can act as molecular chaperone that prevents unspecific interactions between histones and the acidic DNA (Dilworth and Dingwall, 1988). In general, assembly factors need an appropriate ionic environment, which prevents initial non-specific charge interactions between the two main chromatin components. This property allows even RNA and non-classical histone chaperones such as HMGs to potentially act as assembly factors (Nelson et al., 1981; Bonne-Andrea et al., 1984; Schubert et al., 2012).

Crude cellular extracts capable of forming chromatin *in vitro* have been applied to investigate processes resembling those observed *in vivo*. During oogenesis all components required for the initial steps of embryogenesis are accumulated. This includes also a large pool of maternal histones and chaperones and makes embryonic extracts a perfect tool to study chromatin assembly *in vitro* (Kleinschmidt and Franke, 1982; Bulger et al., 1995). *In vitro* assembly systems recapitulate many aspects of chromatin assembly *in vivo* (Becker and Wu, 1992; Kamakaka et al., 1993). As seen *in vivo*,

histone H3 and H4 are first deposited as a tetramer followed by two dimers of H2A and H2B (Worcel et al., 1978; Ladoux et al., 2000; Wagner et al., 2005). H4 is deposited in a preacetylated form, which gets rapidly deacetylated during assembly (Shimamura and Worcel, 1989; Scharf et al., 2009). This deacetylation step is facilitated by the monomethylation of H4K20 and requires the continuous presence of ATP suggesting that it is coupled to chromatin maturation (Scharf et al., 2009).

The organisation of genomic nucleosomes was thought to be intrinsically DNA-encoded and depend on statistical positioning. In fact, *in vitro* experiments with yeast whole cell extract could show that biochemical reconstitution of chromatin by salt gradient dialysis is not sufficient to recapitulate the same nucleosome positions observed *in vivo* (Zhang et al., 2011). ATP-dependent, trans-acting factors are required for proper spacing and occupancy levels. Thus, embryonic extracts are an invaluable resource to investigate chromatin organisation as they can be modified in different ways. For example, chromatin can be assembled from histones with defined modification patterns (Nightingale et al., 1998). This allows not only characterising and comparing distinct chromatin templates but also facilitates studies on the role of histone mutants and variants. The binding behaviour of chaperones, specific chromatin binders and remodellers during assembly, transcription and replication can be analysed independent of a cellular context and their dependency on specific histone modifications can further be investigated (Alexiadis et al., 1998; Nightingale et al., 1998; Moggs et al., 2000; Eskeland et al., 2007).

A multitude of chromatin-associated proteins regulate chromatin structure, but a complete picture of the changes that occur during chromatin assembly and maturation is missing (Ohta et al., 2010; Torrente et al., 2011; Dutta et al., 2012). The main questions are: What are the key players during chromatin assembly? In which order do they bind to chromatin? Do distinct chromatin intermediate states exist during chromatin assembly? To what degree does DNA sequence contribute to binding of chromatin-associated proteins? Those elementary questions regarding chromatin assembly can be easily studied in an *in vitro* reconstitution system.

An additional advantage of extracts and their use in assembly systems is the easy manipulation of distinct aspects of chromatin assembly such as the level of histone chaperones and the concentration of chromatin-binding factors. A very precise study of their functional role and the transfer of conclusions can thus be drawn from *in vitro* experiments to the *in vivo* system. The use of embryonic extracts of organisms that also provide tools for genetic manipulations and a well-established tissue culture cell system allows a detailed systematic and functional analysis and the verification of predictions that are based on the *in vitro* experiments.

1. INTRODUCTION

A recent advance in the field is the isolation of nascent chromatin with subsequent proteomic analysis (Kliszczak et al., 2011; Sirbu et al., 2012). This enables generation of comprehensive data sets of chromatin-associated proteins and the monitoring of their spatiotemporal dynamics.

1.5 Aims of the thesis

The maintenance of chromatin structure is critical for many aspects of cellular physiology. During processes such as DNA replication, repair, recombination and transcription, chromatin is extensively disassembled and reassembled. It is important that this happens in a highly ordered manner as mistakes during nucleosome assembly can have severe impact on a cell's viability.

The principal components of chromatin are the histone proteins, but recent studies have revealed that mature chromatin is structurally much more complex than initially thought (Ohta et al., 2011; Torrente et al., 2011; Dutta et al., 2012). Little is known on how all these chromatin-associated factors interact among each other and how they regulate chromatin structure and assembly kinetics. The high complexity of chromatin assembly and maturation *in vivo* makes it extremely difficult to analyse the key aspects of chromatin assembly. In this regard, *in vitro* assembly systems offer a great advantage as they recapitulate many aspects of chromatin assembly *in vivo* but at the same time allow the dissection of different aspects of chromatin reconstitution.

To analyse the molecular mechanisms involved in chromatin assembly and the impact of protein binding, a proteomic approach in combination with a well-characterised *in vitro* chromatin assembly system was chosen (Becker and Wu, 1992). This system uses embryonic extract from *Drosophila melanogaster*, which comprises all protein functions needed during chromatin assembly. The technology of fast quantitative proteomics applied in this assay allows a detailed proteomic analysis of important steps during chromatin assembly.

Aim of this project was to establish the described method and to progress in answering the following questions:

- How is chromatin structure assembled?
- In which order do factors bind to chromatin?
- Do distinct chromatin intermediates exist?

Over the past years many studies showed that RNA is an integral component of chromatin. RNA is stably associated to chromatin and can account for up to 10% of the total nucleic acids found in

chromatin. Depletion of these chromatin-associated RNAs was shown to have severe effects in different cellular aspects, e.g.:

- Disorganisation of chromosomal territories (Ma et al., 1999)
- Incorrect mitotic spindle assembly in *Xenopus* (Blower et al., 2005)
- Disruption of the cytokeratin cytoskeleton and interference with proper formation of the subsequent development of the germline in *Xenopus* oocytes (Kloc, 2005)

In some cases the effects of RNA on chromatin structure are not mediated by RNA alone, but by so-called ribonucleoprotein (RNP) complexes, which consist of RNA and one or several proteins. In agreement with this, initial *in vitro* assemblies revealed a high number of RNA-binding proteins being associated to the chromatin. Findings by the group of Gernot Längst in Regensburg further substantiated the functional importance of RNA on chromatin. They observed changes in chromatin structure upon depletion of chromatin-associated RNA. The *in vitro* assembly system, described above, was applied to investigate the following questions:

- Does RNA alone mediate the effect of higher order formation or does it also involve chromatin-binding proteins?
- How is the binding of proteins to chromatin affected by RNA?
- Can we perform functional analysis of the identified RNA-binding proteins?

1. INTRODUCTION

2. MATERIALS & METHODS

2. MATERIALS & METHODS

2.1 Materials

Plasmids

Plasmid	Insert	Application	Remark
pMT	FLAG-HA-Df31	Expression in L2-4	(Schubert et al., 2012)
pAI61 (pBS SK(-))	13 repeats of the 5S rRNA gene of <i>L.variegatus</i>	Bacterial expression	(Eskeland et al., 2007)
pCS2+	snoRNA Me28S-G980	<i>In vitro</i> transcription	(Schubert et al., 2012)
pUC	snoRNA Me28S-U2134b roX2 552 (full length)	<i>In vitro</i> transcription	(Maenner et al., 2013)

Oligonucleotides

All oligonucleotides were ordered from Eurofins MWG Operon or Sigma Aldrich.

Name	Alternative name	Application	Sequence 5'-3'
oMiP009	Df31_RNAi_for	RNAi of Df31	TTAATACGACTCACTATAGGGAGACATTCGGCGTTTTCTTTGTGACTGTG
oMiP010	Df31_RNAi_rev		TTAATACGACTCACTATAGGGAGACTTCTTTTGCTCAGCCACATCAGCC
oMiP011	Df31_exon2_for	qPCR	CGTCTGAGCCCACTGTTTCT
oMiP012	Df31_exon2_rev	Primer	CAGCTTCGCTGCTCTCTTTT
oMiP017	Df31NotI	Cloning of Df31	TTTGCGGCCGCGCTGATGTGGCTGAGCAAAAGAATGAGAC
oMiP018	Df31XbaI		TTTTCTAGATCAGGCGGCCACTTCGCTAGCCTC
oMiP037	snoRNA_U2134b_for	<i>In vitro</i> Transcription	TTTATCGATCCTCTCAGTTATGTTTTGTT
oMiP038	snoRNA_U2134b_rev		TTTTCTAGATAGGAGTTCATGATGTTT
oMiP039	snoRNA_G980_for		TTTATCGATCTGGTCAGCAGTGAAGTT
oMiP040	snoRNA_G980_rev		TTTTCTAGAGCTAGCGTGATGAGTTTATTACT
TSP_27	Me-S28 U2134b for	PCR Amplification	AGTTCATGATGTTTTCAAACCTCT
TSP_28	Me-S28 U2134b rev		CCTCTCAGTTATGTTTTGTT
TSP_29	Me-S28 G980 for		GCTAGCGTGATGAGTTTATTAC
TSP_30	Me-S28 G980 rev		CTGGTCAGCAGTGAAGTTGA
ON130	pMT for	Sequencing of pMT	CATCAGTTGTGGTCAGCA
ON152	pMT rev		CAATCCTAAACCCATTTG

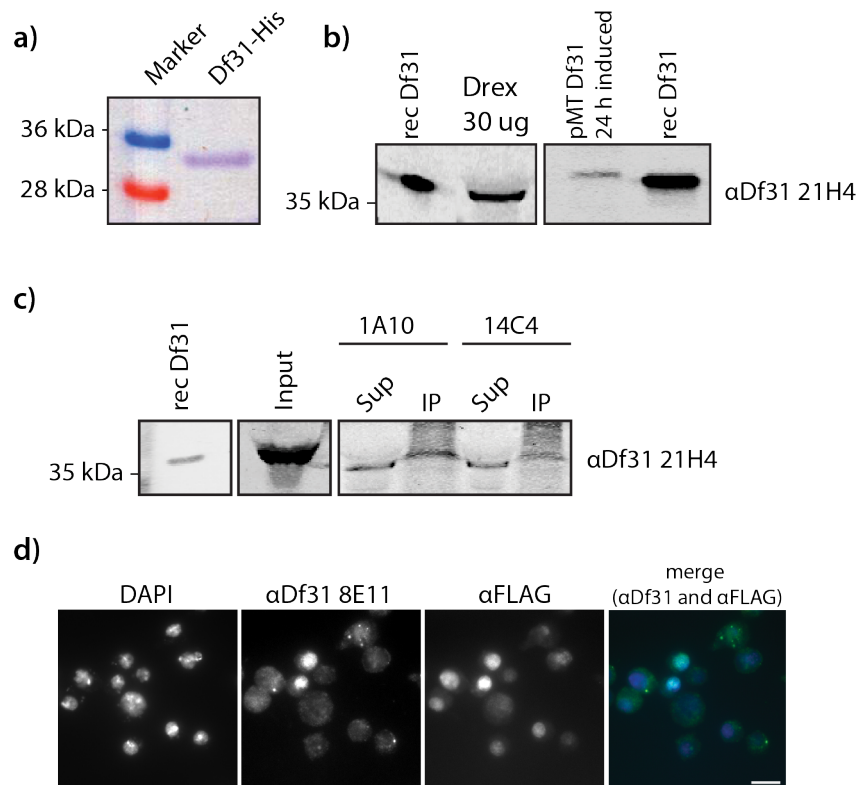
Antibiotics

Name	Concentration of stock solution	Working concentration
Ampicillin	100 mg/ml (1000x) in H ₂ O	100 µg/ml
Hygromycin	50 mg/ml	150 µg/ml

Antibodies - primary antibodies

Name	Supplier	Dilution
αDf31	Dr. E. Kremmer	Western Blotting 1:20 (21H4) Immunofluorescence 1:40 (8E11) Immunoprecipitation (1A10, 14C4)
αDig	Sigma	IF 1:250
αORC	Chesnokov et al., 2001	Western 1:1000
αH3	Abcam (ab1791)	Western 1:5000
αHA R005	Dr. E.Kremmer	IF und Western: 1:50
αFLAG M2	Sigma	IF 1:200

-> All dilutions in 1-5% BSA or 1-5% milk in PBS

Df31 antibody screening

a) Bacterially expressed Df31-His was purified using Ni-NTA beads (performed by Thomas Schubert). Purified protein was used for production of monoclonal antibodies (by Dr. Elisabeth Kremmer, IMI, HelmholtzZentrum). Supernatants of antibody producing hybridoma cells were prescreened in ELISA and positive clones were analysed in different applications.

b) The Df31 antibodies were tested with 30 μ g *Drosophila* embryo extract and 50 ng recombinant Df31-His as positive control. The supernatant 21H4 showed best results in Western Blotting. The corresponding hybridoma clone was recloned and expanded to be used in subsequent experiments.

c) Supernatants were tested in immunoprecipitation as described under “Df31-IP from *Drosophila* embryo extract” (see below). After washing, proteins were eluted in 20 μ l SDS Sample buffer and subjected to SDS-PAGE. Recombinant protein and input were run on the same gel as comparison. Input: 3%, Supernatant: 10%, IP: 100%.

d) Immunofluorescence was tested with a 1:1 mixture of wildtype L2-4 cells and cells expressing HA-FLAG-tagged Df31. Expression of Df31 was induced 24 h before harvesting. Scalebar 12 μ m.

2. MATERIALS & METHODS

Antibodies - secondary antibodies

Type	Supplier	Dilution
Western Blot antibodies	LI-COR	1:10000
ECL antibodies	VWR	1:5000
Immunofluorescence antibodies	Jackson Immuno Research	1:500

-> All dilutions in PBS-Tween (0.1%)

Protease inhibitors and reducing agents

Name	Stock concentration	Dilution
Aprotinin	1 mg/ml in H ₂ O	
Leupeptin	1 mg/ml in H ₂ O	
Pepstatin	0.7 mg/ml in Ethanol	all 1:1000
PMSF	0.2 M in Isopropanol	
DTT	1 M in 10 mM sodium acetate pH 5.2	

2.2 Methods

2.2.1 Microbiology Methods

Plasmid transformation

A maximum of 5 µl plasmid DNA was added to 100 µl chemically competent cells, which were thawed on ice. After 45 min incubation on ice the cell suspension was heat-shocked at 42°C for 90 s and immediately chilled on ice for 2 min. 900 µl of LB medium were added and the cells were incubated for at least 45 min at 37°C in a shaking incubator at 750 rpm. 100 µl of the cell suspension was directly plated on LB agar plates with the appropriate antibiotics. Cells were then centrifuged for 3 min at 800 g, the supernatant was taken off leaving in 100 µl for resuspension and the remaining cell suspension was plated on a second agar plate. Both plates were incubated for 12-16 h at 37°C.

E. coli strain - Genotype

DH5α *fhuA2Δ(argF-lacZ)U169 phoA glnV44 Φ80 Δ(lacZ)M15 gyrA96 recA1 relA1 endA1 thi-1 hsdR17* (New England Biolabs, #C2987)

Media for *E. coli* - Luria-Bertani (LB) medium

1.0% (w/v) Bacto-Tryptone

1.0% (w/v) NaCl

0.5% (w/v) Bacto-Yeast extract

The pH was adjusted to 7.0 with 10 M NaOH. The medium was autoclaved at 120°C for 20 min. Once cooled down to 60°C the appropriate antibiotics were added to the medium. Plates were prepared by adding 1.5% agar to the LB medium.

Extraction and purification of plasmid DNA from *E. coli*

Plasmid DNA from *E. coli* LB was obtained by inoculating medium supplemented with the appropriate antibiotics with a single bacteria colony. The culture was incubated o/n at 37°C at 180 rpm in a shaker (Infors Multitron). The subsequent isolation of the plasmid DNA was done using Qiagen Plasmid Kits according to manufacturer`s instructions.

2.2.2 Nucleic Acid Methods

Storage of DNA and RNA

DNA obtained from isolations and purifications was stored at -20°C in TE buffer (10 mM Tris pH 8.0, 1 mM EDTA). RNA was stored in RNase free water at -20°C. All RNA applications were performed in RNase-free, low-binding tubes (Biozym).

DNA and RNA quantification

DNA and RNA concentration was quantified by measuring the absorbance at the wavelength of 260 nm using a NanoDrop ND-1000 UV spectrophotometer (Peqlab).

Agarose gel electrophoresis

Agarose gel electrophoresis was performed to analyse and separate DNA fragments obtained from PCR and restriction digests (Sambrook et al. 2000). DNA shows different migration behavior depending on size and conformation. The smaller the fragments for analysis the higher the percentage of agarose solution was chosen. Agarose was dissolved in 1x TBE buffer by boiling in the microwave. DNA samples were mixed with 5x loading dye prior to loading onto the gel. To distinguish different fragment length DNA ladders (1 kb or 100 bp, NEB) were used as size standard. Electrophoresis was performed with 10 V/cm gel length. To visualize, DNA-staining was either carried out by adding ethidium bromide to a final concentration of 1 µg/ml prior to pouring the solution into the gel tray or by staining the gel in ethidium bromide solution (1 µg/ml in TBE) after running for 30 min followed by a 15 min destaining in pure 1x TBE. Gels were analysed by radiation with UV light (254-366 nm) and documented with the help of a gel documentary system.

1x TBE: 90 mM Tris, 90 mM Boric acid, 2 mM EDTA

5x loading dye: 0.3% (w/v) Orange G, 5 mM EDTA, 50% (v/v) Glycerol

2. MATERIALS & METHODS

Restriction digest

Buffer conditions and temperatures for restriction digests were used as suggested by the manufacturer. Units of enzymes were calculated according to their unit definition. All restriction endonucleases were purchased from New England Biolabs (NEB). The reaction products were analysed by agarose gel electrophoresis.

Polymerase Chain Reaction (PCR)

DNA was amplified by Polymerase Chain Reaction according to Sambrook et al., 2000. The following PCR conditions were used:

Template	10 ng of plasmid DNA 10-100 ng cDNA 100-500 ng of genomic DNA		
10x Buffer (NEB)	2 µl		
Primer	0.5 µl each		
dNTP mix (10 mM of each nucleotide, NEB)	1 µl		
Taq (5 U/µl, NEB)	0.5 µl		
ddH ₂ O	ad. to 20 µl		
Reaction	Temperature [°C]	Time	
Initial Denaturation	94	5 min	1x
Denaturation	94	30 s - 1min	
Annealing	adjusted to primer size	30 s	25-30 cycles
Elongation	72	1 min/kb	
Final Elongation	72	10 min	1x

Fragments above 1 kb which were later on used in cloning reactions were amplified using the Phusion Polymerase. This polymerase has in contrast to Taq polymerase a proof reading function. Denaturation was performed at 98°C and the final volume was increased up to 50 µl.

Amplified fragments were analysed by agarose gel electrophoresis. Bands of interest for ligations were cut out, purified using a gel extraction kit (Qiagen) and sent to GATC or MWG for sequencing.

RT-PCR

RNA was extracted using the Qiagen RNeasy[®] Kit according to the manufacturer's manual and dissolved in RNase-free water. 1 µg of total RNA per sample was reverse transcribed using the DyNAmo cDNA Synthesis Kit (Thermo Scientific). Reverse transcription was primed with 300 ng of random hexamers for 5 min at 65°C. Samples were further incubated with 10 µl of 2x RT buffer for 5 min at 25°C, then incubated with 2 µl of the enclosed M-MuLV RNase H⁺ reverse transcriptase for 5 min at room temperature. The reaction was performed at 48°C for 1 h, the enzyme was inactivated at 85°C for 5 min and cDNA was stored at -20°C.

2.2.3 Tissue Culture Methods

Cultivation and passaging of cells

Schneider cells were cultivated in Schneider's *Drosophila* Medium (GIBCO) supplemented with 10% FCS, 1x Pen/Strep at 26°C and were maintained by diluting the culture twice a week to $0.5 - 1 \times 10^6$ cells/ml. Cells were grown in culturing flasks (Greiner). For selection of transfected cells 150 µM hygromycin was added. Expression of the Df31 transgene was induced 24 h before harvesting by the addition of 0.25 µM copper sulphate solution.

Cryopreservation of cells

Cells of one large cell culture flask (175 cm²) with 80% confluency were harvested and centrifuged at 800 g for 5 min. Cells were then resuspended in 10 ml freezing medium. 1 ml aliquots were frozen in cryovials stored in a freezing container (Fisher Scientific) with a cooling rate of 1°C/min at -80°C. The next day cells were transferred to the -180°C liquid nitrogen freezer. New aliquots were resuspended in fresh media and sown in medium flasks (75 cm²).

Freezing medium: 50% FCS (heat inactivated), 40% Schneider medium, 10% DMSO

Transfection of *Drosophila* Schneider L2-4 cells

To generate stable cell lines 2×10^6 L2-4 cells were transfected using the X-tremeGENE HP DNA Transfection Reagent according to manufacture's instructions (Roche).

Knockdown of Df31 in *Drosophila* S2 cells

Df31 was knocked down by dsRNA incubation as described elsewhere (Worby et al., 2001). An exon sequence was amplified by PCR and flanked by T7 promotor sites with the primers oMiP009 and oMiP010. The PCR product was used for *in vitro* transcription (Ambion MEGAscript T7 kit) to get suitable amounts of dsRNA. 0.75×10^6 *Drosophila* S2 cells were grown in 25 cm² flasks (Greiner) with 1 ml DMEM medium without FCS and supplied with 10-20 µg dsRNA. After 1 h incubation, 2 ml of DMEM containing FCS were added. Knock down efficiency was tested after 5 days by qPCR using the following primer pairs:

Primer pair 1: ACTGTTTCTTTTGCCGCC (for), CTCGCTGCTCTTTTTTTG (rev)

Primer pair 2: TGA CTCAACAGATGCTCCC (for), CCCCATCTGAACCTCATCC (rev)

2. MATERIALS & METHODS

2.2.4 Protein Methods

Preparation of nuclear extract from tissue culture cells

Cells were expanded over approximately four to five weeks leading to a total cell number of at least 3×10^9 cells. Cells were harvested by centrifugation at 1000 g for 20 min and washed twice with cold PBS. Packed cell volume (PCV) was estimated and the cell pellet resuspended in 3x PCV hypotonic Buffer A. After 30 min incubation on ice cells could be homogenised using a Dounce Homogenisator. In order to increase the stabilization of nuclei the salt concentration was increased with 1/10 volume Buffer B. Cytoplasmic components were removed from the extract by centrifugation (8000 g, 15 min, 4°C) and the packed nuclear volume (PNV) was estimated and the pellet resuspended in 3x PNV of Buffer A/B (9:1). Nuclear proteins were extracted by adding 400 mM NH_4SO_4 pH 7.9 and incubation on a rotating wheel for 25 min at 4°C. To further remove DNA and nuclear membrane the solution was centrifuged in an ultracentrifuge at 40000 g for 1.5 h at 4°C. The supernatant was isolated and solubilised proteins were precipitated by slowly adding 0.3 g of solid NH_4SO_4 per ml of nuclear extract under continuous stirring and subsequent centrifugation (15000 rpm, SS34, 35 min, 4°C). The pellet was resuspended in 0.2 – 0.5 PCV of Buffer C, dialysed 3 times against Buffer C (1.5 h each step, Spectra/Pro Dialysis Membrane) and centrifuged once more at 20000 g at 4°C for 15 min to remove precipitated proteins. Protein concentration was determined as described below. Nuclear extract was aliquoted, frozen in liquid nitrogen and stored at -80°C.

	Buffer A	Buffer B	Buffer C
HEPES pH 7.6	10 mM	50 mM	25 mM
KCl	15 mM	1 M	150 mM
MgCl_2	2 mM	30 mM	12.5 mM
EDTA	0.1 mM	0.1 mM	0.1 mM
			10% (v/v) glycerol

1 mM DTT and protease inhibitors were added freshly

FLAG immunoprecipitation from nuclear extract

ANTI-FLAG[®] M2 Affinity Gel agarose beads (Sigma) were equilibrated by washing 3 times in 10x beads volume of Buffer C. After each step the supernatant was taken off by centrifugation of the beads for 2 min at 1000 rpm at 4°C. 2 mg of nuclear extract from a transgenic cell line was added and beads were incubated for 2 h at 4°C on a rotating wheel. Beads were then washed 3 times in Buffer C/0.1% NP-40 for 10 min each, rotating at 4°C. Finally proteins were eluted in 20 μl SDS Sample buffer. SDS Sample buffer was also added to aliquots of input and supernatant for Western Blot analysis. As control the same protocol was performed with wildtype L2-4 nuclear extract.

Protein quantification

Protein concentrations were determined using Bradford solution (Biorad). Three to five concentrations of BSA were used as standard curve. The linear range of the assay for BSA is 0.2-0.9 mg/ml.

SDS-Polyacrylamid-Gelelectrophoresis (SDS-PAGE)

Denaturing SDS-Polyacrylamid-Gels were used to separate protein mixtures according to their electrophoretic mobility (Laemmli, 1970). SDS in the sample buffer and the gel leads to an unfolding of the proteins and imparts a negative charge to the linearized proteins. Each gel consists of a stacking gel in which the sample is concentrated at the border to the separation gel. The resolving gel can have an acrylamide range of 8-18%, depending on the protein mixture under investigation. Protein samples were mixed with SDS Sample buffer and denatured for 5 min at 95°C before loading onto the gel. Protein markers (peqGOLD Protein Marker IV and V, Peqlab) were used to estimate the molecular weight of the proteins. Electrophoresis was performed at 110 V until the protein running front reached the separation gel. Then the voltage was increased up to 160-180 V until proteins were sufficiently separated. Afterwards gels were stained either by Coomassie or silver or subjected to Western blotting.

Gel cassettes and precast gradientgels (4-20%) were purchased from Invitrogen.

Separation gel (18%)

0.9 ml H₂O
3.6 ml acrylamid mix (30/0.8)
1.5 ml 1.5 M Tris pH 8.8
30 µl 20% (w/v) SDS
30 µl 20% (w/v) APS
3 µl TEMED

Stacking gel (5%)

1.4 ml H₂O
340 µl acrylamid mix (30/0.8)
250 µl 1 M Tris pH 6.8
10 µl 20% (w/v) SDS
10 µl 20% (w/v) APS
2 µl TEMED

SDS Running buffer

25 mM Tris
190 mM glycine
0.1% (w/v) SDS

4 x SDS Sample buffer

200 mM Tris pH 6.8
8% (w/v) SDS
40% (v/v) glycerol
0.2% (w/v) bromphenol blue
4.2% (v/v) β-Mercaptoethanol

Coomassie staining

The stacking gel was removed and the separation gel was incubated for 20 min in a fixation and staining solution on a shaker at RT. Gel was transferred to fresh destaining solution and incubated until background was clear. Gels were documented using a gel documentation system (G:BOX). For mass spectrometry analysis, proteins were cut out with a clean scalpel or a gridcutter and stored in 0.2 ml tubes with 100 µl of ddH₂O at 4°C until further analysis.

Fixation and staining solution: 50% (v/v) methanol, 10% (v/v) acetic acid, 0.25% (w/v) Coomassie Brilliant Blue G-250 **Destaining solution:** 10% (v/v) acetic acid

2. MATERIALS & METHODS

Silver staining

Silverstaining was performed as described by Blum et al. (Blum et al., 1987).

Western blotting

SDS-PAGE of protein samples was performed as described above. The gel was removed from the electrophoresis apparatus and assembled in a gel holder in the following order: black bottom support (facing the negative electrode), 1 sponge, 3x whatman paper, gel, membrane, 3x whatman paper, 1 sponge, clear top support (facing the positive electrode). The PVDF membrane was activated for 15 s in methanol and shortly incubated in 1x Western Blot Buffer before assembly. Sponges as well as whatman paper was soaked in 1x Western Blot Buffer. The gel holder was inserted into the holder cassette and the gel transfer cell was filled with 1x Western Blot Buffer and a cooling unit. Protein transfer was performed at 300 mA for 2 h at 4°C or o/n at 40 mA. The membrane was blocked in 5% (w/v) milk in 1x PBS for 30 min RT on a shaker. Subsequently, it was incubated with the primary antibody 2 h at RT or o/n at 4°C on a shaker. After three washing steps (10 min each) in PBS/0.1% Tween the membrane was incubated with the fluorescently labelled secondary antibody again for 1 h at RT while shaking. The blot was washed again as described above, documented and quantified with an Odyssey system from LI-COR (Towbin et al., 1979). For ECL Western blotting a peroxidase-coupled secondary antibody was used. The signal was detected using the Amersham ECL Prime Western Blotting Detection Reagent (GE Healthcare) as described in the manufacture's protocol.

1x PBS

136 mM NaCl
2.7 mM KCl
4 mM Na₂HPO₄
1.7 mM KH₂PO₄
→ adjust pH to 7.4 with HCl

1x PBS Tween

1x PBS
0.1% (v/v) Tween 20

Western blot buffer

25 mM Tris
192 mM Glycine
0.02% (w/v) SDS
15% (v/v) methanol

Df31-IP from *Drosophila* embryo extract

αDf31 1A10 and αHA R001 (both rat monoclonal antibody, IgG-1 subtype) were incubated with 30 µl ProteinG Sepharose beads (GE healthcare) for 2 h at 4°C. Beads were washed and incubated with 1.5 mg of precleared *Drosophila* embryo extract for 3 h at 4°C. Beads were washed 3x with 300 mM EX300/0.1% NP-40. Immunoprecipitated proteins and associated RNAs were isolated using the TRIZOL reagent (Invitrogen) according to manufactures instructions. RNA was reverse transcribed (described above) and PCR was performed using snoRNA-specific primers.

2.2.5 Chromatin Methods

Preparation of chromatin assembly extract from *Drosophila* embryos

Drosophila embryos were collected on agar trays with yeast paste 0-90 min after egg-laying. Using a brush and sieves with descending mesh size (0.71 mm, 0.355 mm, 0.125 mm), embryos were rinsed with cold tap water and allowed to settle into ice-cold embryo wash buffer to arrest further development. After five successive collections, the wash buffer was decanted and replaced with wash buffer at room temperature. For dechorination of the embryos, the volume was adjusted to 200 ml and 60 ml of 13% hypochlorite solution was added. The embryos were stirred vigorously for 3-3.5 min on a magnetic stirrer, poured back into the collection sieve (0.125 mm), and rinsed with tap water for 5 min. Embryos were allowed to settle in 200 ml of wash buffer for about 3 min. Afterwards the supernatant with the containing chorions was poured out. Following two more settlings in 0.7% NaCl and extract buffer at 4°C, the embryos were settled in extract buffer in a 60 ml glass homogeniser on ice. The volume of the packed embryos was estimated before the supernatant was aspirated, leaving packed embryos and additional 2 ml buffer on top. Homogenisation was performed with one stroke at 3000 rpm and 10 strokes at 1500 rpm with a pestle connected to a drill press. The homogenate was supplemented with MgCl₂ to a final MgCl₂ concentration of 5 mM. Nuclei were pelleted by centrifugation for 10 min at 10000 rpm in a SS34 (Sorvall RC6PLUS) rotor. The supernatant was centrifuged again for 2 h at 45000 rpm in a chilled SW 56 rotor (Beckman ultracentrifuge LE-80K). The clear extract was isolated with a syringe, avoiding the top layer of lipids. Extract aliquots were frozen in liquid nitrogen. Protein concentration was determined with the Bradford assay as described above.

Embryo wash

0.7% (w/v) NaCl
0.05% (v/v) Triton X-100

Extract buffer

10 mM HEPES pH 7.6
10 mM KCl
1.5 mM MgCl₂
0.5 mM EGTA
10% (v/v) glycerol
1 mM DTT*
0.2 mM PMSF*
→ * add fresh before use

Preparation of biotinylated and linearized DNA

To obtain linearized and biotinylated DNA, plasmid DNA (pAI61) containing oligomers of the sea urchin 5S rDNA positioning sequence was used. 500 mg plasmid DNA was linearized using the restriction enzyme SacI. Completion of the digest was analysed by running an aliquot of the reaction on an agarose gel. When all plasmid DNA was linearized the restriction enzyme XbaI was added to

2. MATERIALS & METHODS

the reaction and the mixture was incubated for at least 3 h at 37°C. The DNA was precipitated by adding sodiumacetate pH 5.3 to a final concentration of 0.3 M and 0.8 volumes isopropanol. The sample was mixed and incubated on ice for at least 30 min. After 1 h centrifugation at 13000 rpm at 4°C (Eppendorf 5417C) the supernatant was discarded and the pellet was washed with 70% ethanol. For the biotinylation reaction 30 µl 10x NEB buffer 2, 80 mM dCTP and dGTP, 3 mM biotinylated dUTP and dATP, 10 U Klenow Polymerase and ddH₂O was added up to a total volume of 300 µl. The sample was incubated for 2 h at 37°C before inactivation of the Klenow enzyme at 70°C for 20 min. Excessive nucleotides and enzyme were removed by centrifugating the sample through G50 Sephadex spin columns (Roche). Columns were centrifuged twice (1 min, 1000 rpm, 4°C, Sigma 3-18) and the flow through was discarded. 100 µl of the sample was applied to each column and centrifuged for 2 min at 2000 rpm. The flow through was collected and the DNA concentration determined. Finally, DNA concentration was measured and adjusted to 200 ng/µl.

Chromatin assembly on immobilised DNA

Per sample 2 µg linearized and biotinylated DNA was immobilised onto 0.6 mg Dynabeads[®] M280 paramagnetic streptavidin beads (10 mg/ml, Invitrogen) in EX100 buffer. For this, beads were washed once with 2 M Dynawash/0.05% NP-40. DNA as well as 1x volume of TE buffer and 2x volumes of kilobaseBINDER (Invitrogen) was added. Samples were incubated for 1 h at RT on a metal-free rotating wheel. After extensive washing (3x 1M Dynawash/0.05% NP-40, 3x TE buffer) beads were blocked for 30 min with BSA (0.2 µg/µl, NEB) in EX100. After another washing step in EX-NP-40 beads were resuspended in a total volume of 240 µl containing 120 µl DREX, an ATP-regenerating system (McNAP) and EX100.

1 M Dynawash

10 mM Tris HCl pH 8
1 mM EDTA
1 M NaCl

2 M Dynawash

10 mM Tris HCl pH 8
1 mM EDTA
2 M NaCl

EX100

10 mM HEPES pH 7.6
100 mM NaCl
1.5 mM MgCl₂
0.5 mM EGTA
10% (v/v) glycerol
1 mM DTT*
0.2 mM PMSF*

EX-NP-40

10 mM HEPES pH 7.6
1.5 mM MgCl₂
0.5 mM EGTA
10% (v/v) glycerol
0.05% (v/v) NP-40

→ * add fresh before use

McNap

3 mM ATP
30 mM creatine phosphate
10 µg creatine kinase/ml
3 mM MgCl₂
1 mM DTT

Elution buffer

in EX100
0.5 U/µl MNase
2 mM CaCl₂

a) Analysis of chromatin assembly dynamics

For the analysis of chromatin dynamics a total amount of 4 µg of DNA was used, assembled in two individual samples. The assembly reaction was performed at 26°C for 1 h or 4 h. After three wash steps with EX100, beads were resuspended in 40 µl elution buffer. After 30 min of elution at RT the supernatant was taken off, SDS Sample buffer was added and samples were subjected to SDS-PAGE followed by mass spectrometry analysis or Western blotting.

b) Analysis of RNA-dependent protein binding to chromatin

DNA was assembled as described above. After an assembly of 6 h the supernatant was taken off and beads were washed once with EX100 to remove unbound proteins. Beads were then resuspended in 200 µl EX100. To remove chromatin-associated RNAs RNase A was added to a final concentration of 1 µg/µl. After 2 h incubation at 26°C beads were washed twice with EX100 and proteins were eluted in 20 µl SDS Sample buffer. For the proteomic analysis, a total amount 5 µg of chromatin were subjected to SDS-PAGE and subsequent LC-MS/MS mass spectrometry as described below.

c) Chromatin accessibility assay by Micrococcal nuclease digestion

Two microgram of plasmid DNA was reconstituted into chromatin for 1 h to 4 h at 26°C. The sample was subjected to Micrococcal Nuclease digestion (80 U per reaction, Sigma). The MNase digestion reaction was incubated for 40 s, 80 s and 160 s in the presence of 2 mM CaCl₂ and then stopped by the addition of 2 mM EDTA. RNA and proteins were digested with 50 µg/ml RNase A for 30 min at 37°C, followed by the incubation with 0.5 mg/ml Proteinase K and 0.5% SDS for 2 h at 65°C or overnight at 37°C. Nucleic acids were further purified by Phenol-Chloroform extraction using Rotiphenol. The sample was mixed with two volumes Rotiphenol (Phenol:Chloroform:Isoamyl alcohol in relation 25:24:1, Roth) and centrifuged at full speed for 20 min. The upper aqueous phase was taken off and mixed with 1 µl Glycogen. 0.3 M Sodiumacetat pH 5.2 and 0.8 volumes isopropanol were added, sample was mixed and incubated on ice for 30 min. To precipitate the DNA, the sample was centrifuged full speed for 45 min and the pellet was washed with 70% Ethanol. The precipitated and washed DNA was resuspended in TE Buffer and analysed on a 1% agarose gel stained with ethidium bromide.

2. MATERIALS & METHODS

2.2.6 Mass Spectrometry Methods

Preparation of Mass Spectrometry samples

Chromatin was assembled as described above. After the separation of chromatin-bound proteins by SDS-PAGE, the gel was stained with Coomassie and bands were excised manually or by using an OneTouch gridcutter. Each lane was divided into eight fractions, which were individually digested with trypsin as described before with minor modifications (Wilm et al., 1996; Shevchenko et al., 2000). First, gel slices were washed 2x with 100 μ l of mQ H₂O, 3x with 100 μ l of 25 mM NH₄HCO₃, destained in a 1:1 buffer containing 25 mM NH₄HCO₃ and acetonitrile and dehydrated by washing them 3x with 100 μ l of acetonitrile. Gel slices were then incubated 1 h with 50 μ l of 10 mM DTT in 25 mM NH₄HCO₃. Afterwards slices were incubated 30 min in a dark place with 50 μ l of 55 mM iodoacetamide in 25 mM NH₄HCO₃ to carbamidomethylate the reduced cysteines. Gel fragments were washed with 100 μ l of 25 mM NH₄HCO₃ and dehydrated again with 100 μ l of acetonitrile. 20 μ l of 25 ng/ μ l trypsin dissolved in 25 mM NH₄HCO₃ were added to each sample, incubated 45 min at 4°C and then the non-absorbed protease removed. Gel fragments were covered with 25 mM NH₄HCO₃ and digested for 16 h at 37°C. For peptide extraction, gel slices were incubated 2x with 50 μ l of 50% acetonitrile/0.25% TFA and twice more with 50 μ l of 100% acetonitrile. The resulting liquid containing the digested peptides was totally evaporated using a ScanVac (LaboGene™), redissolved with 15 μ l of 0.1% formic acid and stored at -20°C until further processing.

Proteome Analysis

Tryptic peptides were injected in an Ultimate 3000 HPLC system (LC Packings Dionex). Samples were desalted on-line in a C18 microcolumn (300 μ m i.d. x 5 mm, packed with C18 PepMap™, 5 μ m, 100 Å by LC Packings), and peptides were separated with a gradient from 5-60% acetonitrile in 0.1% formic acid over 40 min at 300 nl/min on a C18 analytical column (75 μ m i.d. x 15 cm, packed with C18 PepMap™, 3 μ m, 100 Å by LC Packings). The effluent from the HPLC was directly electrosprayed into a linear trap quadrupole-Orbitrap mass spectrometer (Thermo Fisher Scientific). The MS instrument was operated in data-dependent mode. Survey full-scan MS spectra (from m/z 300–2000) were acquired in the Orbitrap with resolution R = 60000 at m/z 400 (after accumulation to a “target value” of 500000 in the linear ion trap). The six most intense peptide ions with charge states between two and four were sequentially isolated to a target value of 10000, fragmented by collision-induced dissociation and recorded in the linear ion trap. For all measurements with the Orbitrap detector, three lock-mass ions were used for internal calibration (Olsen et al., 2005). Typical MS conditions were: spray voltage 1.5 kV; no sheath and auxiliary gas flow; heated capillary temperature 200°C; normalized collision-induced dissociation energy 35%; activation q = 0.25; and activation time = 30 ms.

Mass spectrometry material and software

Description	Supplier
0.2 ml tubes, strips of eight	Axygen
Acetonitrile	Roth
Ammoniumhydrogencarbonate	Roth
Formic acid	Sigma
Gridcutter One Touch	Gel Company
H ₂ O LC grade LiChrosolv®	Millipore
Trypsin	Promega
Maxquant	Cox and Mann, 2008
Xcalibur	Thermo Scientific
Proteome Discoverer	Thermo Scientific

Proteomic analysis of chromatin-associated proteins

The Proteome Discoverer Software (Version 1.2.0.208) was applied for the analysis of RNA-dependent protein binding to chromatin. The following workflow settings were used: Database: Mascot; NCBIInr, Sequest: uniprot; Taxonomy: *Drosophila melanogaster*; Enzyme Name: Trypsin; Maximum Missed Cleavage Sites: 1; Instrument: Default; Unrecognized Activation Type Replacements: CID; Peptide Cut Off Score: 10; Protein Scoring Options: Use MudPIT Scoring: True; Decoy Search: True; High Confidence: 1% false hits; Medium Confidence: 5% false hits; Precursor Mass Tolerance: 10 ppm; Fragment Mass Tolerance: 0.8 Da; Dynamic Modification: Oxidation (M); Static Modification: Carbamidomethyl (C); Precursor Ions Area Detector: Mass Precision: 4 ppm; S/N Threshold: 1.

Raw data of protein binding kinetics were analysed by MaxQuant (Version 1.2.2.5) with the following parameters: Database: Swissprot 57.10; Taxonomy: *Drosophila melanogaster*; MS tol: 10 ppm; MS/MS tol: 0.5 Da; Peptide FDR: 0.01; Protein FDR: 0.01; Min. peptide Length: 6; Variable modifications: Oxidation (M), Acetylation (K); Fixed modifications: Carbamidomethyl (C); iBAQ option selected. The generated ‘proteingroups.txt’ table was filtered for “contaminants”, “reverse hits” and “only identified by site”. Proteins were grouped according to their log₂ fold enrichment (iBAQ intensity 1h/iBAQ intensity 4h).

Bioinformatic analysis

Functional annotation of chromatin-bound proteins was done using the DAVID Bioinformatics resource 6.7 (<http://david.abcc.ncifcrf.gov/>). DAVID only works with gene lists, therefore proteins were submitted as Flybase Gene IDs (FBgn numbers). Terms for the different categories were extracted from the functional annotation chart with the following settings: Count 10, EASE 0.1.

2. MATERIALS & METHODS

STRING 9.1 (Search Tool for the Retrieval of Interacting Genes/Proteins) was used to evaluate the already described interactions among the proteins identified in the proteomic analyses. Proteins were submitted as Flybase polypeptide (Fbpp) as complete list with *Drosophila melanogaster* as organism. Networks were displayed as confidence view.

2.2.7 Immunohistochemical Methods

Immunolocalisation in Schneider cells

100 µl cell suspension with approximately 3×10^6 cells/ml were pipetted on a microscope slide. Cells were allowed to settle for 30 min and slides were then washed in PBS for 5-10 min at RT in a Coplin Jar. Fixation was done by incubating the slides for 10 min at RT in PBS/3.7% Formaldehyd followed by two washing steps in PBS. Cells were then permeabilised in ice-cold PBS/0.25% Triton X-100 for 6 min, again followed by two washing steps in PBS. Prior to incubation with the first antibody cells were blocked with 50 µl Image-iT FX (Invitrogen) for 45 min at RT. The first antibody was diluted in PBS/0.1% Triton X-100 in 1.2% non-fat milk. 100 µl antibody was pipetted on the microscope slide with cells, covered with parafilm and incubated overnight in a wet chamber in the dark at 4°C. On the following day slides were washed twice with PBS/0.1% Triton X-100 and incubated with the secondary antibody for 1 h at RT followed by two washings in PBS/0.1% Triton X-100. Cells were mounted with 7 µl Vectashield® DAPI (Vector Laboratories), covered with a coverslip and sealed with nailpolish.

Riboprobes

SnoRNA sequences for the two snoRNA Me28S U2134b and G980 were cloned into the pCS2+ Vector. All plasmids were linearized with XbaI and purified using the Qiagen MinElute® PCR Purification Kit. *In vitro* transcription was performed as follows:

Template	2 µg
5x Transcription Buffer	10 µl
labelling mix	0.5 µl each
	10 mM ATP, CTP, GTP
	6.5 mM UTP
	3.5 mM DIG-11-UTP
0.1 mg/ml DTT	0.5 µl
RNAsin 40 U/µl	0.5 µl
RNA-Polymerase	2 µl (SP6 for snoRNA, T7 for roX2)
RNAsin 40 U/µl	0.5 µl
ddH ₂ O	ad to 50 µl

The reaction was incubated at 37°C for 2.5 h. Then 1 µl RNA-Polymerase was added and incubation was continued for 1 h. RNA probes were purified using the RNeasy® Kit from Qiagen with on-column DNase digest as described in the manual.

RNA FISH and Immunostaining of polytene chromosomes

Polytene chromosomes from salivary glands of 3rd instar larvae were prepared as described in Lavrov et al. (Lavrov et al., 2004). Chromosomes were sequentially rehydrated in Methanol/PBT with 90%, 70%, 50% and 30% methanol in PBT for 15 min at RT. Slides were then incubated for 15 min at RT in PBT/hybridization mix in a ratio of 70%/30%, 50%/50%, 30%/70%. Prehybridization was performed in hybridization buffer at 55°C for 1 h. The slides were treated with the same hybridization solution (25 µl) containing single-stranded antisense riboprobes (100-200 ng) labelled with digoxigenin (Roche). Following overnight hybridization at 37°C in a humid chamber, slides were washed 3x 5 min with 2x SSC at 37°C and 1x 5 min with 2x SSC at RT. Immunostaining was performed as described in Lavrov et al., 2004. Antibody concentrations were 1:250 for the mädig antibody (Sigma) and 1:300 for secondary antibodies.

PBT

PBS containing 0.1% Tween

2x SSC

300 mM sodium chloride

30 mM trisodium citrate

pH adjusted to 7.0 with HCl

Hybridization mix

50% formamide

5x SSC

100 µg/ml of fragmented salmon sperm

50 µg/ml heparin

0.1% Tween

Microscopy

All slides were analysed using the Axiovert 200M epifluorescence microscope (Zeiss). Images were taken with the 60x objective and were kept using the Axiovision 4.7 software (Zeiss). Editing of pictures was done using Adobe CS5 Photoshop and Illustrator.

2. MATERIALS & METHODS

3. RESULTS

3. RESULTS

3.1 *In vitro* chromatin assembly

For the establishment of the method two time points of chromatin assembly were initially chosen. Past experiments in which the *in vitro* assembly system was used to perform a time-resolved analysis of histone modifications, indicated that histone deposition occurs within the first hour of assembly (Scharf et al., 2009). Other *in vitro* assembly systems observed deposition of histones within seconds (Ladoux et al., 2000; Wagner et al., 2005). However, until newly assembled chromatin adopts the typical features of bulk chromatin a certain amount of time has to pass by. This process of maturation includes the removal of an acetylation mark on H4K5 and K12. In the present assembly system, deacetylation was observable at a time point of 1 hour and no further remarkable change was seen after 4 hours (Scharf et al., 2009). For this reason those two time points, resembling early and matured chromatin, were chosen for the establishment of the method.

Protein binding at 1 h and 4 h (henceforth also referred to as early and late) was investigated by mass spectrometry and the changes of different protein groups and complexes was further analysed. Assembly reactions were performed using a well-characterised S-150 chromatin assembly extract prepared from early *Drosophila* embryos (Becker and Wu, 1992). This protein extract is able to assemble large fragments of DNA into an ordered nucleosomal array that closely resembles the chromatin structure observed *in vivo* (Blank et al., 1997). Figure 3.1 shows an MNase accessibility assay, which is frequently used to evaluate nucleosomal spacing of chromatin. The endonuclease micrococcal nuclease (MNase) cuts the linker DNA between nucleosomes thereby creating a regular ladder of DNA fragments with a periodicity of about 170 bp. Each fragment represents various numbers of nucleosomes. The median length of those fragments depends on the MNase concentration, incubation time and temperature. Partial digest of the cellular chromatin by MNase leads to a DNA ladder that reaches from small fragments, which are protected by only few nucleosomes to very large fragments that consist of longer arrays of nucleosomes (Figure 3.1).

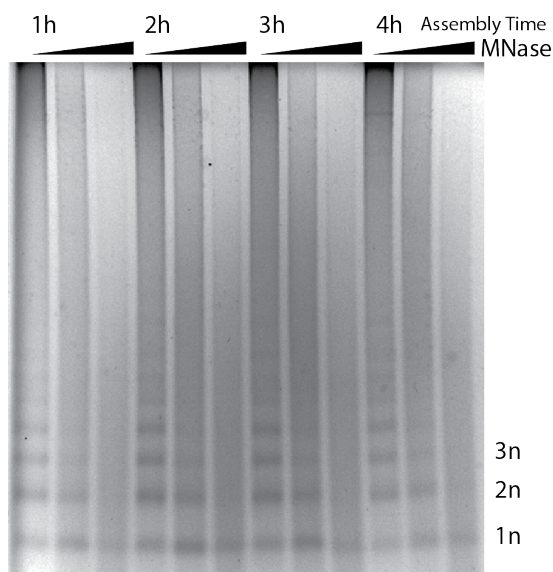
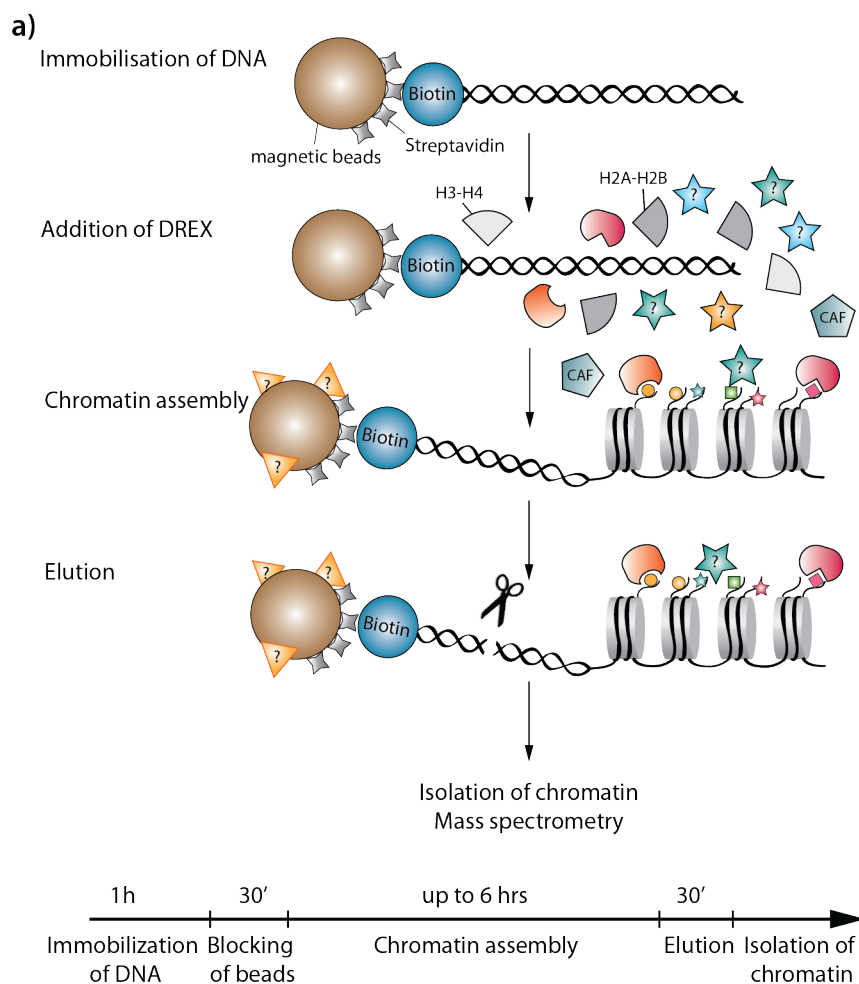


Figure 3.1: *In vitro* assembly leads to a regular spaced array of nucleosomes.

Figure shows a micrococcal accessibility assay of *in vitro* reconstituted chromatin. A total amount of 4 μ g DNA was used. Nucleosomes are already assembled and regularly spaced after 1 h of reconstitution.

The DNA used for the experiments harbours an array of a nucleosome positioning sequence derived from the *Lytechinus variegatus* (Sea urchin) 5S rRNA gene and further consist of the backbone of pBluescript SK(-) (Hansen et al., 1991). Purified plasmid DNA was linearized and cleavage sites were refilled with dCTP, dGTP and biotinylated dATP and dUTP. The template was then immobilised on magnetic streptavidin beads and incubated with the *Drosophila* embryo extract and an ATP-regenerating system for a chosen duration. Using magnetic beads allows to isolate chromatin at any given time point during assembly, investigate protein binding at this specific time point and even interfere with the process of assembly or the already assembled chromatin structure. Due to the sequence of the restriction sites only one end was biotinylated leaving one end unattached to the beads as seen in Figure 3.2 a).

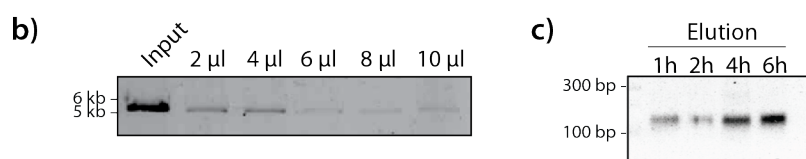
Figure 3.2: Workflow of *in vitro* assembled chromatin with subsequent mass spectrometry.



a) Biotinylated and linearized DNA gets immobilised on streptavidin-coated magnetic beads. Beads are blocked with BSA and incubated with *Drosophila* embryo extract for reconstitution of chromatin. Chromatin is isolated at given time-points, beads are washed and chromatin is eluted by MNase digestion, which processes the chromatin to mononucleosomes (see 2.2 c)). Timeline indicates the duration of the experiment.

b) Binding assay illustrating the binding of biotinylated DNA to streptavidin beads. Shown is the binding of 200 ng biotinylated and linearized DNA to an increasing amount of beads.

c) Chromatin was eluted from beads by digestion with MNase. Shown are different timepoints of assembly.



3. RESULTS

Figure 3.2 b) shows a binding assay of biotinylated DNA in presence of increasing amounts of beads. In all experiments, a certain fraction of DNA seemed to be unefficiently biotinylated and unable to bind to Streptavidin beads. Standard conditions were therefore set to 60 μ l beads per 2 μ g of DNA.

M280 Streptavidin beads are blocked with BSA before and after immobilisation of the DNA. Yet, incubating DNA-free beads with the protein extract showed several protein bands on a protein gel (Figure 3.3 a)). To reduce identification of background proteins beads were extensively washed after assembly and chromatin was eluted by Micrococcal Nuclease (MNase) digest (Figure 3.2 c) and Figure 3.3 b)).

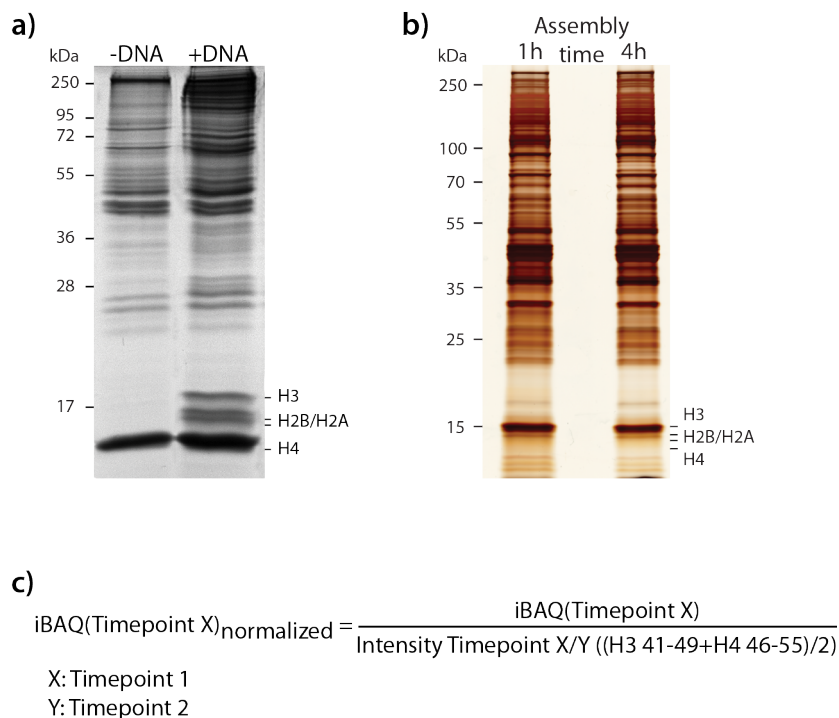


Figure 3.3: *In vitro* assembled chromatin.

a) Coomassie-stained gel comparing a 15 min assembly reaction with and without prior DNA binding. Histones are specifically enriched in the +DNA sample indicating proper chromatin assembly. b) Silverstained gradientgel with MNase-eluted chromatin from two different assembly time points. c) Formula used for the normalization step of chromatin-bound proteins based on the amount of unmodified histone peptides 41-49 of H3 and 46-55 of H4.

3.2 Analysis of chromatin-bound proteins

Chromatin-associated proteins were separated by gel-electrophoresis and subjected to an in-gel tryptic digest to obtain peptides. Four independent replicates of each time point were performed to analyse reproducibility of the method. Depicted in Figure 3.3 b) is a representative silver gel of a 1 h and 4 h chromatin assembly. To identify and quantify chromatin-bound proteins, the Max Quant software and its embedded search engine Andromeda were used. Taking together all four independent replicates a

total number of 1744 proteins was identified. All downstream analysis of mass spec data was based on their iBAQ values. This value stands for intensity based absolute quantification and refers to the sum of intensities of all tryptic peptides for each protein divided by the number of theoretically observable peptides. It should therefore provide an accurate determination of the relative abundance of all proteins identified in a sample (Smits et al., 2012). Based on the assumption that the level of incorporated histones equals the same amount of chromatin in the individual samples, all intensities were normalized to the level of histones (Figure 3.3 c)). Peptides used for this normalization step were the unmodified peptides 41-49 of H3 and 46-55 of H4 which were separately quantified using the Xcalibur software and their ratio between the 1 h and 4 h sample was used to correct all other values.

A comparison of all identified proteins of the two time points showed a robust identification of around 900 to 1000 proteins with an overlap of approximately 60% of all replicates. Figure 3.4 shows a Venn diagram of three of the four replicates for the 1 h and 4 h time point. Replicate 2 and 3, which were performed at the same time, showed the highest overlap with up to 82%.

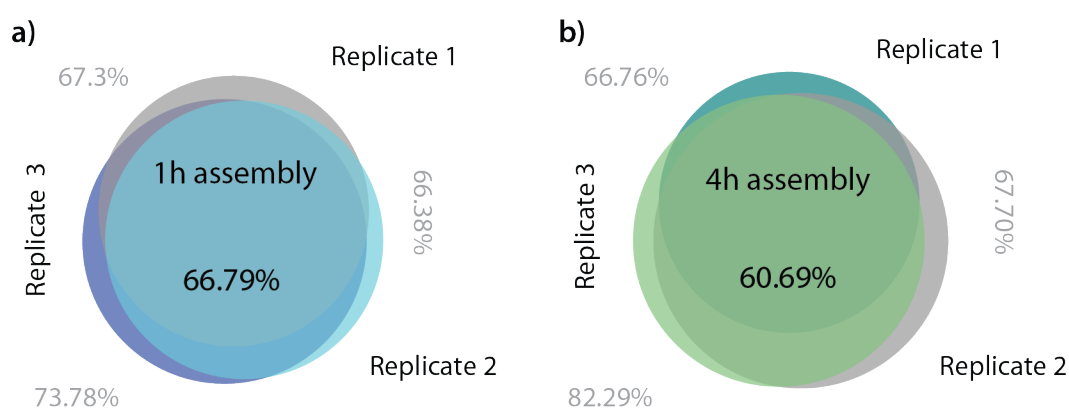


Figure 3.4: Venn diagram showing the overlap of proteins identified by mass spectrometry.

a) Overlap of proteins in three out of four 1 h assemblies. Replicates compared are: SID1319 (Replicate 1, 1306 proteins), SID1373.2 (Replicate 2, 1407 proteins) and SID1373.1 (Replicate 3, 1447 proteins). Over 66% (1096 proteins) are identical in the 1 h sample. **b)** Overlap of proteins in three out of four 4 h assemblies. Replicates compared are: SID1351 (Replicate 1, 1054 proteins), SID1373.2 (Replicate 2, 1334 proteins) and SID1373.1 (Replicate 3, 1289 proteins). Around 61% (911 proteins) are identical in the 4 h sample.

To further analyse the binding behaviour of proteins at those two assembly time points, the ratio of the iBAQ intensities was calculated. Proteins were then grouped according to their ratio of 1 h to 4 h. A five fold higher intensity in one sample over the other resulted in the category “enriched early” or “enriched late” while all other proteins were grouped in the category “unchanged”. For further analysis only proteins present in the same category in three out of four replicates were taken into account, leaving a total number of 1082 proteins (Appendix List 1: Kinetics of chromatin-binding proteins).

3. RESULTS

3.3 Proteomic data interpretation

As in any other -omics technology, the value of proteomic data is defined by the degree of its functional interpretation. Proteomics profiles and their functional analysis are inherently complex. Each of the hundreds of detected proteins can belong to dozens of pathways and can be connected in different context-specific groups by protein interactions (Bessarabova et al., 2012). Based on this complexity a knowledge-based approach was chosen to further evaluate the list of chromatin-associated proteins. List 1 was analysed using DAVID (Database for Annotation, Visualization and Integrated Discovery), an open source database, which provides a comprehensive set of functional annotation tools (Figure 3.5).

GO-Term Biological Process	Count	%	P-Value
Mitotic cell cycle	131	12.3	8.90E-41
Spindle organization	95	8.9	3.60E-35
Mitotic spindle organization	87	8.2	1.50E-34
Microtubule cytoskeleton organization	109	10.2	1.10E-33
Cell cycle	165	15.5	2.90E-32
M phase	141	13.2	4.00E-32
Cell cycle phase	143	13.4	2.00E-31
Cell cycle process	151	14.2	6.10E-31
Microtubule-based process	124	11.6	1.10E-29
Chromosome organization	93	8.7	7.50E-25
DNA metabolic process	80	7.5	2.60E-24
KEGG Pathway			
Proteasome	35	3.3	2.20E-14
DNA replication	24	2.3	9.90E-10
Nucleotide excision repair	21	2	7.80E-07
Mismatch Repair	13	1.2	3.60E-05
Aminoacyl-tRNA biosynthesis	19	1.8	1.30E-04
Pentose phosphate pathway	12	1.1	2.00E-03
Ubiquitin mediated proteolysis	32	3	2.10E-03
InterPro Domain			
Nucleic acid-binding, OB-fold	26	2.4	8.40E-15
Proteasome component region PCI	13	1.2	5.00E-11
Armadillo-like helical	25	2.3	4.30E-09
Like-Sm ribonucleoprotein, core	12	1.1	4.90E-08
Proteasome, subunit alpha/beta	14	1.3	1.10E-07
Glutathione S-transferase, C-terminal-like	16	1.5	1.50E-06
Ubiquitin-conjugating enzyme, E2	14	1.3	1.60E-06
Ubiquitin-conjugating enzyme/RWD-like	15	1.4	2.00E-06
Thioredoxin fold	21	2	1.60E-05
Glutathione S-transferase/chloride channel, C-tr	15	1.4	1.70E-05
ATPase, AAA+ type, core	29	2.7	1.90E-05
Histone-fold	11	1	2.50E-05
Ubiquitin	11	1	3.90E-05

Figure 3.5: DAVID Functional Annotation Analysis

Table shows the top hits of three different functional annotation analyses performed with DAVID. The following parameters were used: minimum number of proteins for a corresponding term (minimum count) was set to 10 for all analyses. All other settings were set to default. Percentages of assigned proteins are: 78.8% (GO-Term), 37.8% (KEGG) and 93% (InterPro). Count: Number of proteins involved in the term, Percentage: involved proteins in percent of total proteins.

Gene Ontology analysis of the Biological Process of List 1 revealed an overrepresentation of proteins carrying the following functions: “Mitotic Cell Cycle”, “Spindle Organization”, “Cell Cycle” and “Chromosome Organization” (P-Values: 8.9E-41, 3.6E-35, 2.9 E-32, 7.5E-25; with 78,8% of all proteins assigned to one or more terms). Those keywords positively relate to chromatin function and structure and point towards an identification of proteins that play a role during chromatin assembly and maintenance. In the functional annotation chart for the GO-term Molecular Function over 22% of the proteins were assigned to the group “Nucleotide binding” (P-Value 6.5E-21) along with related

subgroups such as “Ribonucleotide binding” (18%, 4.5E-20), “Nucleoside binding” (15.9%, 6.3E-17) and “ATP binding”(15.1%, 5.7E-18).

KEGG (Kyoto Encyclopedia of Genes and Genomes) allows the assignment of proteins to the pathways they are involved in. The database is frequently used to understand high-level functions of large-scale molecular datasets. A KEGG pathway analysis indicated “DNA Replication” (P-Value 9.9E-10), “Nucleotide Excision Repair” and “Mismatch Repair” (P-Value: 7.8E-7 and 3.6E-5) as top hits. In all those pathways chromatin disassembly and reassembly plays an indispensable role. Interestingly, KEGG identified the pathway “Proteasome” as top hit with a P-Value of 2.2E-14.

InterPro, a tool to classify proteins into families and to predict domains, denoted “Nucleic acid binding” as top hit (P-Value 1.3E-11, 93% of all proteins assigned). “Armadillo-like helical” and the domain “Like-SM ribonucleoprotein” also belonged to the most prominent domain feature (P-Value: 4.3E-9 and 4.9E-8). Also in this analysis the domain “Proteasome component region PCI” was one of the top hits (P-Value 3.9E-8) linking proteasomal activity to chromatin assembly.

Chromatin-associated proteins are highly interconnected

To find out more about chromatin-bound proteins and their connections among each other a STRING analysis was applied to the set of all bound proteins independently of their binding behaviour to chromatin. STRING is a database of known and predicted protein interactions and can therefore support the analysis of large data sets by clustering proteins in close relation to each other. STRING interactions include direct (physical) and indirect (functional) associations that are derived from e.g. high-throughput experiments or previous knowledge. Integration of proteomic data via STRING enables to evaluate the interconnectedness of the identified proteins and facilitates identification of similar protein groups or complexes. Figure 3.6 shows a STRING network of the obtained chromatin assembly data set. Shown are all proteins with at least one interaction in a so-called confidence view in which associations with higher confidence are represented by thicker lines. Connections are not only visible among well-described complexes but also between subunits of different complexes acting in the same pathways. STRING uses a spring model to generate network images. Thus, the final position of a protein node is computed by minimizing the “energy” of the whole system resulting in close protein nodes whenever a high confidence of their interaction exists. Four protein clusters are highlighted as zoom-in. Those clusters are characterised by an even higher degree of interconnections among the proteins and show the subunits of the proteasome, the MCM Complex and members of the origin recognition complex (ORC), the TFIID Complex and the histone core proteins, and the CHRAC Complex and subunits of the RNA Pol II.

3. RESULTS

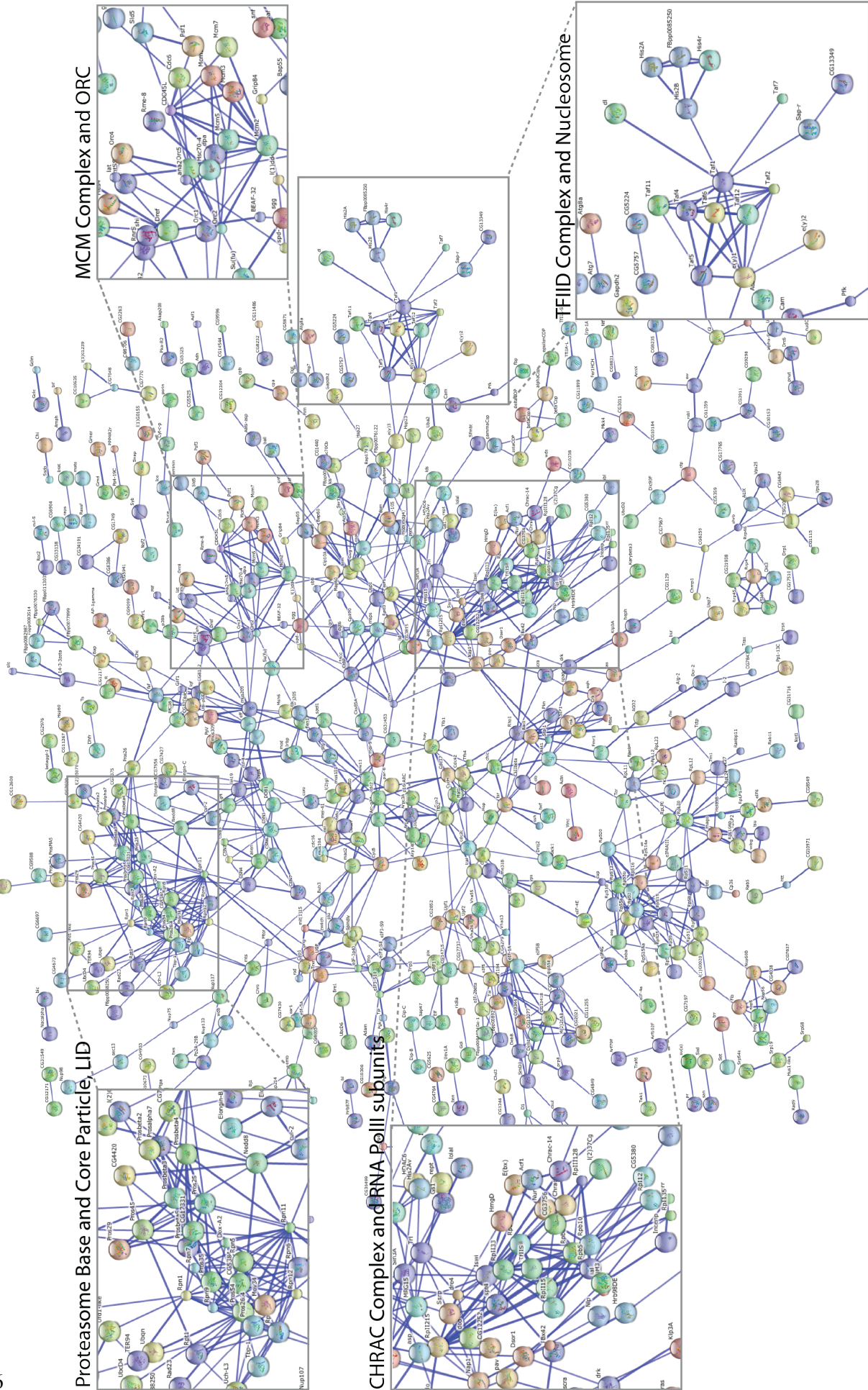


Figure 3.6: STRING network showing chromatin-associated proteins.

The network shows a confidence view with known and predicted protein-protein interactions of chromatin-associated proteins. Only proteins with at least one interaction are included into the network. Line width between nodes visualizes the confidence-score of an interaction between two proteins: the thicker the blue line, the higher the confidence-score of the corresponding interaction. Protein clustering illustrates protein complexes and binding partners with well-described interactions. Node colour differs as visual aid. Nodes with structural information associated to it are displayed at larger size to fit the thumbnail picture

3.4 Early and late chromatin binding profiles differ in their protein composition

Next, the differences between protein binding to early and late chromatin were being analysed. Figure 3.7 a) shows a waterfall plot of all proteins and their \log_2 transformed iBAQ intensities. 20% of all detected factors are more abundant on early chromatin whereas only 2.8 % of all factors were more abundant on matured chromatin (with a threshold of 5 times enriched in one sample over the other). Using the DAVID open source database different subsets of proteins were selected after their GO-term assignment. Proteins of each group were plotted according to their iBAQ intensity ratio. Panel b) to d) of Figure 3.7 show the binding characteristics of proteins with special features and functions.

Except for the proteins that belong to the KEGG pathway “Proteasome” all proteins showed a similar but less pronounced tendency of chromatin binding as seen in the overall analysis. A slightly larger fraction of proteins is found more abundant at the early time point of assembly whereas only few proteins bind preferentially late. Proteins present in the group of “Chromatin remodelling” showed the smallest difference in protein binding early compared to late. Proteins assigned to the KEGG “Proteasome” pathway were equally abundant on early versus late chromatin. The group of “Ribonucleotide binding“ proteins represents 18% of all identified proteins. 17.6% of those RNA-binding proteins bind preferentially to early chromatin whereas only 3% of those proteins are found more abundantly on the late chromatin fraction. Taken together early chromatin seems to be more accessible and prone to protein binding.

3. RESULTS

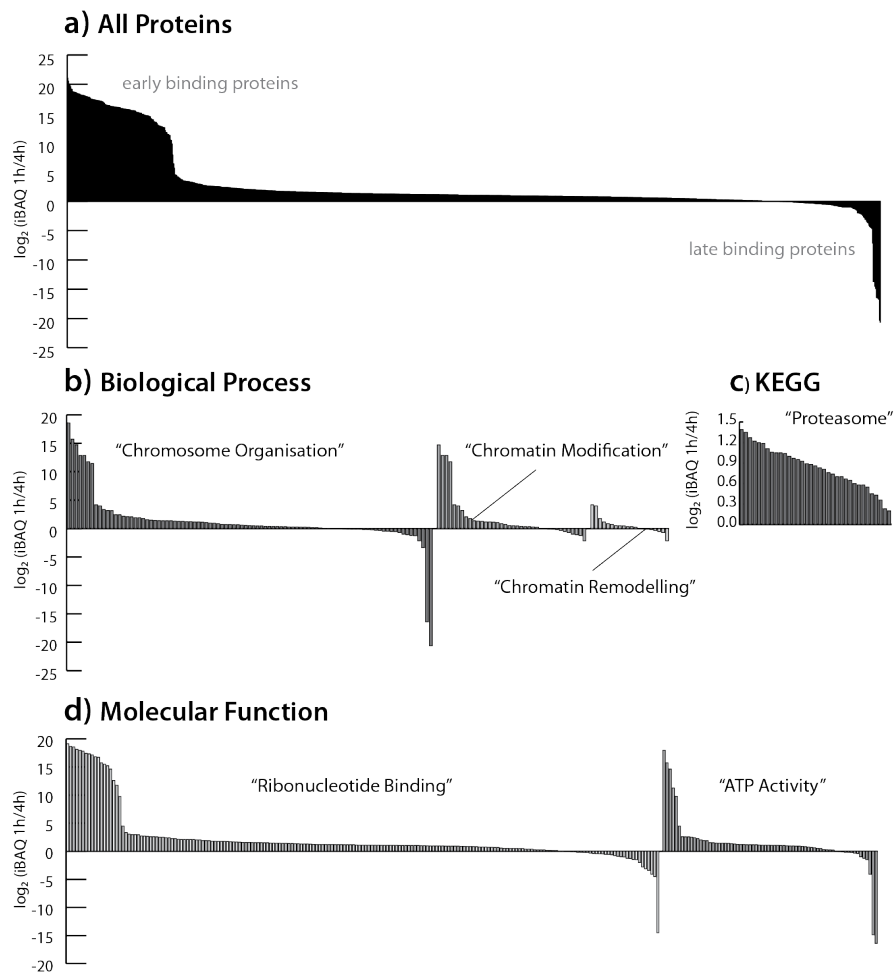


Figure 3.7: Waterfall plot illustrating the protein binding behaviour during assembly

Plotted are the \log_2 ratios of single proteins. **a)** Analysis of all proteins of List 1. **b) – d)** Analysis of functional subclasses of proteins. Assignment was done using the DAVID bioinformatic database. **b)** Shown are proteins that belong to the GO-terms “Chromosome Organisation”, “Chromatin Modification” and “Chromatin Remodelling” (93, 38, 20 proteins respectively). **c)** Shown are all proteins that belong to the KEGG pathway “Proteasome” (35 proteins). **d)** Binding behaviour of proteins that have the molecular function “Ribonucleotide Binding” (193 proteins) and “ATP activity” (70 proteins).

Chromatin complexes show distinct binding behaviour during assembly

The STRING network (Figure 3.6) already indicated that many protein complexes are involved in the establishment and maintenance of chromatin. To further assess their binding behaviour the iBAQ values of both time points were \log_2 transformed and plotted as heat map (Figure 3.8, Appendix List 2: Chromatin-associated complexes).

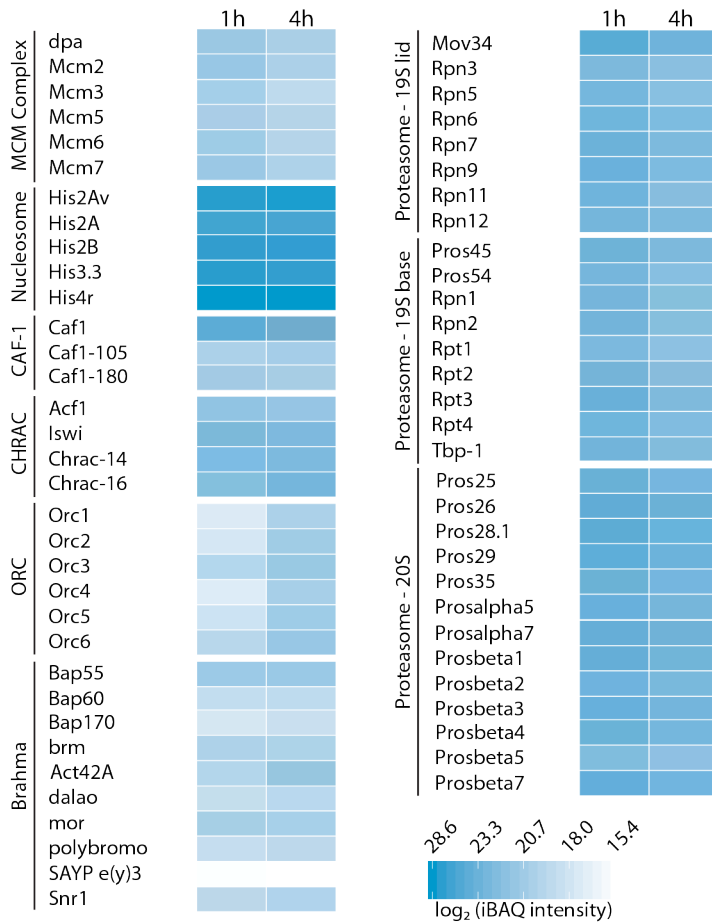


Figure 3.8: Protein binding of complexes during chromatin assembly

Heatmap displaying the relative abundance of chromatin-related complexes at early and late chromatin assembly time points. The highest and lowest log₂ values were taken as maximum and minimum to optimise visualisation. Abundant complexes are illustrated in dark blue, complexes with lower abundance are shown with pale blue squares. The figure further allows appreciating changes in abundance on chromatin of each subunit of the chosen complexes. Note: 20S Proteasome subunit alpha1 is not displayed, as it was not identified in the MS analysis. Corresponding log₂ values and standard deviations can be found in the Appendix, List 2: Chromatin-associated complexes.

Subunits of well-known chromatin-related complexes show similar binding characteristics in early and late chromatin assembly, confirming the accuracy of the obtained MS data. Additionally, the three subunits of the 26S proteasome are included as a previously performed bioinformatic analysis already indicated its link to chromatin assembly (Figure 3.5). The representation further allows the extraction of information about the relative abundance of the displayed complexes to each other. The histone proteins have the highest iBAQ values and can therefore be considered as being the most abundant proteins associated to chromatin. This is in agreement with what is known as histones occupy roughly every 170 bp of the DNA used in this study. The proteasome subunits also belong to group of proteins, which numerously bind to chromatin. On the opposite the MCM Complex was only identified with low iBAQ values suggesting a minor role of this complex in assembly and maintenance of chromatin.

Similar to the waterfall plot in Figure 3.7 a) the binding behaviour of complexes during assembly can also be assessed from Figure 3.8. Whereas the origin recognition complex shows clear binding preferences towards matured chromatin, all other complexes seem to either bind stronger to early assembled chromatin or bind similar to both analysed time points. Figure 3.9 shows the binding of three ORC subunits to chromatin over the assembly time of four hours. Elevated binding was observed for all three subunits, confirming the results of the proteomic MS analysis.

3. RESULTS

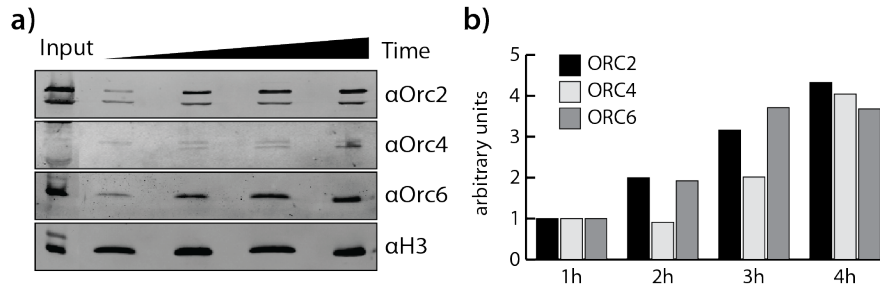


Figure 3.9: Binding of the origin recognition complex changes during assembly

a) Western Blot evaluating the binding of the origin recognition complex to chromatin during assembly. Empty lanes were cut for presentation purposes. b) Quantification of Western blot signal. All values were normalised to their corresponding H3 signal. The signal of the 1 h time point was set to 1 and all other values are plotted accordingly.

3.5 RNA is a structural component of chromatin in *Drosophila melanogaster*

The bioinformatics analysis of chromatin-bound proteins (Figure 3.7) revealed a considerable number of RNA-binding proteins. Proteomic analyses of assemblies that were performed during the first phase of method establishment and improvement already led to the conclusion that ribonucleic acids are a functional component of chromatin and also pointed to an involvement of RNA-binding proteins. This hypothesis gained further credence by findings from the group of Gernot Längst in Regensburg. They examined the effect of RNA depletion on chromatin structure. In their experiment, nuclei of *Drosophila* Schneider cells were permeabilised with 0.1% NP40, a concentration that does not change the cellular integrity (Stewart et al., 1991; Iborra et al., 2001). Chromatin was then treated with Ribonuclease (RNase) to hydrolyse cellular RNA and probed for its accessibility to MNase. The accessibility of cellular chromatin to the endonuclease correlates with the depletion of RNA, seen by the disappearance of smaller DNA fragments simultaneously to the decrease of RNA (Figure 3.10 a) and b)), performed by Thomas Schubert). Increasing concentrations of MNase in turn generate shorter fragments of DNA implicating that chromatin goes over into a higher order structure, in which nucleosomes are kept in regular arrays (Figure 3.10 c)), performed by Thomas Schubert). Taken together these results suggest a structural role of RNA in chromatin structure *in vivo*.

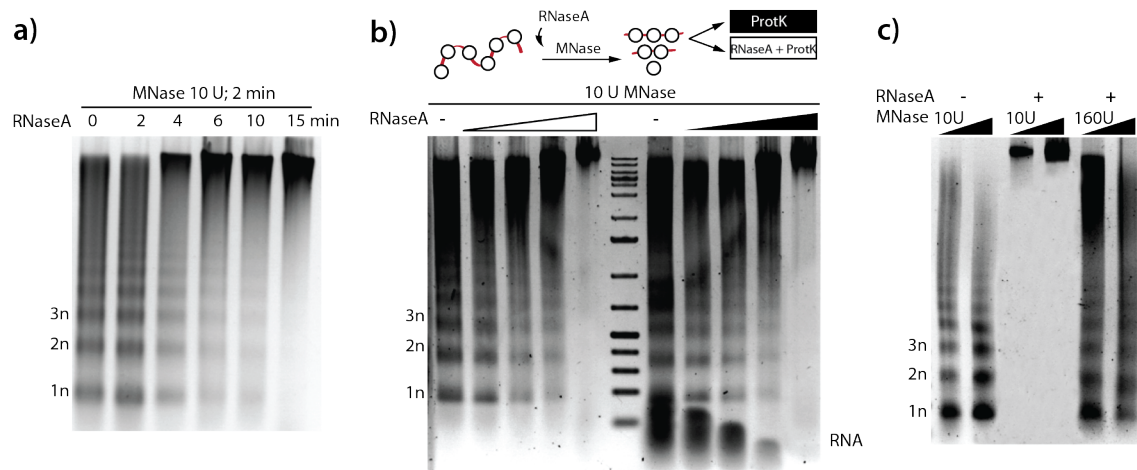


Figure 3.10: RNA influences chromatin accessibility in *Drosophila* cells

a) RNase-dependent kinetics of chromatin accessibility *in vivo*. Permeabilised *Drosophila* cells were treated with 150 µg/ml RNase A for 0 to 15 min and afterwards incubated with 10 U MNase for 2 min. The purified DNA was then analysed by agarose gel electrophoresis. **b)** Chromatin compaction correlates with the loss of RNA. S2 cells were incubated with increasing amount of RNase A 10 to 50 µg/ml for 5 min and then subjected to an MNase accessibility assay with 10 U enzyme for 2 min. Samples were split in half and depleted for either protein alone (black) or protein and RNA (white). **c)** S2 cells were treated with or without RNase A. Chromatin was then hydrolysed with two different amounts of MNase (10 U and 160 U). Experiments performed by Thomas Schubert (Figure adapted from Schubert et al., 2012).

3.6 *In vitro* reconstituted chromatin recapitulates the RNA-dependent accessibility of chromatin

The *Drosophila* embryo extract used in this study contains amongst all the proteins needed for chromatin assembly high levels of RNA. This circumstance makes it an optimal tool to study the mechanism of RNaseA-dependent chromatin compaction *in vitro*. Incubation of plasmid DNA with the extract led to efficient assembly (Figure 3.11, performed by Thomas Schubert). Similar to what was observed *in vivo* the addition of increasing amounts of RNase prior to the accessibility assay resulted in a compaction of the chromatin structure as indicated by a disappearance of smaller nucleosomal fragments. Again, this compaction follows the depletion of RNAs. Furthermore, by increasing the MNase concentration 16 fold, it was possible to obtain a similar digestion degree as observed without RNase A treatment. This argues against a non-specific aggregation of the DNA and proves that *in vitro* assembled nucleosomes are regularly spaced even in the compacted chromatin form.

3. RESULTS

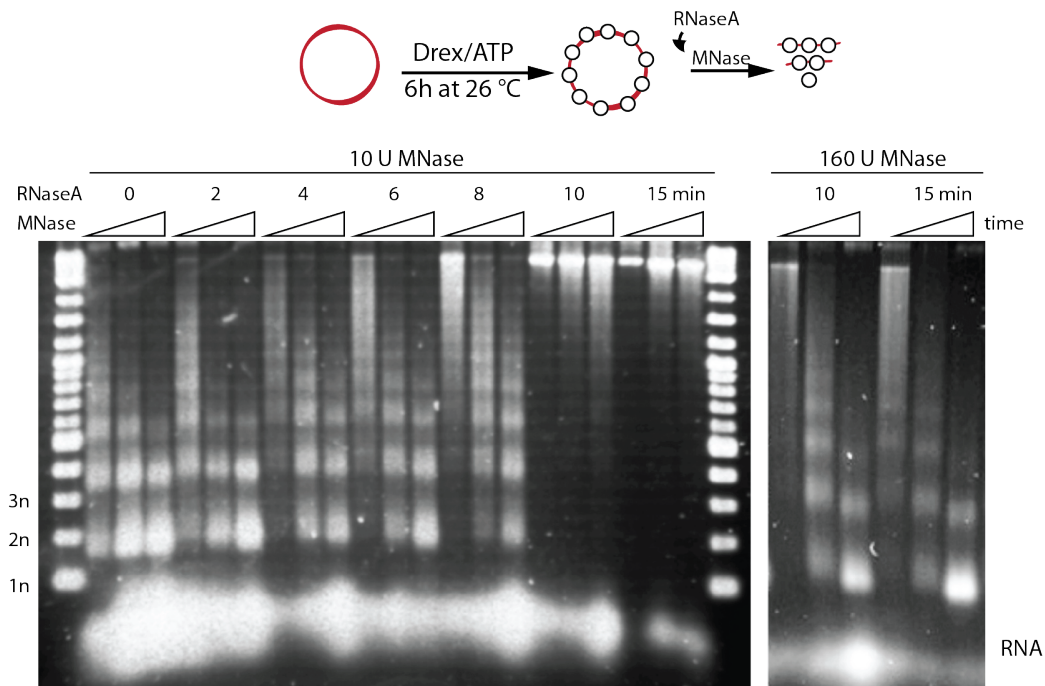


Figure 3.11: Effects of RNA on *in vitro* assembled chromatin resemble those *in vivo*

In vitro reconstituted chromatin was depleted from associated RNAs for the indicated time points and subsequently incubated with 10 U of MNase for 30 s to 3 min. Proteins were digested with Proteinase K and DNA as well as RNA were visualized on an agarose gel. Additionally, chromatin fractions that were incubated for 10 and 15 min with RNase A were subjected to a higher dose of MNase (160 U). Experiments performed by Thomas Schubert (Figure adapted from Schubert et al., 2012).

3.7 Chromatin accessibility is regulated by snoRNAs

Chromatin-interacting RNAs were further analysed by the group of Gernot Längst by high throughput sequencing. RNAs isolated from chromatin fibres that were purified by density gradient centrifugation were used for library preparation and subsequent sequencing on the Illumina platform (accession number on the ArrayExpress database: E-MTAB-1237; Schubert et al., 2012). A reference file was created from the embryonic transcriptome of *Drosophila melanogaster* and fold-enrichments of chromatin-associated RNA fractions were calculated in comparison to it. Annotation and quantification of the transcripts revealed that the chromatin-associated RNAs (caRNAs) constitute a small but highly specific subset of the total RNA pool. Non-coding RNA species were enriched approximately 3 fold in the caRNA fraction whereas protein-coding transcripts showed no enrichment (Schubert et al., 2012). Surprisingly, the most enriched fraction comprised a subset of small nucleolar RNA (snoRNA) (Figure 3.12, performed by Thomas Schubert). Those RNAs are primarily known to guide chemical modifications of other RNA species, such as ribosomal RNAs. 30 out of 186 snoRNAs present in the embryonic *Drosophila* transcriptome were enriched more than 10 fold on chromatin. The highest enriched snoRNAs showed an enrichment factor of over 100, like the snoRNAs Me28S-U214b and Me28S-G980. Notably, there is a negative correlation between the abundance of ncRNA in

the embryonic extract and their enrichment on chromatin. The association of low abundant snoRNAs with chromatin suggests that their binding to chromatin is highly specific (Schubert et al., 2012).

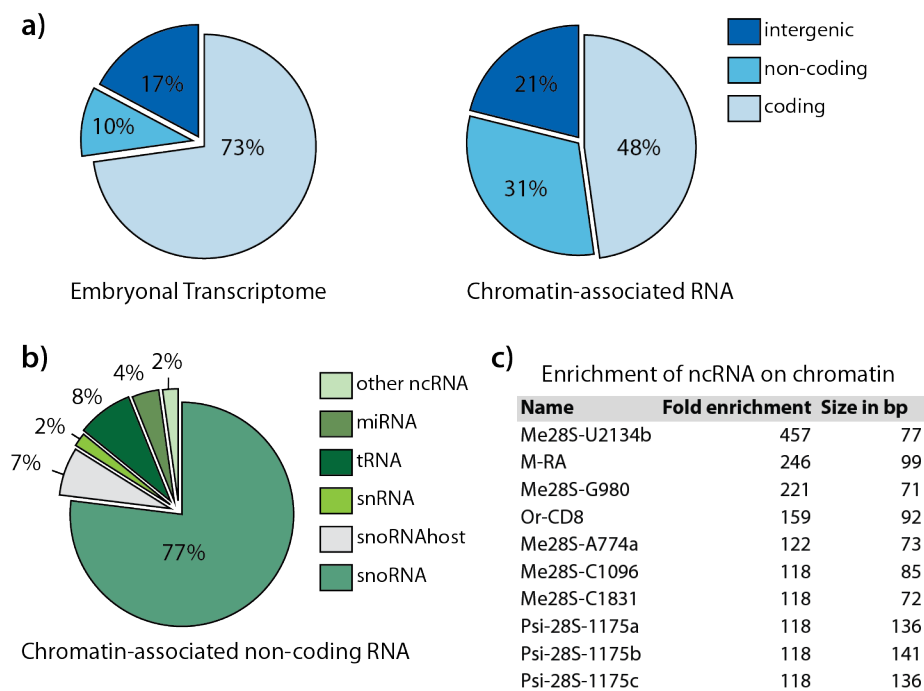


Figure 3.12: Characterisation of chromatin-associated RNAs

a) Shown is the analysis of RNA deep sequencing data from RNAs derived from embryonic extract and from the pool of chromatin-associated RNAs. **b)** A detailed analysis of the ncRNA fraction of the caRNAs revealed different subgroups with snoRNAs comprising the biggest class. **c)** Table showing the most enriched ncRNAs within the data set of caRNA. Fold-enrichments were calculated using the abundance of RNAs in the embryonal transcriptome as reference. Experiments performed by Thomas Schubert and Sarah Diermeier (Figure adapted from Schubert et al., 2012).

3.8 Decondensation factor 31 is involved in chromatin opening

To investigate if the structural changes of chromatin also involve proteins, chromatin-bound proteins were analysed in presence or absence of RNA. Linearized and biotinylated DNA was prepared for assembly as described above. Reconstitution was performed for the duration of six hours, a time point at which chromatin assembly and maturation is completed (Scharf et al., 2009). Unbound proteins were washed away and chromatin was subjected to an RNase A digest or mock treated for additional two hours. Chromatin-bound proteins were then separated via SDS-PAGE and analysed by LC-MS/MS. A representative gel is shown in Figure 3.13. Label-free quantitative analysis using the Proteome Discoverer software (Thermo Scientific) revealed a total number of 158 proteins. Of those, 59 had a lower affinity to RNase A treated chromatin whereas 15 proteins showed an enriched binding upon RNA depletion (Figure 3.13 c)), complete protein list can be found in the Appendix List 3: RNA-dependent protein binding). As the depletion of RNA caused mainly a decreased binding of

3. RESULTS

proteins, all 59 proteins were further investigated. Ten of those proteins had been shown to bind RNA *in vitro* but there was no described RNA-binding domain for the other 49 proteins.

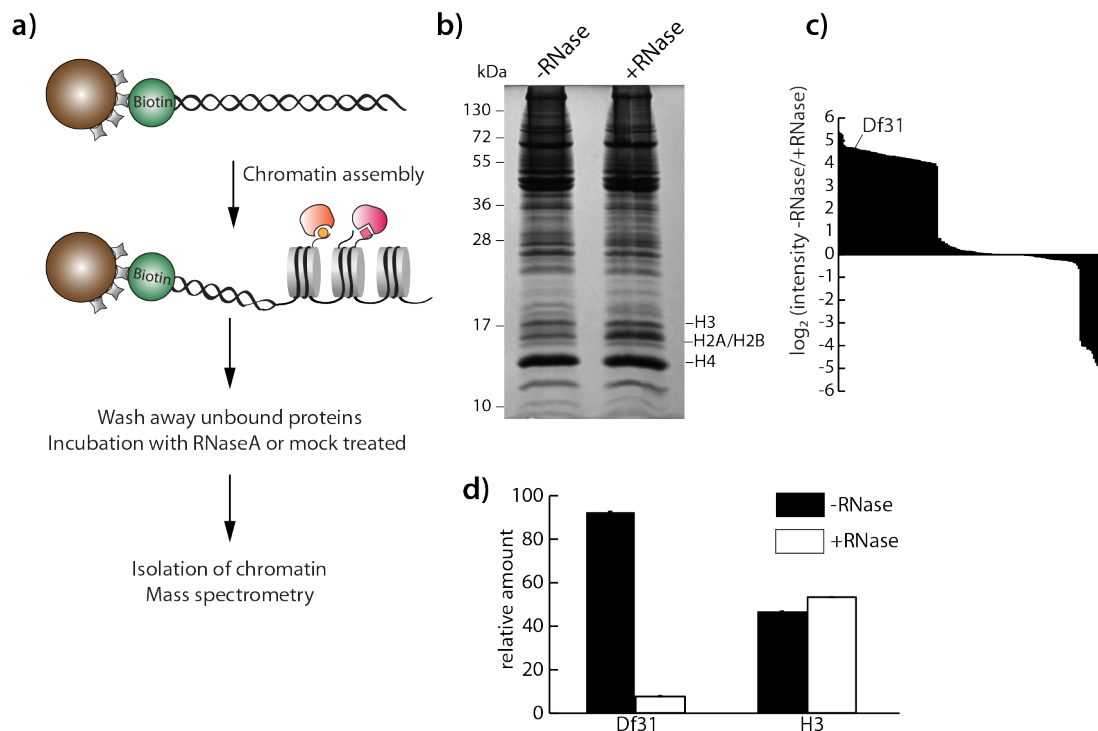


Figure 3.13: Quantitative analysis of RNA associated with accessible and inaccessible chromatin

a) Biotinylated DNA was immobilised on magnetic beads and chromatin was fully assembled. Unbound beads were washed away and depleted from associated RNAs. Chromatin-bound proteins of both samples were separated via SDS gel-electrophoreses and subjected to an in-gel tryptic digest with subsequent LC-MS/MS identification. **b)** Coomassie-stained gel showing representative samples of chromatin-associated proteins in presence or absence of RNA. **c)** Waterfall plot shows the \log_2 fold change of protein association with or without caRNAs. Protein identification and quantification was performed using the Proteome Discoverer software. Only proteins that were identified by at least two unique peptides are shown. **d)** Quantification of Df31 and H3 was done using the ion chromatograms of the peptides 17–26, 29–39 and 40–55 for Df31 and 41–49 and 54–63 for H3. The relative ratio of the respective protein intensity comparing RNase A-treated (+RNase) and mock-treated samples (-RNase) is displayed. Data represent the mean \pm SD for two independent experiments.

One factor with reduced affinity to RNA-depleted chromatin is the protein Decondensation factor 31 (Df31) (Figure 3.13). Df31 was first identified to play a role in *Drosophila* sperm compaction (Crevel and Cotterill, 1995). It is an abundant protein and was described to be involved in the formation of higher order structures *in vivo* (Crevel et al., 2001). The exact mechanisms however remained unclear. Systematic localisation mapping via Dam-ID determined Df31 as preferential binding factor of Red and Yellow chromatin regions which represent euchromatic regions in *Drosophila* (Filion et al., 2010). Those characteristic traits made Df31 a good candidate, which could be involved in the observed RNA-dependent chromatin accessibility.

3.9 Df31 is a chromatin and RNA-binding protein

Df31 was already described as histone chaperone specific for histone H3, with a binding affinity towards the N-terminal tail (Guillebault and Cotterill, 2007). Microscale thermophoresis experiments using fluorescently labelled snoRNAs further proved that Df31 exhibits an RNA-binding ability *in vitro* (Schubert et al., 2012).

To proceed in the functional characterisation of Df31, monoclonal antibodies were produced in close collaboration with the group of Dr. Elisabeth Kremmer at the Institute of Molecular Immunology at the Helmholtz Centre in Munich. Df31-His was bacterially expressed, purified and used for immunisation of rats (expression and purification performed by Thomas Schubert). Prescreening in an enzyme-linked immunosorbent assay (ELISA) yielded 20 positive clones whose specificity was further tested in different applications (see under “Df31 antibody screening”, Materials and Methods). Recloned and expanded antibodies were then used in the following experiments.

To assess whether Df31 can also directly bind to the identified caRNA species *in vivo*, Df31 was immunoprecipitated from embryonic extracts using an antibody against the endogenous protein and an antibody against HA as negative control. The associated RNAs were purified and reverse transcribed to complementary DNA (cDNA). The cDNA was then used in a Reverse Transcription PCR (RT-PCR) with specific primers for snoRNA U2134b and G980. Both snoRNAs could be co-purified with an anti-Df31 antibody but not with the nonspecific control antibody suggesting that Df31 can also interact with snoRNAs *in vivo* (Figure 3.14).

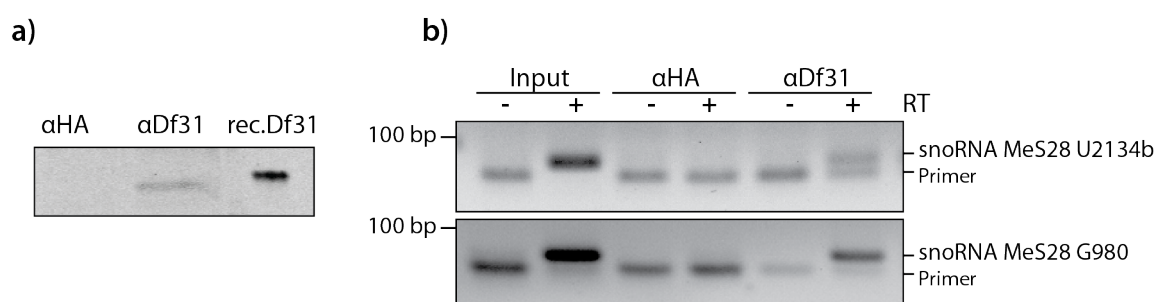


Figure 3.14: Df31 can bind to caRNA *in vivo*.

a) Df31 was immunoprecipitated from a *Drosophila* embryonic extract. As control an HA antibody was used. Proteins were analysed by western blotting using a Df31 specific antibody. **b)** Df31 associated RNAs were isolated via TRIzol extraction, reverse transcribed and used as template in a PCR reaction. For this, primers of two abundant RNAs were used. The positions of specific amplification products and primer excess are indicated.

3. RESULTS

3.10 Df31 and snoRNA both act on euchromatic regions *in vivo*

Df31 localises to euchromatic regions across the genome and is associated to caRNAs. To further demonstrate their activity in euchromatic regions, binding of two abundant snoRNAs to chromatin was assayed by RNA FISH on polytene chromosomes. SnoRNA sequences were cloned into the pCS2+ Vector and transcribed from the linearized template using the SP6 polymerase and a nucleotide labelling mix with Digoxigenin-UTP. SnoRNAs abundantly localised to the nucleolus, the cellular compartment in which they are transcribed and known to function. Additionally, both snoRNAs localise to the interbands of polytene chromosomes, regions of low chromatin compaction and active transcription (Figure 3.15). This novel localisation of snoRNAs supports their important role in the maintenance of euchromatin structure.

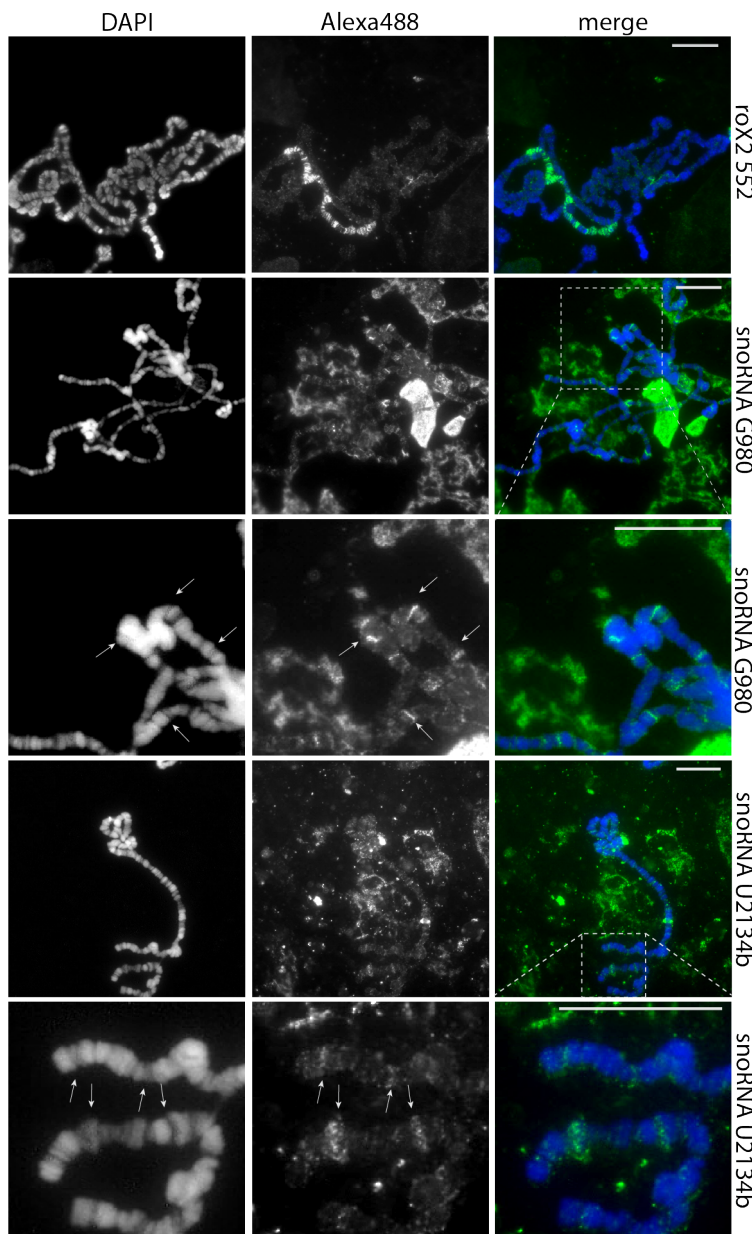


Figure 3.15: SnoRNAs localise to euchromatic regions on polytene chromosomes.

RNA fluorescence in situ hybridization was performed with two different snoRNA probes and the roX2 RNA as control. Left panel shows DAPI dense regions on the polytene chromosome. Middle panel indicates the binding of the RNA probes (Alexa488). Whereas the roX2 antisense probe only binds to the X chromosome, snoRNA antisense probes cover the nucleolus and the interbands of polytene chromosomes. Right panel shows an overlay of both channels and emphasizes the interband binding of snoRNA G980 and U2134b. Two magnifications of both snoRNA hybridizations are shown as indicated in the merge picture (dotted line). Arrows point towards interbands of polytene chromosomes. Scalebar 20 μm .

3.11 Df31 interactome

Df31 and snoRNAs are associated in a ribonucleoprotein. Still, further interaction partners could contribute to the maintenance of chromatin structure. To identify potential binding partners, the interactome of Df31 was analysed by co-immunoprecipitation (Co-IP). For this, a stable transgenic fly cell line was established expressing Flag- and HA-tagged Df31 under the control of an inducible promoter. Localisation of Df31 was assayed by immunofluorescence to confirm that the localisation of the transgenic protein equals the endogenous protein localisation (Figure 3.16).

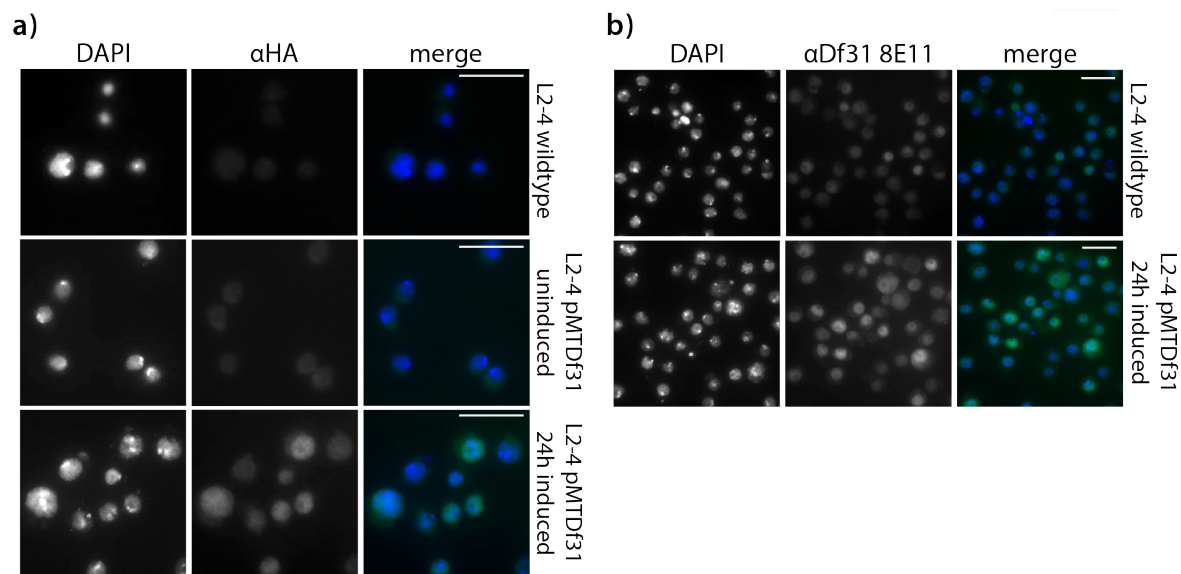


Figure 3.16: Immunofluorescence analysis of Df31 localisation in wildtype and transgenic Schneider cells.

a) and **b)** Localisation of transgenic and endogenous Df31 was analysed using an HA **(a)** or a Df31 specific antibody **(b)**, respectively. Transgene expression was induced by addition of copper sulphate 24 hours before harvesting. Scalebar 20 μm .

A Flag-immunoprecipitation was performed from nuclear extract prepared from cells with induced expression of Df31 and wildtype Schneider cells. Df31 and its interacting proteins as well as the proteins in the negative control were eluted from the beads by boiling in SDS Sample buffer and separated via SDS-PAGE (Figure 3.17). LC-MS/MS and a computational analysis with the MaxQuant software were performed for identification and quantification of proteins. The average of the iBAQ intensities of three independent replicates was taken and the \log_2 fold enrichment of all proteins over the control was calculated. As expected Df31 was the top hit with an enrichment factor of 27 (iBAQ enrichment: $\sim 170 \times 10^6$ fold). In addition, 318 proteins with an enrichment factor over five were considered as potential interaction partners of Df31. DAVID was used to perform a functional annotation and select candidate proteins. Figure 3.17 d) shows a selection of Df31's interaction partners and their assignment to functional groups. Among the 318 proteins, over 10% exhibit a

3. RESULTS

function in positive regulation of transcription, such as the Taf subunits and Tbp, components of the TBP/TAF-Complex. A similar analysis was performed in the lab of Artavanis-Tsakonas (Guruharsha et al., 2011). They generated a large-scale *Drosophila* Protein interaction Map (DPiM) by performing 3500 coaffinity purifications of FLAG-HA tagged *Drosophila* proteins. Associated proteins were identified by mass spectrometry and potential interaction partners determined via a semi-quantitative statistical approach. This analysis led to the identification of 290 Df31-associating proteins of which 175 were also identified in the present study. 105 of those proteins were enriched in the Df31 pulldowns, 37 more than five fold over the control IP. Among those proteins were AGO1, Stonewall (stwl) and CG2982, encoding the histone demethylase No66, that interact with Df31 either directly or as part of a highly interactive network in case of Stonewall (shown in a follow-up study by Rohrbaugh et al., 2013).

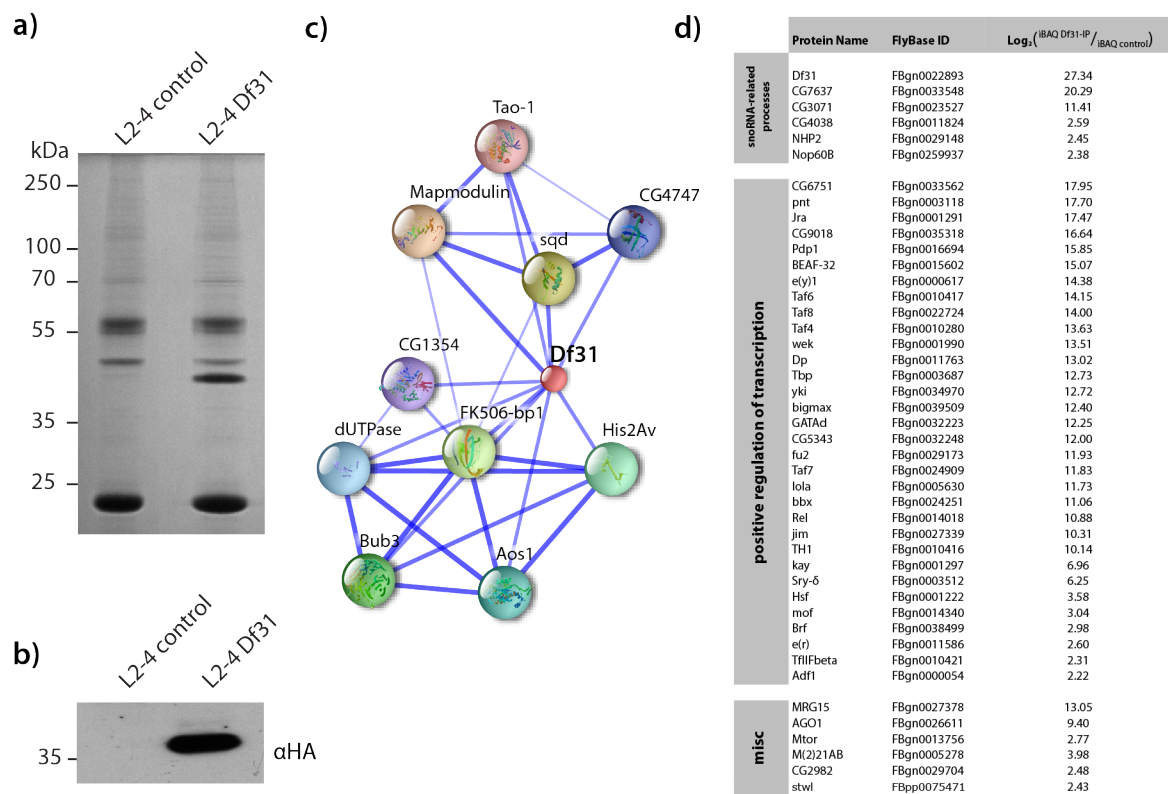


Figure 3.17: Analysis of the Df31 interactome.

a) Representative gel of a Flag purification performed with nuclear extract from Df31 expressing cells and a control cell line. **b)** Western Blot confirming the presence of HA-FLAG tagged Df31 in the Df31 IP. **c)** STRING network showing the predicted functional partners of Df31. **d)** Table shows a chosen selection of the identified Df31 interaction partners. Proteins were grouped according to their function or the process they are involved in.

So far unknown interaction partners are the proteins CG3071, CG4038 and NHP2, which supposedly associate with snRNAs analogue to Df31. The STRING network in Figure 3.17 c) displays the predicted functional partners of Df31 that were identified by different means. The results from

Guruharsha et al. are not included into this network. From the STRING interaction partners only sqd, FK506-bp1, Bub3, His2Av and CG4747 were identified in the present analysis. From those proteins only Bub3 and His2Av were enriched in the Df31 IP (1.8 and 4.8 times over control IP). Df31 resides mainly in euchromatic regions (Filion et al., 2010). This is in accordance with the identified interaction partners, including many proteins with link to positive regulation in transcription. In addition, the interactome of Df31 relates back to its role as RNP with other protein-RNA complexes such as NHP2 being present. Whether those other RNPs act in a similar fashion to the Df31-RNP remains to be answered.

3. RESULTS

4. DISCUSSION

4. DISCUSSION

4.1 Towards a detailed temporal proteomic analysis of chromatin assembly

The coalescence of a well-described *in vitro* chromatin reconstitution system and the technology of quantitative proteomics allowed the fast and detailed analysis and temporal dissection of the process of chromatin assembly. This study was aimed to provide a proof of principle of the method and generate first proteomic data on the process of stepwise chromatin assembly. The analysis of two time points led to the identification of distinct protein complexes at specific time points during assembly. With the help of open source databases it was possible to characterise and group the identified proteins according to their biological function, binding domains and the pathways they are involved in and thus provide a detailed picture of early and late steps during chromatin assembly.

4.2 Reproducibility of the system and future improvements

In quantitative proteomics it is important to be aware of the effect of experimental variation. Errors in quantitation are introduced during various steps in the sample preparation and in the mass spectrometric analysis of it. Whereas the latter is usually caused by the instrument itself, errors in sample preparation can be minimized by e.g. preparing replicates in the very same set of experiments. In the present study the reproducibility of three independent replicates yielded a robust identification of 900 proteins with a total overlap of ~60%. Replicate 2 and replicate 3, prepared in parallel and analysed consecutively, showed an even higher overlap of over 73% in the early assembly and 82% in the late assembly time point (Figure 3.4).

Many studies aim to investigate the variation in sample preparation for comparative proteomics (Wang et al., 2003; Higgs et al., 2005; Old et al., 2005; Wang et al., 2006). Often those studies neglect the actual variation among samples by focussing on those analyses that provide the smallest deviation. Although mass spectrometry-based proteomics is now well established in all kind of research fields, comparable studies are seldom.

The reproducibility of the present *in vitro* chromatin assembly system is within the variation, which was observed by other labs. In a SILAC (stable isotope labelling by amino acid in cell culture) based approach by the Neubert lab, the relative standard deviation of an anti-phosphotyrosine (pY) IP from NG108 cell lysates (mouse neuroblastoma and rat glioma hybrid) was calculated to be quite low (0.080) (Zhang et al., 2009). In contrast, the overall overlap of identified proteins in all replicates was ~50%, with a maximum of 70% overlap when comparing two replicates (Zhang et al., 2009) (comparison of supplementary data). Other studies report median coefficients of variation of around 26% for peak intensity ratios in proteome analysis (Wang et al., 2003). Reproducibility in label-free quantitative proteomics is thus a crucial issue and the development and improvement of technology in

this field an active research area. The *in vitro* chromatin assembly system presented in this study works with a protein extract made out of *Drosophila* embryos. Therefore, a certain variation is expected due to its biological background.

LC-MS/MS is still the most accurate method for large-scale relative protein quantitation. Hence, improvement in accuracy can more easily be achieved in the steps prior to sample measurement. One major step in mass spec sample preparation is the enzymatic protein digestion, which is either performed as in-gel or as in-solution digestion. In-gel tryptic digestion involves running of an SDS-PAGE, dicing of gel slices, extensive destaining and washing, and peptide extraction after digestion. At all those steps loss of material can occur by unequal sample loading and/or inefficient extraction. Division of one sample into several fractions reduces the complexity, which facilitates peptide identification but introduces variability at the same time. Advantages of in-gel tryptic digestion include that it provides information about the observed proteins. Having a visual output can help to get a first idea of the experimental outcome. Furthermore, contaminations that might occur are unlikely to interfere with the digestion as it takes place inside the gel pieces. In-solution digestion is a detergent-free method in which proteins are extracted with strong chaotropic reagents such as urea. Proteins are then precipitated and digestion is performed under denaturing conditions. Sample recovery is reported to be more efficient as in in-gel digestion, as little or no protein is lost during preparation (Wiśniewski et al., 2009). However, depending on the constitution of the solution additional clean-up steps may be necessary before analysing the sample.

A recent technique, called FASP (filter-aided sample preparation), combines the advantages of both sample preparation methods (Wiśniewski et al., 2009). In FASP, the sample is solubilized in SDS and further retained and concentrated in an ultrafiltration device, which helps to remove detergents and exchange buffers. This technique allows an increase in sample volume, which will have a beneficial effect on the elution efficiency in the presented chromatin assembly method. Samples are not fractionated and all steps are performed in solution, which will decrease variability. On the other hand the missing fractionation can reduce the number of proteins identified as more proteins elute at the same time. To counteract the risk of low protein identification, a pre-fractionation of peptides could be an optional step to include in the protocol. With FASP the time demand of individual experiments can be substantially decreased, even with pre-fractionation, as only one analytic LC-MS/MS run is needed which minimizes the total analysis time. Especially in light of the many replicates which are needed to perform proper bioinformatics analysis this is an advantage.

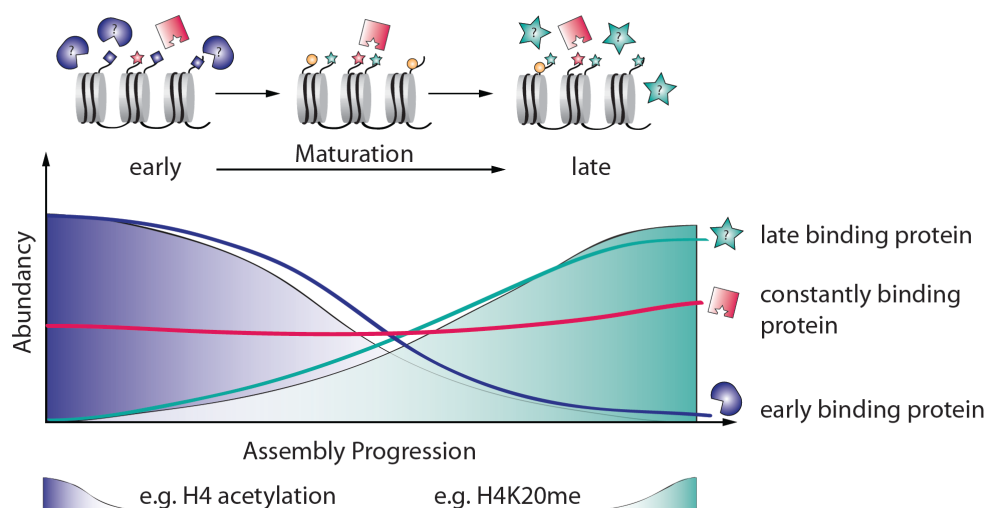
A drawback of the FASP method is the simultaneous analysis of histones and non-histone proteins. Trypsin, the protease commonly used in MS, cleaves proteins after lysine and arginine. Especially in

4. DISCUSSION

histone tails, those amino acids are quite abundant, leading to very short fragments in a trypsin digestion, which are inefficiently analysed by MS. Therefore histones are usually treated with propionic anhydride, which blocks lysines from tryptic cleavage. This step cannot be included into FASP if proteomic samples shall be investigated at the same time. Histones therefore have to be analysed separately. To obtain a complete picture of chromatin maturation it is important to also include the presence of histone modifications to the analysis and to observe their changes over time. Additionally, elution efficiency can vary between individual samples (Figure 3.2 c)). As the method works with label-free quantification a normalisation step is advisable and histones are the most suited proteins to normalise to. Although the analysis of unmodified histone peptides is an adequate option, evaluating all present histone peptides would improve the quantification.

The continuous improvement of accuracy and sensitivity in mass spectrometry and proteomic sample preparation will enable a fast analysis of biological replicates and their assessment by statistical tools. An advance in MS-based experiments can already be extracted from the proteomic results presented in this work. Whereas the analysis of RNA-dependent protein binding revealed a total number of 158 proteins (Appendix List 3), later proteomic experiments that were performed to investigate protein kinetics (Appendix List 1) yielded over 1000 proteins. This discrepancy can be explained by two main reasons: one is probably due to a slightly different experimental setup. In the screen for RNA-dependent protein binding, chromatin was assembled for six hours, washed and then incubated in EX100 with or without RNase A. In comparison to the analysis of protein kinetics this additional incubation step probably led to a removal of proteins also independent of RNA depletion. A second reason is the proceeding improvement in mass spectrometry. The experiments that led to the identification of Df31 were performed while the method for analysing the binding kinetics was still under improvement. The data of chromatin dynamics presented in this thesis were obtained at a time when mass spectrometry was already more sensitive and accurate. Additionally, new software tools were available that were especially designed for protein identification and label-free quantification.

Already now proteomic mass spectrometry has reached a level, which enables a detailed, quantitative analysis of protein kinetics during assembly. The results obtained from the presented study allow the estimation of the dependency of chromatin-associated proteins on histone modifications and between each other (Figure 4.1). Future findings will add to this work.



4.1: Model of chromatin-associated protein binding

Mass spectrometry-based proteomics of *in vitro* assembled chromatin enables the evaluation of protein binding dependent on histone modifications and on other sets of proteins.

A recent advance is the use of iBAQ values as tool for stoichiometric calculation of protein complexes in label-free quantitative proteomics (Smits et al., 2012). This technique can also be implemented in the present study, however with limitations. From Figure 3.8 it can be inferred that histones are the most prominent chromatin-associated proteins. The three proteasomal complexes are moderately abundant in comparison to other complexes which was also confirmed by the DAVID enrichment analysis (Figure 3.5). For the proteomic analysis of protein binding kinetics in this study 4 μg of DNA were used. This roughly equals a molecular weight of 2.4×10^{18} Dalton, which in turn equals the amount of 3.65×10^{15} bp. In the *in vitro* assembled chromatin, DNA is occupied by an octamer of histones every 170 to 180 bp. This assumption leads to a value of 2.0×10^{13} histones. From this a rough estimation of the amount of molecules of chromatin-binding proteins can be calculated (Figure 4.2). As example the number of molecules for the proteasome, the origin recognition complex and the histone chaperone CAF-1 are presented below. To simplify and as values were in the same magnitude, number of molecules were calculated from the mean value of all subunits for the proteasome and ORC. For the CAF-1 complex one of the subunits was remarkably more abundant than the other two subunits. This points towards a role of Caf1 (p55) in other protein complexes as well, e.g. in the NURF complex. It is important to keep in mind, that binding and elution efficiency of DNA is rarely achieved to a 100%. In addition, MS measurements were performed using only a fraction of the sample. Thus, the calculated values are only a rough estimation of the actual state. A further advance in accuracy in the present method will allow a more precise evaluation of the relative abundance of chromatin-associated proteins and complexes and the efficient discrimination of different interactions of the same subunit, e.g. p55.

4. DISCUSSION

	1 h	4 h
Histone Octamer	2.0E+13	2.0E+13
Proteasome 19S lid	3.1E+12	1.4E+12
Proteasome 19S base	2.6E+12	1.1E+12
Proteasome 20S	4.0E+12	2.2E+12
ORC	8.7E+10	3.1E+11
Caf1	5.6E+12	4.0E+12
Caf1-180	3.7E+11	2.6E+11
Caf1-105	2.2E+11	2.5E+11

Figure 4.2: Estimation of the relative abundance of histone octamers and chromatin-associated proteins in number of molecules.

Numbers of molecules were calculated based on the theoretical abundance of histones and the respective iBAQ values. Mean values were taken for the proteasome subunits 19S lid, 19S base and 20S and the origin recognition complex.

4.3 Ubiquitination in chromatin assembly and regulation

Among the chromatin-associated proteins identified were not only proteins, which were previously linked to chromatin-based processes but also proteins with so far unknown function in chromatin assembly. The enrichment analysis of KEGG pathways and InterPro domains identified for both time points proteins with a strong link to the proteasome suggesting that ubiquitination and proteolysis are important steps in chromatin assembly (Figure 3.5). Histones have long been described to be targets of ubiquitination. The conjugation of this modification involves an enzymatic cascade comprising an activating enzyme E1, a conjugating enzyme E2 and an ubiquitin ligase E3. The concerted action of all three enzymes results in the ubiquitin transfer to lysine residues on the protein substrate via an isopeptide bond or to the amino group of the N-terminus via a peptide bond (Komander and Rape, 2012). Although found on only very few residues, ubiquitination is linked to chromatin regulation. H2A monoubiquitylation is associated with silencing of the Hox gene cluster in mammals (Endoh et al., 2012). Ubiquitination of H2B has emerged as important modification during RNA Pol II transcription (Weake and Workman, 2008). Furthermore, cycles of ubiquitination and deubiquitination were shown to regulate gene expression by stabilizing the elongating Pol II (Henry, 2003; Osley et al., 2006). Recent findings now also connect ubiquitination and chromatin replication. In budding yeast, ubiquitination of H2B seems to facilitate the assembly and stability of nucleosomes on newly replicated DNA. In this way the modification contributes to replication fork progression (Trujillo and Osley, 2012). Additionally, H2Bub is required for H3K4 and K79 methylation (Sun and Allis, 2002; Nakanishi et al., 2009). Ubiquitination of H3 by Rtt101 regulates replication-coupled nucleosome deposition via weakening the interaction to Asf1. The transfer to other histone chaperones is thereby facilitated (Han et al., 2013). A similar mechanism was also found in human cells, where the E3 ligase Cul4A-Ddb1 is involved (Han et al., 2013). Ubiquitination by Cul4A-Ddb1 in *Schizosaccharomyces pombe* has also been linked to proper heterochromatin formation. Its action leads to proteasomal degradation of the protein Epe1 thereby restricting its presence to heterochromatic boundaries (Braun et al., 2011). In human, polyubiquitination of the largest ORC subunit, ORC1p, by SCF_{Skp2} results in

its degradation and provides a mechanism for cell-cycle-dependent oscillating protein concentrations (Méndez et al., 2002). Taken together, those data suggest that proteasomal degradation is an important mechanism that regulates the abundance of specific chromatin factors and avoids the spreading of inappropriate chromatin features. The relative abundance of proteins on early chromatin was higher compared to the later time point (Figure 3.7 a)). Also the proteasome was already abundant on early chromatin (Figure 3.6 c)). This correlation could indicate that the proteasome is involved in the degradation of early binding proteins and serves as means of shaping chromatin structure. If this is the case and how this regulation functions in a genomic context needs to be experimentally addressed in the future.

4.4 Chromatin-associated proteins and their interactions

The STRING network nicely illustrates the high degree of connections among chromatin-binding proteins (Figure 3.6). As STRING only depicts known and predicted interactions not all proteins of the proteomic analysis are connected amongst each other. Some proteins build up sub-networks, which are not connected to the main network. Additional experiments will be needed to further prove a function in chromatin assembly of those proteins with low numbers of or not existing interaction partners.

Mass spectrometry allows the identification of large numbers of proteins and bioinformatics analysis are beneficial in understanding the meaning behind those large scale data. Still, some aspects of chromatin assembly and dynamics are still difficult to gather. Do proteins distribute equally on the assembling chromatin or do different types of chromatin exist? Is chromatin assembly a uniform process or are there chromatin states with characteristic binding patterns of proteins? Does the binding of some proteins mutually exclude binding of other proteins? Although many identified proteins in the proteomic analysis were shown to interact with each other this does not necessarily imply that they interact with each other during chromatin assembly. Those questions will be extremely difficult to answer using mass spectrometry. Other state of the art visual techniques might be helpful in approaching those questions. The technique of DNA combing already allows looking at single DNA fibres. Together with the fast development and improvement of high-resolution microscopy it could be possible to look at single fibres of assembling chromatin and determine their homogeneity.

The *in vitro* system presented here is limited with regards to the identifications of proteins. Only the kinetics of proteins present in the early embryo (90 min after egg deposition) can be investigated. Although this is a developmental stage of high replication and nucleosome assembly factors are present in abundance one can not dismiss the possibility that certain proteins playing a role during *in vivo* assembly are missing in the embryonic extracts.

4. DISCUSSION

4.5 Chromatin proteins and complexes show distinct kinetics

20% of all chromatin-associated proteins were found to preferentially bind to early chromatin (Figure 3.7 a)). This fraction of proteins cannot be assigned to a particular function or process during chromatin assembly. The analysis of subclasses of proteins revealed that proteins from all analysed classes show a similar binding pattern. A likely explanation for this observation is that during early steps of assembly, chromatin is more accessible and offers more potential binding sites for proteins. During assembly the chromatin structure adopts a higher order structure, which offers limited space for protein binding. Many proteins are known DNA binders. The high number of proteins at the early time point could therefore also result from unspecific binding of those proteins to DNA. After this initial binding of proteins, chromatin undergoes a systematic ordering and regulation of protein binding in which only necessary proteins are kept on chromatin. This process could also involve degradation, explaining the presence of proteasomal subunits at the onset of chromatin maturation.

One protein complex specifically favouring matured chromatin was the origin recognition complex. All six subunits of the complex were identified with higher intensities in the late chromatin fraction. A modification linked to the presence of the ORC complex is H2B ubiquitination. This modification is set by the ubiquitin ligase Bre1 (Hwang et al., 2003; Wood et al., 2003). Interestingly, Bre1 is one of the proteins found to bind more abundantly to early chromatin ($\log_2(\text{iBAQ}_{1\text{h}/4\text{h}}) = 12.9$). The presence of Bre1 during early steps of chromatin assembly could involve ubiquitination of H2B, which in turn stabilizes the new deposited nucleosomes. In this way H2B ubiquitination levels could contribute to chromatin stability thereby regulating binding of the origin recognition complex.

Earlier studies using this assembly system could show that the maturation of chromatin is linked to an increase in monomethylation of H4K20 (Scharf et al., 2009). Interestingly, certain subunits of the ORC complex favour a distinct methylation status. ORC2 and 3 were shown to co-purify with the repressive histone marks H4K20me3 and H3K9me (Chan and Zhang 2012). Although the ORC complex is known to be involved in initiation of DNA replication, ORC2 and other components of the complex are also needed for heterochromatin maintenance in mice (Chan and Zhang, 2012). Additionally, the BAH domain of ORC1 binds to H4K20me2 and with a slightly weaker affinity to H4K20 mono- and trimethylation in various organisms (Kuo et al., 2013). ORC1 is an evolutionary conserved protein and its bromo adjacent homology (BAH) domain a common property in diverse metazoans. It has been postulated that the BAH domain is important for loading and stabilization of the ORC complex onto chromatin in human cells (Noguchi et al., 2006). Chromatin-association of ORC components is compromised in cells expressing an ORC1 mutant lacking the ability to bind H4K20me2 (Kuo et al., 2013). H4K20 monomethylation, set by Pr-Set7, is assumed to serve as template for the Su(var) enzymes which catalyse H4K20 di- and trimethylation (Schotta et al., 2008;

Oda et al., 2009). However, both modifications were not detectable in the present *in vitro* assembly system (Scharf et al., 2009). ORC could still be targeted to the chromatin via the affinity of ORC1 towards H4K20me. This in turn could lead to the assembly of the other ORC components. To substantiate this hypothesis one could interfere the assembly reaction by the addition of S-adenosylhomocysteine, an inhibitor of methyltransferases. The absence of methylation on H4 should lead to decreased binding of the origin recognition complex. As ORC has a natural affinity towards DNA by itself, binding should not be completely abolished but the difference in binding between early and late chromatin should be negligible.

It is important to understand the dynamics of histone modifications throughout chromatin assembly and the way they regulate binding of proteins and adjust their abundance. *In vivo* monomethylation as well as dimethylation are regulatory modifications that seem to be dynamic throughout the cell cycle. A study in HeLa cells investigating combinatorial modification patterns of H4 during cell cycle, described an increase of monomethylation during G1/S to S/G2 phase and a decrease of mono- and dimethylated H4 during G2 to mid G1 phase (Pesavento et al., 2008). Newly synthesized histones are progressively methylated to the dimethylation state with a small subset even being trimethylated. The H4K20me2 mark stays relatively high during the whole cell cycle, ranging between 53-63% in abundance (Pesavento et al., 2008). All three different methylation states as well as other histone modifications fulfil distinct functions in the cell and it seems as if each modification has its own temporal and spatial availability. Thus, their function will also have impact on the presence of writers and readers of those modifications.

4.6 RNA is involved in structural properties of chromatin

Not only histone modifications and protein binding influences chromatin states but also RNA turned out to be an important component of chromatin by playing a role in its regulation. Early analyses of protein binding kinetics during chromatin assembly indicated a role of RNA-binding proteins in chromatin dynamics (also observed in later experiments, Figure 3.6 d). In addition, the depletion of chromatin-associated RNAs was accompanied by chromatin compaction, visible through the complete disappearance of smaller nucleosomal bands, which are indicative of accessible chromatin (Schubert et al., 2012). Further experiments helped to stepwise characterise the RNA species mediating this effect. The inhibition of RNA Polymerase II by α -amanitin treatment resulted in a genome wide compaction of chromatin *in vivo* (Schubert et al., 2012). The compaction degree was markedly dependent on the remaining level of RNA suggesting that the chromatin-associated RNAs are indeed RNA Pol II transcripts. Similar effects were seen in HeLa cells by microscopic and EM studies upon RNA depletion or transcriptional inhibition (Bouvier et al., 1985; Nickerson et al., 1989). A related

4. DISCUSSION

study investigating the effects of RNA depletion on human chromatin structure likewise observed condensation of the overall chromatin (Caudron-Herger et al., 2011).

The effect of chromatin compaction in *Drosophila* could experimentally be defined to single-stranded RNAs as the depletion of RNAs by RNaseH, an enzyme hydrolysing RNA-DNA hybrids, did not lead to any changes in chromatin compaction (Schubert et al., 2012). In contrast, all enzymes with ssRNA as substrate affected the chromatin accessibility.

4.7 Chromatin compaction can be reversed by specific subtypes of RNA

In vitro experiments can recapitulate the RNA-dependent accessibility of chromatin observed *in vivo*. Initial characterisations showed that the association between chromatin and RNA is stable even under high salt conditions and does not require supercoiled chromatin as template (Schubert et al., 2012). Sucrose gradient centrifugation allows the differentiation between open and closed chromatin states as more compacted chromatin runs at fractions of higher sucrose concentrations. Studies using this technique indicated that the compaction by chromatin could be reversed by addition of RNA purified from *Drosophila* embryonic extracts but not by the addition of tRNA and random oligonucleotides. Additionally, RNA purified from HeLa cells led to reassociation of RNA molecules to chromatin and a shift in the density of chromatin fibres towards an open chromatin state (Schubert et al., 2012). Together with the fact that RNA-dependent accessibility is also seen in other organisms, this points towards a conserved role of a specific RNA species in chromatin organisation.

4.8 Chromatin structure is regulated by a ribonucleoprotein complex

The identification of chromatin-associated RNAs and Df31 led to the discovery of a new RNP complex with function in chromatin structure. Whereas Df31 was already described to feature affinity to chromatin, the description of small nucleolar RNAs and their effect on chromatin structure was a novel finding.

The snoRNA U2134b and G980 were among the most enriched snoRNA found on chromatin and therefore chosen for further experiments. The enrichment factor however generates a misleading impression on the role of other snoRNAs. Abundant RNAs that are found associated to chromatin in equimolar amounts in comparison to the above mentioned snoRNAs appear less significant due to their lower enrichment factor. From the 186 transcribed snoRNAs in *Drosophila*, over 30 were found being bound to chromatin (Schubert et al., 2012). A number, which is quite surprising as snoRNAs were known to be mainly implicated in RNA-editing of rRNA, tRNA and possibly even mRNA (Bachellerie et al., 2002). Two major classes of snoRNAs have been identified to date and have been

named after the presence of short consensus sequence motifs; the box C/D and H/ACA snoRNAs (Balakin et al., 1996). They catalyse site-specific pseudouridylation and 2'-O-ribose methylation, respectively, and act in ribonucleoprotein complexes together with proteins such as Nop and Nhp (Watkins and Bohnsack, 2011). The modifications seem to be important for proper folding and function of their target RNA. An increasing number of snoRNAs have been described as “orphan” guides with tissue-specific expression but no obvious sequence complementarity in the transcriptome (Bachellerie et al., 2002). Those snoRNAs may give rise to other regulatory RNA species or act in a different fashion. The identification of a class of RNAs in human cells that act as miRNA in complex with Ago1 and Ago2 but originate from snoRNA precursors further strengthens this hypothesis (Ender et al., 2008). The general function of snoRNAs in cellular organism is quite diverse. Therefore their mode of action in chromatin structure should be part of further investigations in the future.

Df31 was already described to have certain characteristics that reasoned for an involvement in chromatin-based processes. First, it was shown to decondense sperm chromatin by removing sperm specific proteins and loading histones onto naked DNA *in vitro* (Crevel and Cotterill, 1995). Further experiments suggested a more general role of Df31 in the organisation of higher order structures (Crevel et al., 2001). Secondly, it was shown to bind to histone H3 tails and promote interstrand bridging of chromatin fibres, which is mediated by indirect binding to DNA (Guillebault and Cotterill, 2007). Df31 furthermore belongs to the group of intrinsically disordered proteins (IDPs), which are characterised by a lack of stable tertiary structures. A high level of disorder has already been described in transcription factors, DNA repair proteins and general chromatin organisation factors, such as HMGs (Bell et al., 2002; Reeves and Adair, 2005). Structural disorder transfers specific advantages such as the ability to bind different partners with distinct functional outcomes, also referred to as binding promiscuity (Szöllösi et al., 2008). Df31 can benefit from this feature, as it has to bind two dissimilar cellular components, protein in form of histones and RNA. The possible binding of Df31 to DNA could clearly be ruled out by microscale thermophoresis experiments, in which the protein discriminates single-stranded as well as double-stranded DNA and exhibits a strong preference towards snoRNA compared to other single-stranded RNAs (Schubert et al., 2012).

4.9 SnoRNP complexes and their mode of action

Interestingly, several RNP complexes cooperating with snoRNAs have been linked to chromatin related processes. In mouse, biochemical fractionation of an *in vitro* assembled snoRNP complex led to the identification of two pairs of highly conserved proteins; namely the nucleolar proteins Nop56p and Nop58p and the two proteins p50 and p55 (Watkins et al., 1998; Newman et al., 2000). Those proteins associate with the sequence motif box C/D of the snoRNA U14. The Nop56p/Nop58p homologues proteins MARBP-1 and MARBP-2 in plants interact with matrix-attached regions

4. DISCUSSION

(MARs), which play a structural role in the organisation of chromatin (Hatton and Gray, 1999). p50 and p55 in mouse localise to the nucleoplasm and are linked to replication and transcriptional events (Newman et al., 2000). Furthermore, rat p55 was found together in a complex with the TATA-binding protein (Tbp) where it acts as a putative ATP-dependent DNA helicase (Kanemaki et al., 1997). These findings support the idea that snoRNPs influence chromatin structure and regulation. How those snoRNPs are targeted to chromatin remains unclear. There are examples of RNA-mediated targeting in fission yeast and mouse. The RNA-induced transcriptional silencing complex (RITS) in yeast is recruited to chromatin via the formation of ncRNA-DNA hybrids (Nakama et al., 2012). Those ncRNAs are transcribed from heterochromatic repeats, bind to the RITS complex and lead to RNAi-mediated assembly of heterochromatin. In mice, a promoter-associated RNA (pRNA) interacts with a transcription factor and forms a DNA-RNA triplex. This triplex further recruits DNMT3b thereby triggering de novo DNA methylation and transcriptional silencing (Schmitz et al., 2010). Whether snoRNAs also form a DNA-RNA hybrid or additional proteins are involved in the recruitment of Df31 needs to be clarified by additional experiments.

4.10 Mechanisms of snoRNP-dependent chromatin opening

Df31 was suggested to bind euchromatic regions in the *Drosophila* genome (Filion et al., 2010). The binding preference towards histone H3 tails could indicate that certain histone modifications play a role in the recruitment of Df31 to chromatin. Knockdown of Df31 in Schneider cells caused only moderate compaction of chromatin. Taken together, these results point towards a specific role of Df31 in the regulation of euchromatic structure. On the opposite, depletion of RNA had an overall effect on chromatin accessibility (Schubert et al., 2012). Other studies showing genome-wide association of RNAs to chromatin further encourage the assumption that snoRNA have a more global function in maintaining chromatin structure. How snoRNA and Df31 keep chromatin in an open state remains elusive. The RNP complex could somehow disturb internucleosomal interactions, which are a key requisite for a stable chromatin fibre. The interference of this stability could be mediated by different possible mechanisms:

Df31 also shows weak association to H4 (Schubert et al., 2012). Once Df31 is in close proximity to the nucleosome via its binding to H3, it could destabilize internucleosomal interactions between the H4 N-terminus and the surface of H2A-H2B dimers of another nucleosome, thereby causing an opening of the 30 nm fibre. The interaction between H4 and the H2A-H2B dimer is mediated by a region of highly basic amino acids (16-25) (Luger et al., 1997). The RNP complex could provoke a retargeting of this basic region to the negatively charged snoRNA, which would also result in a destabilisation of chromatin.

H3 tails are involved in internucleosomal interactions upon formation of condensed secondary and tertiary chromatin structures (Zheng, 2005). Binding of Df31 to the H3 tail could disturb these interarray formations and thereby decondensing the chromatin fibre.

Df31 is a highly abundant protein and amounts to approximately 0.1% of the total protein content in *Drosophila* embryos (Crevel et al., 2001). This value is comparable to H1 levels. In eukaryotic genomes, H1 is present in nearly stoichiometric abundance with the nucleosome and is important for the formation of nucleosomal arrays and secondary chromatin structures (Widom, 1998). Df31 does not interfere with the formation of the chromosome in *in vitro* reconstituted arrays (Guillebault and Cotterill, 2007). Supercoiling and MNase assays further revealed that the RNA and Df31 dependent chromatin accessibility is not the result of changes in histone and nucleosome density (Schubert et al., 2012). Yet, due to its abundance, Df31 could take over a role similar to H1 in which it binds certain nucleosomes and thereby regulates accessibility of the underlying genomic region. The protein's ability to mediate interstrand bridging could further promote a loosely packaging of chromatin fibres. In this way, the chromatin structure could be maintained via a direct interaction between the nucleosome and individual Df31 molecules, which are in turn linked by snoRNAs (Figure 4.3).

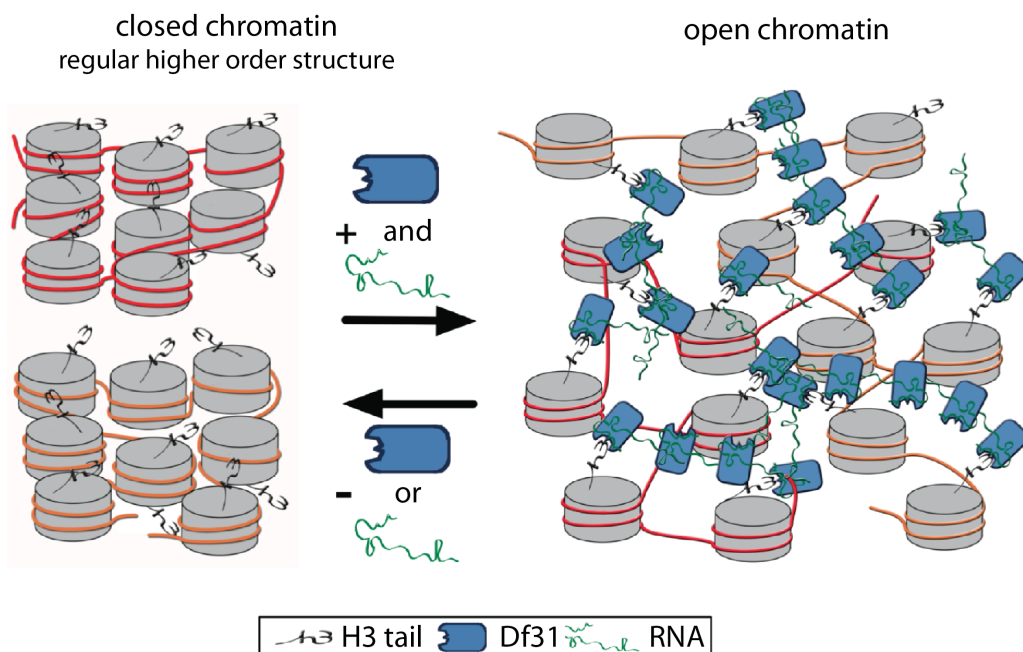


Figure 4.3: Model of snoRNP-mediated chromatin higher order formation

The Df31-RNA complex keeps chromatin in an open state via binding of Df31 to H3 tails and bridging of Df31 by RNA molecules. This net-like structure guarantees chromatin accessibility in euchromatic regions. Loss of either complex component causes higher order formation but can be reversed by replacement of the missing molecule (Schubert et al., 2012).

4. DISCUSSION

4.11 Df31 and its interactome

Df31 is included in a large-scale *Drosophila* protein interaction map (DPiM) generated by the Artavanis-Tsakonas lab and collaborators (Guruharsha et al., 2011). They performed over 3500 co-affinity purifications on Flag-HA epitope tagged *Drosophila* proteins with combinatorial MS analysis. In this study, they recovered many known but also previously uncharacterised protein complexes, in which Df31 appeared as interactor. An additional study investigating the distribution pattern of *Drosophila* protein trap lines, led to the observation that Df31 parts the nucleus in four different compartments, one of them inclosing the male X chromosome (Rohrbaugh et al., 2013). Data of both publications further suggest that Df31 together with Stwl and dNlp belong to a large protein network that comprises a common subset of proteins. However, the functional impact of those common binding partners was not discussed. The Df31 co-immunoprecipitation presented in this study led to the identification of 318 potential interaction partners. The relatively small overlap with previous studies and open source interaction data can be caused by different reasons. Although Guruharsha et al. followed the same experimental approach by tagging the protein with a FLAG-HA epitope, there are evident differences between the used protocols. In the following the experimental differences should be specified: The cell line used by Guruharsha et al. was the *Drosophila* S2R+ line, in contrast to the L2-4 cell. Both cell lines derive from the same primary embryonic culture but most likely differ slightly in their genomic and proteomic make-up. The IP presented in this thesis was performed using nuclear extract from stably transfected cells with induced expression. Proteins were eluted in SDS Sample buffer, separated by SDS-PAGE and digested with trypsin in-gel. Guruharsha et al. used whole cell extract from transiently transfected cells with induced expression. In both cases the gene was under the control of a metallothionein promoter. Immunoprecipitation was then performed using HA-beads and bound proteins were eluted with synthetic HA-peptide. The eluate was prepared for MS analysis by in-solution digest. Furthermore different software tools and set-ups were used for the data analysis, which most likely introduced additional variance between the two Df31 IPs. Thus, although not entirely confirmed by other studies, the interaction partners in this thesis were considered as potential candidates and further characterised.

To evaluate if proteins with similar functions or relation in distinct pathways were enriched in the Df31 IP, the open source database DAVID was used. The bioinformatics analysis identified many factors with an activating role in transcription. Examples are the transcription initiation factors Taf4, 6, 7 and 8. They bind to promoters and serve as scaffold for the assembly of the RNA Polymerase II and other proteins that coordinate transcription such as Tbp (Malkowska et al., 2013). Tbp is known to interact with the Taf proteins but there is also evidence that it associates with fu2 and Brf, two other Df31 interactors (data extracted from STRING). Also enriched are several other transcription factors

such as Jra, Pdp1, e(y)1, Dp, bigmax, lola, Rel and TfiIFbeta. This observation further strengthens Df31's function in genomic regions with active transcription.

In addition, the proteins CG7637, CG3071, CG4038, NHP2 and Nop60B were co-purified and are linked to snoRNA-related processes. The appearance of snoRNA-associated proteins confirms the link between Df31 and snoRNA. One of those snoRNA-associated protein is the protein CG7637, which was markedly enriched in the Df31 pull down. It belongs to the Nop10 family, a class of nucleolar proteins, and is involved in H/ACA ribonucleoprotein complex formation. CG3071 is an U3 snoRNA-associated protein, which harbours a WD40 repeat. This repeat is also a common feature found in transcription factors and other chromatin-associated proteins such as p55, a subunit of PRC2, NURF and CAF-1 (Wen et al., 2012). Affinity purification of snR30 snoRNPs in yeast identified not only NHP2 and Nop10 as interaction partners but also H2B and H4 (Lemay et al., 2011). Loss of an NHP2 containing RNP in human has been linked to reduced telomerase activity, mitotic dysfunction and genomic instability (Stedingk et al., 2013). SnoRNP complexes probably mainly act in the ribosome biogenesis, but increasing evidence points towards important functions also outside the nucleolus.

The protein MRG15, one of the top hits in the Df31 pull down, is predicted to bind to chromatin via an interaction with methylated histone tails. The family of MRG15 proteins is evolutionary conserved across a large number of species and has a chromodomain as common binding feature (Zhang et al., 2010). Studies in human tissue culture cells and *Drosophila* suggested a role for MRG15 in chromatin remodelling (Pardo, 2002). In *Drosophila*, MRG15 is present in the Tip60/KAT5 complex, which is implicated in the repair of dsDNA breaks (Kusch, 2004). Consistent with this H2Av is found slightly enriched in the co-immunoprecipitation experiment (\log_2 enrichment: 2.3). Other members of the Tip60 complex could not be co-immunoprecipitated with Df31. Moreover, MRG15 was linked to compaction of interphase chromatin via an interaction with the condensin II subunit Cap-H2 in *Drosophila* (Smith et al., 2013). Consequently, MRG15 could fulfil an antagonizing role in the maintenance of chromatin accessibility and hence act as counterpart of Df31. It is also conceivable that MRG15 is acting in chromatin compaction and opening as part of two distinct complexes as MRG15 was described to also act in both histone acetyltransferase (HAT) and histone deacetylase (HDAC) complexes (Yochum and Ayer, 2002; Cai, 2003; Peña et al., 2011). The human MRG15 is found in a complex together with hMOF, the human homologue of the acetyltransferase MOF in flies (Pardo, 2002). The *Drosophila* protein MOF is involved in dosage compensation, which is achieved by positive regulation of transcription through acetylation of target genes. MOF also belongs to the group of moderately enriched proteins in the pulldown (\log_2 enrichment: 3.0) and links Df31 again to regions of active transcription.

4. DISCUSSION

The protein megator (Mtor; \log_2 enrichment: 2.77) is predicted to function in a ribonucleoprotein complex (inferred from sequence/structural similarity with *Saccharomyces* MLP1). Furthermore, it is found in distinct chromosomal territories that represent active regions of the genome (Vaquerizas et al., 2010). Comparison of male and female cells revealed that these domains are particularly enriched on the male X chromosome in *Drosophila*. Mtor and Nup153, found in complex with MOF, bind to 25% of the genome and create so-called “nucleoporin-associated regions” (NAR), which are characterised by active regions, high RNA Pol II occupancy and histone H4K16 acetylation (Vaquerizas et al., 2010). The interaction of Df31 with MOF and Mtor is particularly interesting in the light of Df31’s distinct localisation to a compartment which encloses the male X chromosome (Rohrbaugh et al., 2013). Rohrbaugh et al. also found MSL-1, another member of the DCC, confined within the Df31 compartment. These results suggest a role of Df31 in chromatin compartmentalisation and maintenance in particular on the male X chromosome in *Drosophila melanogaster*.

Gel filtration experiments could reveal if Df31 is present in several distinct complexes. Depending on the composition of the complex one could speculate about the exact role of those complexes in chromatin regulation. RNA immunoprecipitation via Df31 precipitation would help to further characterise the already described Df31 containing snoRNP complex. So far only chromatin-associated RNAs have been isolated and sequenced. Therefore, it would be interesting to investigate the overlap between caRNAs and Df31-associated RNAs. In this study, immunoprecipitation of Df31 was performed to investigate specific binding partners. However, histones and the evaluation of their modification pattern were not included in the analysis. A Df31 ChIP or even ChIPseq with histone modification analysis would reveal whether Df31 binds to regions with specific modification marks. As Df31 was found in two distinct types of euchromatin, one would forecast to find Df31 localising to regions with active marks such as H3K4me2 and H3K79me3 (Filion et al., 2010). In addition, ChIPseq data would allow the analysis of the exact binding sites of Df31 to euchromatic regions.

Using the same *in vitro* assembly system, it was possible to look at two different biological questions; at the characterisation of binding kinetics during chromatin assembly and at the dependency of binding factors on RNA. Additional data points and future technical improvements will help to refine the present findings. Moreover, the knowledge obtained by applying the *in vitro* system can easily be transferred to the *in vivo* context as shown for Df31. Top-down proteomic approaches combined with label-free quantification as presented in this thesis will support further systematic investigations in this research field and help to shed light on different aspects of chromatin assembly and maintenance.

ABBREVIATIONS

ABBREVIATIONS

3C	Chromosome conformation capture
α	Anti
ac	Acetylation
ACF	ATP-dependent chromatin assembly factor
ADP	Adenosindiphosphate
ASF1	Antisilencing function 1
BAH	Bromo-adjacent homology
bp	Basepair
BSA	Bovine serum albumin
CAF-1	Chromatin assembly factor 1
CARM1	Histone-arginine methyltransferase
caRNA	chromatin-associated RNA
cDNA	complementary DNA
ChIP	Chromatin immunoprecipitation
CHRAC	Chromatin accessibility complex
Co-IP	Co-Immunoprecipitation
dATP, dUTP, dCTP, dGTP	deoxy Adenosin-, Uridin-, Cytidin,Guanosin triphosphate
DAVID	Database for Annotation, Visualization and Integrated Discovery
DAXX	Death domain-associated protein
DCC	Dosage Compensation Complex
Df31	Decondensationfactor 31
DMSO	Dimethylsulfoxide
DNA	Deoxyribonucleic acid
DNMT	DNA methyltransferase
dNTP	Desoxyribonucleotidetriphosphate
DREX	Drosophila embryonic extract
DSB	Doublestrand break
DTT	Dithiothreitol
<i>E.coli</i>	<i>Echerichia coli</i>
EDTA	Ethylendiamintetraacetate
EGTA	Ethylene glycol tetraacetic acid
ELISA	Enzyme-linked-immunosorbent
EM	Electron microscopy
EX	Extraction Buffer
FACT	Facilitates chromatin transcription
FASP	Filter aided sample preparation
FCS	Fetale Calf Serum
H1, H2A, H2B, H3, H4	Histones
HAT	Histone acetyltransferase
HDAC	Histone deacetylase
HeLa cells	Henrietta Lacks cells
HEPES	(4-(2-hydroxyethyl)-1-piperazineethanesulfonic acid)
HMG	High mobility group protein
HP1	Heterochromatin protein 1
HPLC	High-performance liquid chromatography
iBAQ	Intensity based absolute quantification

ABBREVIATIONS

ISWI	Imitation switch
K	Lysine
kb	Kilobase
kDa	Kilodalton
LC-MS/MS	Liquid chromatography mass spectrometry
lincRNA	long non-coding RNA
LSD	Lysine-specific demethylase
MCM	Mini-Chromosome Maintenance
me	Methylation
miRNA	microRNA
MNase	Micrococcal nuclease
mRNA	messenger RNA
MS	Mass spectrometry
NAP1	Nucleosome assembly protein
ncRNA	Non-coding RNA
NER	Nucleotide excision repair
NTD	N-terminal domain
NURF	Nucleosomes remodelling factor
ORC	Origin Recognition Complex
P-TEFb	Positive transcription elongation factor
PBS	Phosphate buffered saline
PCNA	Proliferating cell nuclear antigen
PCR	Polymerase chain reaction
Pen/Strep	Penicillin/Streptomycin
PMSF	Phenylmethanesulfonyl fluoride
PRC2	Polycomb repressive complex
PRMT1	Protein arginine methyltransferase 1
pRNA	promoter-associated RNA
rDNA	Ribosomal DNA
RNA	Ribonucleic acid
RNA FISH	RNA Fluorescence in situ hybridization
RNA Pol II	RNA Polymerase II
RNase A	Ribonuclease
RNP	Ribonucleoprotein
rRNA	ribosomalRNA
RT	Room temperature
SDS	Sodium dodecyl sulfate
SDS-PAGE	SDS-Polyacrylamide gel electrophoresis
SID	Sample identification number
SILAC	Stable isotope labelling with amino acids in cell culture
snoRNA	small nucleolar RNA
ssRNA	single-stranded RNA
STRING	Search Tool for the Retrieval of Interacting Genes/Proteins
SUMO	Small ubiquitin-related modifier
SUV	Suppressor of position-effect variegation
TBP	TATA-box-binding protein

ABBREVIATIONS

TF	Transcriptionfactor
TFA	Trifluor acetic acid
Tris	Tris(hydroxymethyl)aminomethane
tRNA	transferRNA
ub	Ubiquitination
v/v	Volume per volume
w/v	Weight per volume
Xist	X-inactive specific transcript

REFERENCES

REFERENCES

- Annunziato, A. (2008) DNA packaging: Nucleosomes and chromatin. *Nature Education* 1(1):26.
- Ahmad, K., and Henikoff, S. (2002). Histone H3 variants specify modes of chromatin assembly. *Proc. Natl. Acad. Sci. U.S.A.* 99 *Suppl 4*, 16477–16484.
- Alexiadis, V., Varga-Weisz, P.D., Bonte, E., Becker, P.B., and Gruss, C. (1998). In vitro chromatin remodelling by chromatin accessibility complex (CHRAC) at the SV40 origin of DNA replication. *Embo J.* 17, 3428–3438.
- Arents, G., and Moudrianakis, E.N. (1995). The histone fold: a ubiquitous architectural motif utilized in DNA compaction and protein dimerization. *Proc. Natl. Acad. Sci. U.S.A.* 92, 11170–11174.
- Artman, M., and Roth, J.S. (1971). Chromosomal RNA: an artifact of preparation? *J. Mol. Biol.* 60, 291–301.
- Avvakumov, N., Nourani, A., and Côté, J. (2011). Histone chaperones: modulators of chromatin marks. *Mol. Cell* 41, 502–514.
- Bachelier, J.P., Cavaillé, J., and Hüttenhofer, A. (2002). The expanding snoRNA world. *Biochimie* 84, 775–790.
- Balakin, A.G., Smith, L., and Fournier, M.J. (1996). The RNA world of the nucleolus: two major families of small RNAs defined by different box elements with related functions. *Cell* 86, 823–834.
- Bao, Y., and Shen, X. (2007). SnapShot: Chromatin Remodeling Complexes. *Cell* 129, 632.e1–632.e2.
- Barth, T.K., and Imhof, A. (2010). Fast signals and slow marks: the dynamics of histone modifications. *Trends in Biochemical Sciences* 35, 618–626.
- Bauer, U.-M., Daujat, S., Nielsen, S.J., Nightingale, K., and Kouzarides, T. (2002). Methylation at arginine 17 of histone H3 is linked to gene activation. *EMBO Rep* 3, 39–44.
- Becker, P.B., and Hörz, W. (2002). ATP-DEPENDENT NUCLEOSOME REMODELING. *Annu. Rev. Biochem.* 71, 247–273.
- Becker, P.B., and Wu, C. (1992). Cell-free system for assembly of transcriptionally repressed chromatin from *Drosophila* embryos. *Mol. Cell. Biol.* 12, 2241–2249.
- Bednar, J., Horowitz, R.A., Grigoryev, S.A., Carruthers, L.M., Hansen, J.C., Koster, A.J., and Woodcock, C.L. (1998). Nucleosomes, linker DNA, and linker histone form a unique structural motif that directs the higher-order folding and compaction of chromatin. *Proc. Natl. Acad. Sci. U.S.A.* 95, 14173–14178.
- Bell, A.J., Xin, H., Taudte, S., Shi, Z., and Kallenbach, N.R. (2002). Metal-dependent stabilization of an active HMG protein. *Protein Eng.* 15, 817–825.
- Belton, J.-M., McCord, R.P., Gibcus, J.H., Naumova, N., Zhan, Y., and Dekker, J. (2012). HiC: A comprehensive technique to capture the conformation of genomes. *Methods* 58, 268–276.
- Benson, L.J. (2005). Modifications of H3 and H4 during Chromatin Replication, Nucleosome Assembly, and Histone Exchange. *Journal of Biological Chemistry* 281, 9287–9296.
- Bessarabova, M., Ishkin, A., JeBailey, L., Nikolskaya, T., and Nikolsky, Y. (2012). Knowledge-based analysis of proteomics data. *BMC Bioinformatics* 13, S13.
- Blank, T.A., Sandaltzopoulos, R., and Becker, P.B. (1997). Biochemical analysis of chromatin structure and function using *Drosophila* embryo extracts. *Methods* 12, 28–35.
- Blower, M.D., Nachury, M., Heald, R., and Weis, K. (2005). A Rae1-Containing Ribonucleoprotein Complex Is Required for Mitotic Spindle Assembly. *Cell* 121, 223–234.
- Blum, H., Beier, H. and Gross, H. J. (1987), Improved silver staining of plant proteins, RNA and DNA in polyacrylamide gels. *ELECTROPHORESIS*, 8: 93–99. doi: 10.1002/elps.1150080203.
- Bonne-Andrea, C., Harper, F., Sobczak, J., and De Recondo, A.M. (1984). Rat liver HMG1: a physiological nucleosome assembly factor. *Embo J.* 3, 1193–1199.
- Bonner, J. (1971). Problematic chromosomal RNA. *Nature* 231, 543–544.
- Bonner, J., and Widholm, J. (1967). Molecular complementarity between nuclear DNA and organ-specific chromosomal RNA. *Proc. Natl. Acad. Sci. U.S.A.* 57, 1379–1385.
- Bouvier, D., Hubert, J., Sève, A.P., and Bouteille, M. (1985). Nuclear RNA-associated proteins and their relationship to the nuclear matrix and related structures in HeLa cells. *Can. J. Biochem. Cell Biol.* 63, 631–643.
- Bönisch, C., and Hake, S.B. (2012). Histone H2A variants in nucleosomes and chromatin: more or less stable? *Nucleic Acids Research* 40, 10719–10741.
- Braun, S., Garcia, J.F., Rowley, M., Rougemaille, M., Shankar, S., and Madhani, H.D. (2011). The Cul4-Ddb1Cdt2 Ubiquitin Ligase Inhibits Invasion of a Boundary-Associated Antisilencing Factor into Heterochromatin. *Cell* 144, 41–54.
- Bulger, M., Ito, T., Kamakaka, R.T., and Kadonaga, J.T. (1995). Assembly of regularly spaced nucleosome arrays by *Drosophila* chromatin assembly factor 1 and a 56-kDa histone-binding protein. *Proc. Natl. Acad. Sci. U.S.A.* 92, 11726–11730.

- Burgess, R.J., and Zhang, Z. (2013). Histone chaperones in nucleosome assembly and human disease. *Nat Struct Mol Biol* 20, 14–22.
- Bynum, J.W., and Volkin, E. (1980). Chromatin-associated RNA: differential extraction and characterization. *Biochim. Biophys. Acta* 607, 304–318.
- Cai, Y. (2003). Identification of New Subunits of the Multiprotein Mammalian TRRAP/TIP60-containing Histone Acetyltransferase Complex. *Journal of Biological Chemistry* 278, 42733–42736.
- Caudron-Herger, M., Müller-Ott, K., Mallm, J.-P., Marth, C., Schmidt, U., Fejes-Tóth, K., and Rippe, K. (2011). Coding RNAs with a non-coding function: Maintenance of open chromatin structure. *Nucleus* 2, 410–424.
- Chadwick, B.P., and Willard, H.F. (2001). A novel chromatin protein, distantly related to histone H2A, is largely excluded from the inactive X chromosome. *J. Cell Biol.* 152, 375–384.
- Chan, K.M., and Zhang, Z. (2012). Leucine-rich Repeat and WD Repeat-containing Protein 1 Is Recruited to Pericentric Heterochromatin by Trimethylated Lysine 9 of Histone H3 and Maintains Heterochromatin Silencing. *Journal of Biological Chemistry* 287, 15024–15033.
- Chen, C.-C., Carson, J.J., Feser, J., Tamburini, B., Zabaronick, S., Linger, J., and Tyler, J.K. (2008). Acetylated Lysine 56 on Histone H3 Drives Chromatin Assembly after Repair and Signals for the Completion of Repair. *Cell* 134, 231–243.
- Chesnokov, I., Remus, D., and Botchan, M. (2001). Functional analysis of mutant and wild-type *Drosophila* origin recognition complex. *Proc. Natl. Acad. Sci. U.S.A.* 98, 11997–12002.
- Corpet, A., De Koning, L., Toedling, J., Savignoni, A., Berger, F., Lemaître, C., O'Sullivan, R.J., Karlseder, J., Barillot, E., Asselain, B., et al. (2011). Asf1b, the necessary Asf1 isoform for proliferation, is predictive of outcome in breast cancer. *Embo J.* 30, 480–493.
- Costanzi, C., and Pehrson, J.R. (1998). Histone macroH2A1 is concentrated in the inactive X chromosome of female mammals. *Nature* 393, 599–601.
- Cox, J., and Mann, M. (2008). MaxQuant enables high peptide identification rates, individualized p.p.b.-range mass accuracies and proteome-wide protein quantification. *Nat. Biotechnol.* 26, 1367–1372.
- Craig, J.M. (2005). Heterochromatin--many flavours, common themes. *Bioessays* 27, 17–28.
- Cremer, T., and Cremer, M. (2010). Chromosome Territories. *Cold Spring Harbor Perspectives in Biology* 2, a003889–a003889.
- Crevel, G., and Cotterill, S. (1995). DF 31, a sperm decondensation factor from *Drosophila melanogaster*: purification and characterization. *Embo J.* 14, 1711–1717.
- Crevel, G., Huikeshoven, H., and Cotterill, S. (2001). Df31 is a novel nuclear protein involved in chromatin structure in *Drosophila melanogaster*. *Journal of Cell Science* 114, 37–47.
- D'Arcy, S., Martin, K.W., Panchenko, T., Chen, X., Bergeron, S., Stargell, L.A., Ben E Black, and Luger, K. (2013). Chaperone Nap1 Shields Histone Surfaces Used in a Nucleosome and Can Put H2A-H2B in an Unconventional Tetrameric Form. *Mol. Cell* 1–16.
- Deem, A.K., Li, X., and Tyler, J.K. (2012). Epigenetic regulation of genomic integrity. *Chromosoma* 121, 131–151.
- Dekker, J. (2002). Capturing Chromosome Conformation. *Science* 295, 1306–1311.
- Dilworth, S.M., and Dingwall, C. (1988). Chromatin assembly in vitro and in vivo. *Bioessays* 9, 44–49.
- Dutta, B., Adav, S.S., Koh, C.G., Lim, S.K., Meshorer, E., and Sze, S.K. (2012). Elucidating the temporal dynamics of chromatin-associated protein release upon DNA digestion by quantitative proteomic approach. *Journal of Proteomics* 75, 5493–5506.
- Earnshaw, W.C., Honda, B.M., Laskey, R.A., and Thomas, J.O. (1980). Assembly of nucleosomes: the reaction involving *X. laevis* nucleoplasmin. *Cell* 21, 373–383.
- Eberharter, A., Ferrari, S., Längst, G., Straub, T., Imhof, A., Varga-Weisz, P., Wilm, M., and Becker, P.B. (2001). Acf1, the largest subunit of CHRAC, regulates ISWI-induced nucleosome remodelling. *Embo J.* 20, 3781–3788.
- Eilebrecht, S., Benecke, B.-J., and Benecke, A. (2011a). 7SK snRNA-mediated, gene-specific cooperativity of HMGA1 and P-TEFb. *Rnabiology* 8, 1084–1093.
- Eilebrecht, S., Brysbaert, G., Wegert, T., Urlaub, H., Benecke, B.J., and Benecke, A. (2011b). 7SK small nuclear RNA directly affects HMGA1 function in transcription regulation. *Nucleic Acids Research* 39, 2057–2072.
- Elgin, S.C. (1996). Heterochromatin and gene regulation in *Drosophila*. *Curr. Opin. Genet. Dev.* 6, 193–202.
- Elgin, S.C.R., and Grewal, S.I.S. (2003). Heterochromatin: silence is golden. *Curr. Biol.* 13, R895–R898.
- Elsässer, S.J., and D'Arcy, S. (2012). Towards a mechanism for histone chaperones. *BBA - Gene Regulatory Mechanisms* 1819, 211–221.
- Ender, C., Krek, A., Friedländer, M.R., Beitzinger, M., Weinmann, L., Chen, W., Pfeffer, S., Rajewsky, N., and Meister, G. (2008). A Human snoRNA with MicroRNA-Like Functions. *Mol. Cell* 32, 519–528.

REFERENCES

- Endoh, M., Endo, T.A., Endoh, T., Isono, K.-I., Sharif, J., Ohara, O., Toyoda, T., Ito, T., Eskeland, R., Bickmore, W.A., et al. (2012). Histone H2A Mono-Ubiquitination Is a Crucial Step to Mediate PRC1-Dependent Repression of Developmental Genes to Maintain ES Cell Identity. *PLoS Genet* 8, e1002774.
- English, C.M., Adkins, M.W., Carson, J.J., Churchill, M.E.A., and Tyler, J.K. (2006). Structural basis for the histone chaperone activity of Asf1. *Cell* 127, 495–508.
- Eskeland, R., Eberharter, A., and Imhof, A. (2007). HP1 binding to chromatin methylated at H3K9 is enhanced by auxiliary factors. *Mol. Cell. Biol.* 27, 453–465.
- Felsenfeld, G., and Groudine, M. (2003). The digital code of DNA. *Nature* 421, 444–448.
- Filion, G.J., van Bommel, J.G., Braunschweig, U., Talhout, W., Kind, J., Ward, L.D., Brugman, W., de Castro, I.J., Kerkhoven, R.M., Bussemaker, H.J., et al. (2010). Systematic Protein Location Mapping Reveals Five Principal Chromatin Types in Drosophila Cells. *Cell* 143, 212–224.
- Finch, J.T., and Klug, A. (1976). Solenoidal model for superstructure in chromatin. *Proc. Natl. Acad. Sci. U.S.A.* 73, 1897–1901.
- Fischle, W., Tseng, B.S., Dormann, H.L., Ueberheide, B.M., Garcia, B.A., Shabanowitz, J., Hunt, D.F., Funabiki, H., and Allis, C.D. (2005). Regulation of HP1–chromatin binding by histone H3 methylation and phosphorylation. *Nature* 438, 1116–1122.
- Fischle, W., Wang, Y., and Allis, C.D. (2003). Histone and chromatin cross-talk. *Current Opinion in Cell Biology* 15, 172–183.
- Fletcher, T.M., and Hansen, J.C. (1995). Core histone tail domains mediate oligonucleosome folding and nucleosomal DNA organization through distinct molecular mechanisms. *J. Biol. Chem.* 270, 25359–25362.
- Fraser, P., and Bickmore, W. (2007). Nuclear organization of the genome and the potential for gene regulation. *Nature* 447, 413–417.
- Fussner, E., Ching, R.W., and Bazett-Jones, D.P. (2011). Living without 30nm chromatin fibers. *Trends in Biochemical Sciences* 36, 1–6.
- Gambus, A., Jones, R.C., Sanchez-Diaz, A., Kanemaki, M., van Deursen, F., Edmondson, R.D., and Labib, K. (2006). GINS maintains association of Cdc45 with MCM in replisome progression complexes at eukaryotic DNA replication forks. *Nat. Cell Biol.* 8, 358–366.
- Goldberg, A.D., Banaszynski, L.A., Noh, K.-M., Lewis, P.W., Elsaesser, S.J., Stadler, S., Dewell, S., Law, M., Guo, X., Li, X., et al. (2010). Distinct factors control histone variant H3.3 localization at specific genomic regions. *Cell* 140, 678–691.
- Grewal, S.I.S., and Elgin, S.C.R. (2002). Heterochromatin: new possibilities for the inheritance of structure. *Curr. Opin. Genet. Dev.* 12, 178–187.
- Grewal, S.I.S., and Jia, S. (2007). Heterochromatin revisited. *Nature Publishing Group* 8, 35–46.
- Grigoryev, S.A., and Woodcock, C.L. (2012). Chromatin organization — The 30nm fiber. *Experimental Cell Research* 318, 1448–1455.
- Groth, A., Rocha, W., Verreault, A., and Almouzni, G. (2007). Chromatin Challenges during DNA Replication and Repair. *Cell* 128, 721–733.
- Gruber, A.R., Koper-Emde, D., Marz, M., Tafer, H., Bernhart, S., Obernosterer, G., Mosig, A., Hofacker, I.L., Stadler, P.F., and Benecke, B.-J. (2008). Invertebrate 7SK snRNAs. *J. Mol. Evol.* 66, 107–115.
- Guglielmi, B., La Rochelle, N., and Tjian, R. (2013). Gene-Specific Transcriptional Mechanisms at the Histone Gene Cluster Revealed by Single-Cell Imaging. *Mol. Cell* 51, 480–492.
- Guillebault, D., and Cotterill, S. (2007). The Drosophila Df31 Protein Interacts with Histone H3 Tails and Promotes Chromatin Bridging In vitro. *J. Mol. Biol.* 373, 903–912.
- Guruharsha, K.G., Rual, J.-F., Zhai, B., Mintseris, J., Vaidya, P., Vaidya, N., Beekman, C., Wong, C., Rhee, D.Y., Cenaj, O., et al. (2011). A Protein Complex Network of Drosophila melanogaster. *Cell* 147, 690–703.
- Gürsoy, H.C., Koper, D., and Benecke, B.J. (2000). The vertebrate 7S K RNA separates hagfish (*Myxine glutinosa*) and lamprey (*Lampetra fluviatilis*). *J. Mol. Evol.* 50, 456–464.
- Han, J., Zhang, H., Zhang, H., Wang, Z., Zhou, H., and Zhang, Z. (2013). A Cul4 E3 Ubiquitin Ligase Regulates Histone Hand-Off during Nucleosome Assembly. *Cell* 155, 817–829.
- Hansen, J.C., van Holde, K.E., and Lohr, D. (1991). The mechanism of nucleosome assembly onto oligomers of the sea urchin 5 S DNA positioning sequence. *J. Biol. Chem.* 266, 4276–4282.
- Hatton, D., and Gray, J.C. (1999). Two MAR DNA-binding proteins of the pea nuclear matrix identify a new class of DNA-binding proteins. *Plant J.* 18, 417–429.
- Haushalter, K.A., and Kadonaga, J.T. (2003). Chromatin assembly by DNA-translocating motors. *Nature Publishing Group* 4, 613–620.

- Heidemann, M., Hintermair, C., Voß, K., and Eick, D. (2013). Dynamic phosphorylation patterns of RNA polymerase II CTD during transcription. *BBA - Gene Regulatory Mechanisms* 1829, 55–62.
- Heitz, E. (1935): Chromosomenstruktur und Gene. *Mol. Gen. Genet.* 70, 402–447.
- Henry, K.W. (2003). Transcriptional activation via sequential histone H2B ubiquitylation and deubiquitylation, mediated by SAGA-associated Ubp8. *Genes Dev.* 17, 2648–2663.
- Heyden, von, H.W., and Zachau, H.G. (1971). Characterization of RNA in fractions of calf thymus chromatin. *Biochim. Biophys. Acta* 232, 651–660.
- Higgs, R.E., Knierman, M.D., Gelfanova, V., Butler, J.P., and Hale, J.E. (2005). Comprehensive label-free method for the relative quantification of proteins from biological samples. *J. Proteome Res.* 4, 1442–1450.
- Hoek, M., and Stillman, B. (2003). Chromatin assembly factor 1 is essential and couples chromatin assembly to DNA replication in vivo. *Proc. Natl. Acad. Sci. U.S.A.* 100, 12183–12188.
- Holoubek, V., Deacon, N.J., Buckle, D.W., and Naora, H. (1983). A small chromatin-associated RNA homologous to repetitive DNA sequences. *Eur. J. Biochem.* 137, 249–256.
- Houlard, M., Berlivet, S., Probst, A.V., Quivy, J.-P., Héry, P., Almouzni, G., and Gérard, M. (2006). CAF-1 is essential for heterochromatin organization in pluripotent embryonic cells. *PLoS Genet* 2, e181.
- Huang, R.C., and Bonner, J. (1965). Histone-bound RNA, a component of native nucleohistone. *Proc. Natl. Acad. Sci. U.S.A.* 54, 960–967.
- Hwang, W.W., Venkatasubrahmanyam, S., Ianculescu, A.G., Tong, A., Boone, C., and Madhani, H.D. (2003). A conserved RING finger protein required for histone H2B monoubiquitination and cell size control. *Mol. Cell* 11, 261–266.
- Iacovoni, J.S., Caron, P., Lassadi, I., Nicolas, E., Massip, L., Trouche, D., and Legube, G. (2010). High-resolution profiling of gammaH2AX around DNA double strand breaks in the mammalian genome. *Embo J.* 29, 1446–1457.
- Iborra, F.J., Jackson, D.A., and Cook, P.R. (2001). Coupled transcription and translation within nuclei of mammalian cells. *Science* 293, 1139–1142.
- Ito, T., Bulger, M., Pazin, M.J., Kobayashi, R., and Kadonaga, J.T. (1997). ACF, an ISWI-containing and ATP-utilizing chromatin assembly and remodeling factor. *Cell* 90, 145–155.
- Ito, T., Levenstein, M.E., Fyodorov, D.V., Kutach, A.K., Kobayashi, R., and Kadonaga, J.T. (1999). ACF consists of two subunits, Acf1 and ISWI, that function cooperatively in the ATP-dependent catalysis of chromatin assembly. *Genes Dev.* 13, 1529–1539.
- Jamai, A., Imoberdorf, R.M., and Strubin, M. (2007). Continuous histone H2B and transcription-dependent histone H3 exchange in yeast cells outside of replication. *Mol. Cell* 25, 345–355.
- Jasencakova, Z., Scharf, A.N.D., Ask, K., Corpet, A., Imhof, A., Almouzni, G., and Groth, A. (2010). Replication Stress Interferes with Histone Recycling and Predeposition Marking of New Histones. *Mol. Cell* 37, 736–743.
- Jenuwein, T. (2001). Translating the Histone Code. *Science* 293, 1074–1080.
- Kamakaka, R.T., Bulger, M., and Kadonaga, J.T. (1993). Potentiation of RNA polymerase II transcription by Gal4-VP16 during but not after DNA replication and chromatin assembly. *Genes Dev.* 7, 1779–1795.
- Kan, P.-Y., Lu, X., Hansen, J.C., and Hayes, J.J. (2007). The H3 tail domain participates in multiple interactions during folding and self-association of nucleosome arrays. *Mol. Cell. Biol.* 27, 2084–2091.
- Kan, P.Y., Caterino, T.L., and Hayes, J.J. (2008). The H4 Tail Domain Participates in Intra- and Internucleosome Interactions with Protein and DNA during Folding and Oligomerization of Nucleosome Arrays. *Mol. Cell. Biol.* 29, 538–546.
- Kanduri, C., Whitehead, J., and Mohammad, F. (2009). The long and the short of it: RNA-directed chromatin asymmetry in mammalian X-chromosome inactivation. *FEBS Letters* 583, 857–864.
- Kanemaki, M., Makino, Y., Yoshida, T., Kishimoto, T., Koga, A., Yamamoto, K., Yamamoto, M., Moncollin, V., Egly, J.M., Muramatsu, M., et al. (1997). Molecular cloning of a rat 49-kDa TBP-interacting protein (TIP49) that is highly homologous to the bacterial RuvB. *Biochem. Biophys. Res. Commun.* 235, 64–68.
- Kim, J.-A., and Haber, J.E. (2009). Chromatin assembly factors Asf1 and CAF-1 have overlapping roles in deactivating the DNA damage checkpoint when DNA repair is complete. *Proc. Natl. Acad. Sci. U.S.A.* 106, 1151–1156.
- Kimura, H., and Cook, P.R. (2001). Kinetics of core histones in living human cells: little exchange of H3 and H4 and some rapid exchange of H2B. *J. Cell Biol.* 153, 1341–1353.
- Kireeva, M.L., Walter, W., Tchernajenko, V., Bondarenko, V., Kashlev, M., and Studitsky, V.M. (2002). Nucleosome remodeling induced by RNA polymerase II: loss of the H2A/H2B dimer during transcription. *Mol. Cell* 9, 541–552.
- Kleinschmidt, J.A., and Franke, W.W. (1982). Soluble acidic complexes containing histones H3 and H4 in nuclei of *Xenopus laevis* oocytes. *Cell* 29, 799–809.
- Kliszczak, A.E., Rainey, M.D., Harhen, B., Boisvert, F.M., and Santocanale, C. (2011). DNA mediated chromatin pull-down for the study of chromatin replication. *Sci Rep* 1, 95.

REFERENCES

- Kloc, M. (2005). Potential structural role of non-coding and coding RNAs in the organization of the cytoskeleton at the vegetal cortex of *Xenopus* oocytes. *Development* *132*, 3445–3457.
- Komander, D., and Rape, M. (2012). The Ubiquitin Code. *Annu. Rev. Biochem.* *81*, 203–229.
- Kuo, A.J., Song, J., Cheung, P., Ishibe-Murakami, S., Yamazoe, S., Chen, J.K., Patel, D.J., and Gozani, O. (2013). The BAH domain of ORC1 links H4K20me2 to DNA replication licensing and Meier-Gorlin syndrome. *Nature* *484*, 115–119.
- Kusch, T. (2004). Acetylation by Tip60 Is Required for Selective Histone Variant Exchange at DNA Lesions. *Science* *306*, 2084–2087.
- Lachner, M. (2003). An epigenetic road map for histone lysine methylation. *Journal of Cell Science* *116*, 2117–2124.
- Lachner, M., O'Carroll, D., Rea, S., Mechtler, K., and Jenuwein, T. (2001). Methylation of histone H3 lysine 9 creates a binding site for HP1 proteins. *Nature* *410*, 116–120.
- Ladoux, B., Quivy, J.P., Doyle, P., Roure, du, O., Almouzni, G., and Viovy, J.L. (2000). Fast kinetics of chromatin assembly revealed by single-molecule videomicroscopy and scanning force microscopy. *Proc. Natl. Acad. Sci. U.S.a.* *97*, 14251–14256.
- Laemmli, U.K. (1970). Cleavage of structural proteins during the assembly of the head of bacteriophage T4. *Nature* *227*, 680–685.
- Lancôt, C., Cheutin, T., Cremer, M., Cavalli, G., and Cremer, T. (2007). Dynamic genome architecture in the nuclear space: regulation of gene expression in three dimensions. *Nature Publishing Group* *8*, 104–115.
- Laskey, R.A., Honda, B.M., Mills, A.D., and Finch, J.T. (1978). Nucleosomes are assembled by an acidic protein which binds histones and transfers them to DNA. *Nature* *275*, 416–420.
- Lavrov, S., Déjardin, J., and Cavalli, G. (2004). Combined immunostaining and FISH analysis of polytene chromosomes. *Methods Mol. Biol.* *247*, 289–303.
- Lemay, V., Hossain, A., Osheim, Y.N., Beyer, A.L., and Dragon, F. (2011). Identification of novel proteins associated with yeast snR30 small nucleolar RNA. *Nucleic Acids Research* *39*, 9659–9670.
- Levy, A., and Noll, M. (1981). Chromatin fine structure of active and repressed genes. *Nature* *289*, 198–203.
- Lohe, A.R., Hilliker, A.J., and Roberts, P.A. (1993). Mapping simple repeated DNA sequences in heterochromatin of *Drosophila melanogaster*. *Genetics* *134*, 1149–1174.
- Loyola, A., Bonaldi, T., Roche, D., Imhof, A., and Almouzni, G. (2006). PTMs on H3 variants before chromatin assembly potentiate their final epigenetic state. *Mol. Cell* *24*, 309–316.
- Luger, K., Dechassa, M.L., and Tremethick, D.J. (2012). New insights into nucleosome and chromatin structure: an ordered state or a disordered affair? *Nat Rev Mol Cell Biol* *13*, 436–447.
- Luger, K. (2006). Dynamic nucleosomes. *Chromosome Res* *14*, 5–16.
- Luger, K., and Richmond, T.J. (1998). The histone tails of the nucleosome. *Curr. Opin. Genet. Dev.* *8*, 140–146.
- Luger, K., Mäder, A.W., Richmond, R.K., Sargent, D.F., and Richmond, T.J. (1997). Crystal structure of the nucleosome core particle at 2.8 Å resolution. *Nature* *389*, 251–260.
- Ma, H., Siegel, A.J., and Berezney, R. (1999). Association of chromosome territories with the nuclear matrix. Disruption of human chromosome territories correlates with the release of a subset of nuclear matrix proteins. *J. Cell Biol.* *146*, 531–542.
- Ma, X.J., Wu, J., Altheim, B.A., Schultz, M.C., and Grunstein, M. (1998). Deposition-related sites K5/K12 in histone H4 are not required for nucleosome deposition in yeast. *Proc. Natl. Acad. Sci. U.S.a.* *95*, 6693–6698.
- MacAlpine, D.M., and Almouzni, G. (2013). Chromatin and DNA Replication. *Cold Spring Harbor Perspectives in Biology* *5*, a010207–a010207.
- Maenner, S., Müller, M., Fröhlich, J., Langer, D., and Becker, P.B. (2013). ATP-dependent roX RNA remodeling by the helicase maleless enables specific association of MSL proteins. *Mol. Cell* *51*, 174–184.
- Maier, V.K., Chioda, M., and Becker, P.B. (2008). ATP-dependent chromatosome remodeling. *Biol. Chem.* *389*, 345–352.
- Maison, C., Bailly, D., Peters, A.H.F.M., Quivy, J.-P., Roche, D., Taddei, A., Lachner, M., Jenuwein, T., and Almouzni, G. (2002). Higher-order structure in pericentric heterochromatin involves a distinct pattern of histone modification and an RNA component. *Nat. Genet.* *30*, 329–334.
- Malkowska, M., Kokoszynska, K., Rychlewski, L., and Wyrwicz, L. (2013). Structural bioinformatics of the general transcription factor TFIID. *Biochimie* *95*, 680–691.
- Marzluff, W.F., Wagner, E.J., and Duronio, R.J. (2008). Metabolism and regulation of canonical histone mRNAs: life without a poly(A) tail. *Nat Rev Genet* *9*, 843–854.
- McGhee, J.D., Nickol, J.M., Felsenfeld, G., and Rau, D.C. (1983). Higher order structure of chromatin: orientation of nucleosomes within the 30 nm chromatin solenoid is independent of species and spacer length. *Cell* *33*, 831–841.
- Mersfelder, E.L. (2006). The tale beyond the tail: histone core domain modifications and the regulation of chromatin

- structure. *Nucleic Acids Research* *34*, 2653–2662.
- Méndez, J., Zou-Yang, X.H., Kim, S.-Y., Hidaka, M., Tansey, W.P., and Stillman, B. (2002). Human origin recognition complex large subunit is degraded by ubiquitin-mediated proteolysis after initiation of DNA replication. *Mol. Cell* *9*, 481–491.
- Moggs, J.G., Grandi, P., Quivy, J.P., Jonsson, Z.O., Hubscher, U., Becker, P.B., and Almouzni, G. (2000). A CAF-1-PCNA-Mediated Chromatin Assembly Pathway Triggered by Sensing DNA Damage. *Mol. Cell. Biol.* *20*, 1206–1218.
- Mondal, T., Rasmussen, M., Pandey, G.K., Isaksson, A., and Kanduri, C. (2010). Characterization of the RNA content of chromatin. *Genome Research* *20*, 899–907.
- Mosammaparast, N., Ewart, C.S., and Pemberton, L.F. (2002). A role for nucleosome assembly protein 1 in the nuclear transport of histones H2A and H2B. *Embo J.* *21*, 6527–6538.
- Mueller-Planitz, F., Klinker, H., Ludwigsen, J., and Becker, P.B. (2012). The ATPase domain of ISWI is an autonomous nucleosome remodeling machine. *Nat Struct Mol Biol* *20*, 82–89.
- Nagano, T., Mitchell, J.A., Sanz, L.A., Pauler, F.M., Ferguson-Smith, A.C., Feil, R., and Fraser, P. (2008). The Air noncoding RNA epigenetically silences transcription by targeting G9a to chromatin. *Science* *322*, 1717–1720.
- Nahkuri, S., and Paro, R. (2012). The role of noncoding RNAs in chromatin regulation during differentiation. *WIREs Dev Biol* *1*, 743–752.
- Nakama, M., Kawakami, K., Kajitani, T., Urano, T., and Murakami, Y. (2012). DNA-RNA hybrid formation mediates RNAi-directed heterochromatin formation. *Genes to Cells* *17*, 218–233.
- Nakanishi, S., Lee, J.S., Gardner, K.E., Gardner, J.M., Takahashi, Y.H., Chandrasekharan, M.B., Sun, Z.W., Osley, M.A., Strahl, B.D., Jaspersen, S.L., et al. (2009). Histone H2BK123 monoubiquitination is the critical determinant for H3K4 and H3K79 trimethylation by COMPASS and Dot1. *J. Cell Biol.* *186*, 371–377.
- Nambodiri, V.M.H., Dutta, S., Akey, I.V., Head, J.F., and Akey, C.W. (2003). The crystal structure of Drosophila NLP-core provides insight into pentamer formation and histone binding. *Structure* *11*, 175–186.
- Natsume, R., Eitoku, M., Akai, Y., Sano, N., Horikoshi, M., and Senda, T. (2007). Structure and function of the histone chaperone CIA/ASF1 complexed with histones H3 and H4. *Nature* *446*, 338–341.
- Nelson, T., Wiegand, R., and Brutlag, D. (1981). Ribonucleic acid and other polyanions facilitate chromatin assembly in vitro. *Biochemistry* *20*, 2594–2601.
- Newman, D.R., Kuhn, J.F., Shanab, G.M., and Maxwell, E.S. (2000). Box C/D snoRNA-associated proteins: two pairs of evolutionarily ancient proteins and possible links to replication and transcription. *Rna* *6*, 861–879.
- Nguyen, V.T., Kiss, T., Michels, A.A., and Bensaude, O. (2001). 7SK small nuclear RNA binds to and inhibits the activity of CDK9/cyclin T complexes. *Nature* *414*, 322–325.
- Nickerson, J.A., Krochmalnic, G., Wan, K.M., and Penman, S. (1989). Chromatin architecture and nuclear RNA. *Proc. Natl. Acad. Sci. U.S.A.* *86*, 177–181.
- Nightingale, K.P., Wellinger, R.E., Sogo, J.M., and Becker, P.B. (1998). Histone acetylation facilitates RNA polymerase II transcription of the Drosophila hsp26 gene in chromatin. *Embo J.* *17*, 2865–2876.
- Nishino, Y., Eltsov, M., Joti, Y., Ito, K., Takata, H., Takahashi, Y., Hihara, S., Frangakis, A.S., Imamoto, N., Ishikawa, T., et al. (2012). Human mitotic chromosomes consist predominantly of irregularly folded nucleosome fibres without a 30-nm chromatin structure. *Embo J.* *31*, 1644–1653.
- Noguchi, K., Vassilev, A., Ghosh, S., Yates, J.L., and DePamphilis, M.L. (2006). The BAH domain facilitates the ability of human Orc1 protein to activate replication origins in vivo. *Embo J.* *25*, 5372–5382.
- Oda, H., Okamoto, I., Murphy, N., Chu, J., Price, S.M., Shen, M.M., Torres-Padilla, M.E., Heard, E., and Reinberg, D. (2009). Monomethylation of histone H4-lysine 20 is involved in chromosome structure and stability and is essential for mouse development. *Mol. Cell. Biol.* *29*, 2278–2295.
- Ohta, S., Bukowski-Wills, J.-C., Sanchez-Pulido, L., de Lima Alves, F., Wood, L., Chen, Z.A., Platani, M., Fischer, L., Hudson, D.F., Ponting, C.P., et al. (2010). The Protein Composition of Mitotic Chromosomes Determined Using Multiclassifier Combinatorial Proteomics. *Cell* *142*, 810–821.
- Ohta, S., Wood, L., Bukowski-Wills, J.-C., Rappsilber, J., and Earnshaw, W.C. (2011). Building mitotic chromosomes. *Current Opinion in Cell Biology* *23*, 114–121.
- Old, W.M., Meyer-Arendt, K., Aveline-Wolf, L., Pierce, K.G., Mendoza, A., Sevinsky, J.R., Resing, K.A., and Ahn, N.G. (2005). Comparison of label-free methods for quantifying human proteins by shotgun proteomics. *Mol. Cell Proteomics* *4*, 1487–1502.
- Olins, A.L., and Olins, D.E. (1974). Spheroid chromatin units (v bodies). *Science* *183*, 330–332.
- Olsen, J.V., de Godoy, L.M.F., Li, G., Macek, B., Mortensen, P., Pesch, R., Makarov, A., Lange, O., Horning, S., and Mann, M. (2005). Parts per million mass accuracy on an Orbitrap mass spectrometer via lock mass injection into a C-trap. *Mol. Cell Proteomics* *4*, 2010–2021.

REFERENCES

- Osley, M.A., Fleming, A.B., and Kao, C.-F. (2006). Histone ubiquitylation and the regulation of transcription. *Results Probl Cell Differ* 41, 47–75.
- Pardo, P.S. (2002). MRG15, a Novel Chromodomain Protein, Is Present in Two Distinct Multiprotein Complexes Involved in Transcriptional Activation. *Journal of Biological Chemistry* 277, 50860–50866.
- Peña, A.N., Tominaga, K., and Pereira-Smith, O.M. (2011). MRG15 activates the *cdc2* promoter via histone acetylation in human cells. *Experimental Cell Research* 317, 1534–1540.
- Pesavento, J.J., Bullock, C.R., LeDuc, R.D., Mizzen, C.A., and Kelleher, N.L. (2008). Combinatorial Modification of Human Histone H4 Quantitated by Two-dimensional Liquid Chromatography Coupled with Top Down Mass Spectrometry. *Journal of Biological Chemistry* 283, 14927–14937.
- Polo, S.E., Roche, D., and Almouzni, G. (2006). New histone incorporation marks sites of UV repair in human cells. *Cell* 127, 481–493.
- Quivy, J.P., Grandi, P., and Almouzni, G. (2001). Dimerization of the largest subunit of chromatin assembly factor 1: importance in vitro and during *Xenopus* early development. *Embo J.* 20, 2015–2027.
- Reeves, R., and Adair, J.E. (2005). Role of high mobility group (HMG) chromatin proteins in DNA repair. *DNA Repair* 4, 926–938.
- Reik, W., and Walter, J. (2001). Genomic imprinting: parental influence on the genome. *Nat Rev Genet* 2, 21–32.
- Richards, E.J., and Elgin, S.C.R. (2002). Epigenetic codes for heterochromatin formation and silencing: rounding up the usual suspects. *Cell* 108, 489–500.
- Rinn, J.L., Kertesz, M., Wang, J.K., Squazzo, S.L., Xu, X., Bruggmann, S.A., Goodnough, L.H., Helms, J.A., Farnham, P.J., Segal, E., et al. (2007). Functional Demarcation of Active and Silent Chromatin Domains in Human HOX Loci by Noncoding RNAs. *Cell* 129, 1311–1323.
- Rodríguez-Campos, A., and Azorín, F. (2007). RNA Is an Integral Component of Chromatin that Contributes to Its Structural Organization. *PLoS ONE* 2, e1182.
- Rogakou, E.P., and Sekeri-Pataryas, K.E. (1999). Histone variants of H2A and H3 families are regulated during in vitro aging in the same manner as during differentiation. *Exp* 34, 741–754.
- Rohrbaugh, M., Clore, A., Davis, J., Johnson, S., Jones, B., Jones, K., Kim, J., Kithuka, B., Lunsford, K., Mitchell, J., et al. (2013). Identification and Characterization of Proteins Involved in Nuclear Organization Using *Drosophila* GFP Protein Trap Lines. *PLoS ONE* 8, e53091.
- Sado, T. (2004). De novo DNA methylation is dispensable for the initiation and propagation of X chromosome inactivation. *Development* 131, 975–982.
- Scharf, A.N.D., Meier, K., Seitz, V., Kremmer, E., Brehm, A., and Imhof, A. (2009). Monomethylation of lysine 20 on histone H4 facilitates chromatin maturation. *Mol. Cell Biol.* 29, 57–67.
- Schmitz, K.M., Mayer, C., Postepska, A., and Grummt, I. (2010). Interaction of noncoding RNA with the rDNA promoter mediates recruitment of DNMT3b and silencing of rRNA genes. *Genes Dev.* 24, 2264–2269.
- Schotta, G., Sengupta, R., Kubicek, S., Malin, S., Kauer, M., Callén, E., Celeste, A., Pagani, M., Opravil, S., La Rosa-Velazquez, De, I.A., et al. (2008). A chromatin-wide transition to H4K20 monomethylation impairs genome integrity and programmed DNA rearrangements in the mouse. *Genes Dev.* 22, 2048–2061.
- Sambrook, J., and Russell, D. W. (2000). *Molecular Cloning: A Laboratory Manual*, 3 Vol. 0003rd ed. (Cold Spring Harbor Laboratory).
- Schubert, T., Pusch, M.C., Diermeier, S., Benes, V., Kremmer, E., Imhof, A., and Längst, G. (2012). Df31 protein and snoRNAs maintain accessible higher-order structures of chromatin. *Mol. Cell* 48, 434–444.
- Sexton, T., Yaffe, E., Kenigsberg, E., Bantignies, F., Leblanc, B., Hoichman, M., Parrinello, H., Tanay, A., and Cavalli, G. (2012). Three-Dimensional Folding and Functional Organization Principles of the *Drosophila* Genome. *Cell* 148, 458–472.
- Shevchenko, A., Chernushevich, I., Wilm, M., and Mann, M. (2000). De Novo peptide sequencing by nanoelectrospray tandem mass spectrometry using triple quadrupole and quadrupole/time-of-flight instruments. *Methods Mol. Biol.* 146, 1–16.
- Shibahara, K., and Stillman, B. (1999). Replication-dependent marking of DNA by PCNA facilitates CAF-1-coupled inheritance of chromatin. *Cell* 96, 575–585.
- Shimamura, A., and Worcel, A. (1989). The assembly of regularly spaced nucleosomes in the *Xenopus* oocyte S-150 extract is accompanied by deacetylation of histone H4. *J. Biol. Chem.* 264, 14524–14530.
- Shopland, L.S., Lynch, C.R., Peterson, K.A., Thornton, K., Kepper, N., Hase, J.V., Stein, S., Vincent, S., Molloy, K.R., Kreth, G., et al. (2006). Folding and organization of a contiguous chromosome region according to the gene distribution pattern in primary genomic sequence. *J. Cell Biol.* 174, 27–38.
- Shroff, R., Arbel-Eden, A., Pilch, D., Ira, G., Bonner, W.M., Petrini, J.H., Haber, J.E., and Lichten, M. (2004). Distribution and dynamics of chromatin modification induced by a defined DNA double-strand break. *Curr. Biol.* 14, 1703–1711.
- Sirbu, B.M., Couch, F.B., and Cortez, D. (2012). Monitoring the spatiotemporal dynamics of proteins at replication forks and

- in assembled chromatin using isolation of proteins on nascent DNA. *Nat Protoc* 7, 594–605.
- Smerdon, M.J. (1991). DNA repair and the role of chromatin structure. *Current Opinion in Cell Biology* 3, 422–428.
- Smith, C.L., and Peterson, C.L. (2005). A conserved Swi2/Snf2 ATPase motif couples ATP hydrolysis to chromatin remodeling. *Mol. Cell. Biol.* 25, 5880–5892.
- Smith, H.F., Roberts, M.A., Nguyen, H.Q., Peterson, M., Hartl, T.A., Wang, X.-J., Klebba, J.E., Rogers, G.C., and Bosco, G. (2013). Maintenance of interphase chromosome compaction and homolog pairing in *Drosophila* is regulated by the condensin cap-h2 and its partner mrg15. *Genetics* 195, 127–146.
- Smith, S., and Stillman, B. (1989). Purification and characterization of CAF-I, a human cell factor required for chromatin assembly during DNA replication in vitro. *Cell* 58, 15–25.
- Smits, A.H., Jansen, P.W.T.C., Poser, I., Hyman, A.A., and Vermeulen, M. (2012). Stoichiometry of chromatin-associated protein complexes revealed by label-free quantitative mass spectrometry-based proteomics. *Nucleic Acids Research* 41, e28–e28.
- Sobel, R.E., Cook, R.G., Perry, C.A., Annunziato, A.T., and Allis, C.D. (1995). Conservation of deposition-related acetylation sites in newly synthesized histones H3 and H4. *Proc. Natl. Acad. Sci. U.S.A.* 92, 1237–1241.
- Song, Y., He, F., Xie, G., Guo, X., Xu, Y., Chen, Y., Liang, X., Stagljar, I., Egli, D., Ma, J., et al. (2007). CAF-1 is essential for *Drosophila* development and involved in the maintenance of epigenetic memory. *Developmental Biology* 311, 213–222.
- Soria, G., Polo, S.E., and Almouzni, G. (2012). Prime, Repair, Restore: The Active Role of Chromatin in the DNA Damage Response. *Mol. Cell* 46, 722–734.
- Stedingk, von, K., Koster, J., Piqueras, M., Noguera, R., Navarro, S., Pählman, S., Versteeg, R., Ora, I., Gisselsson, D., Lindgren, D., et al. (2013). snoRNPs Regulate Telomerase Activity in Neuroblastoma and Are Associated with Poor Prognosis. *Transl Oncol* 6, 447–457.
- Stewart, A.F., Reik, A., and Schütz, G. (1991). A simpler and better method to cleave chromatin with DNase 1 for hypersensitive site analyses. *Nucleic Acids Research* 19, 3157.
- Strahl, B.D., and Allis, C.D. (2000). The language of covalent histone modifications. *Nature* 403, 41–45.
- Strahl, B.D., Briggs, S.D., Brame, C.J., Caldwell, J.A., Koh, S.S., Ma, H., Cook, R.G., Shabanowitz, J., Hunt, D.F., Stallcup, M.R., et al. (2001). Methylation of histone H4 at arginine 3 occurs in vivo and is mediated by the nuclear receptor coactivator PRMT1. *Curr. Biol.* 11, 996–1000.
- Straub, T., and Becker, P.B. (2011). Transcription modulation chromosome-wide: universal features and principles of dosage compensation in worms and flies. *Curr. Opin. Genet. Dev.* 21, 147–153.
- Sun, Z.-W., and Allis, C.D. (2002). Ubiquitination of histone H2B regulates H3 methylation and gene silencing in yeast. *Nature* 418, 104–108.
- Szöllösi, E., Bokor, M., Bodor, A., Perczel, A., Klement, E., Medzihradsky, K.F., Tompa, K., and Tompa, P. (2008). Intrinsic structural disorder of DF31, a *Drosophila* protein of chromatin decondensation and remodeling activities. *J. Proteome Res.* 7, 2291–2299.
- Tagami, H., Ray-Gallet, D., Almouzni, G., and Nakatani, Y. (2004). Histone H3.1 and H3.3 complexes mediate nucleosome assembly pathways dependent or independent of DNA synthesis. *Cell* 116, 51–61.
- Tan, M., Luo, H., Lee, S., Jin, F., Yang, J.S., Montellier, E., Buchou, T., Cheng, Z., Rousseaux, S., Rajagopal, N., et al. (2011). Identification of 67 Histone Marks and Histone Lysine Crotonylation as a New Type of Histone Modification. *Cell* 146, 1016–1028.
- Thoma, F., Koller, T., and Klug, A. (1979). Involvement of histone H1 in the organization of the nucleosome and of the salt-dependent superstructures of chromatin. *J. Cell Biol.* 83, 403–427.
- Thomas, J.O. (1999). Histone H1: location and role. *Current Opinion in Cell Biology* 11, 312–317.
- Thomas, J.O., and Kornberg, R.D. (1975). Cleavable cross-links in the analysis of histone-histone associations. *FEBS Letters* 58, 353–358.
- Torigoe, S.E., Patel, A., Khuong, M.T., Bowman, G.D., and Kadonaga, J.T. (2013). ATP-dependent chromatin assembly is functionally distinct from chromatin remodeling. *eLife* 2, e00863–e00863.
- Torrente, M.P., Zee, B.M., Young, N.L., Baliban, R.C., LeRoy, G., Floudas, C.A., Hake, S.B., and Garcia, B.A. (2011). Proteomic interrogation of human chromatin. *PLoS ONE* 6, e24747.
- Towbin, H., Staehelin, T., and Gordon, J. (1979). Electrophoretic transfer of proteins from polyacrylamide gels to nitrocellulose sheets: procedure and some applications. *Proc. Natl. Acad. Sci. U.S.A.* 76, 4350–4354.
- Tremethick, D.J. (2007). Higher-Order Structures of Chromatin: The Elusive 30 nm Fiber. *Cell* 128, 651–654.
- Tropberger, P., and Schneider, R. (2010). Going global: novel histone modifications in the globular domain of H3. *Epigenetics* 5, 112–117.
- Tropberger, P., Pott, S., Keller, C., Kamieniarz-Gdula, K., Caron, M., Richter, F., Li, G., Mittler, G., Liu, E.T., Bühler, M., et

REFERENCES

- al. (2013). Regulation of Transcription through Acetylation of H3K122 on the Lateral Surface of the Histone Octamer. *Cell* 152, 859–872.
- Trujillo, K.M., and Osley, M.A. (2012). A Role for H2B Ubiquitylation in DNA Replication. *Mol. Cell* 48, 734–746.
- Tsai, M.C., Manor, O., Wan, Y., Mosammamaparast, N., Wang, J.K., Lan, F., Shi, Y., Segal, E., and Chang, H.Y. (2010). Long Noncoding RNA as Modular Scaffold of Histone Modification Complexes. *Science* 329, 689–693.
- Tsukiyama, T., and Wu, C. (1995). Purification and properties of an ATP-dependent nucleosome remodeling factor. *Cell* 83, 1011–1020.
- Turner, B.M. (2002). Cellular memory and the histone code. *Cell* 111, 285–291.
- Van Holde, K. E. *Chromatin: Springer Series in Molecular Biology* (New York, Springer-Verlag, 1989).
- Vaquerizas, J.M., Suyama, R., Kind, J., Miura, K., Luscombe, N.M., and Akhtar, A. (2010). Nuclear pore proteins nup153 and megator define transcriptionally active regions in the Drosophila genome. *PLoS Genet* 6, e1000846.
- Varga-Weisz, P.D., Wilm, M., Bonte, E., Dumas, K., Mann, M., and Becker, P.B. (1997). Chromatin-remodelling factor CHRAC contains the ATPases ISWI and topoisomerase II. *Nature* 388, 598–602.
- Wagner, G., Bancaud, A., Quivy, J.-P., Clapier, C., Almouzni, G., and Viovy, J.-L. (2005). Compaction kinetics on single DNAs: purified nucleosome reconstitution systems versus crude extract. *Biophys. J.* 89, 3647–3659.
- Wang, G., Wu, W.W., Zeng, W., Chou, C.-L., and Shen, R.-F. (2006). Label-Free Protein Quantification Using LC-Coupled Ion Trap or FT Mass Spectrometry: Reproducibility, Linearity, and Application with Complex Proteomes. *J. Proteome Res.* 5, 1214–1223.
- Wang, H., Cao, R., Xia, L., Erdjument-Bromage, H., Borchers, C., Tempst, P., and Zhang, Y. (2001). Purification and functional characterization of a histone H3-lysine 4-specific methyltransferase. *Mol. Cell* 8, 1207–1217.
- Wang, K.C., Yang, Y.W., Liu, B., Sanyal, A., Corces-Zimmerman, R., Chen, Y., Lajoie, B.R., Protacio, A., Flynn, R.A., Gupta, R.A., et al. (2012). A long noncoding RNA maintains active chromatin to coordinate homeotic gene expression. *Nature* 472, 120–124.
- Wang, W., Zhou, H., Lin, H., Roy, S., Shaler, T.A., Hill, L.R., Norton, S., Kumar, P., Anderle, M., and Becker, C.H. (2003). Quantification of Proteins and Metabolites by Mass Spectrometry without Isotopic Labeling or Spiked Standards. *Anal. Chem.* 75, 4818–4826.
- Wang, Y., Wysocka, J., Perlin, J.R., Leonelli, L., Allis, C.D., and Coonrod, S.A. (2004). Linking Covalent Histone Modifications to Epigenetics: The Rigidity and Plasticity of the Marks. *Cold Spring Harbor Symposia on Quantitative Biology* 69, 161–170.
- Watkins, N.J., and Bohnsack, M.T. (2011). The box C/D and H/ACA snoRNPs: key players in the modification, processing and the dynamic folding of ribosomal RNA. *WIREs RNA* 3, 397–414.
- Watkins, N.J., Newman, D.R., Kuhn, J.F., and Maxwell, E.S. (1998). In vitro assembly of the mouse U14 snoRNP core complex and identification of a 65-kDa box C/D-binding protein. *Rna* 4, 582–593.
- Weake, V.M., and Workman, J.L. (2008). Clearing the way for unpaused polymerases. *Cell* 134, 16–18.
- Wen, P., Quan, Z., and Xi, R. (2012). The biological function of the WD40 repeat-containing protein p55/Caf1 in Drosophila. *Dev. Dyn.* 241, 455–464.
- White, A.E., Leslie, M.E., Calvi, B.R., Marzluff, W.F., and Duronio, R.J. (2007). Developmental and cell cycle regulation of the Drosophila histone locus body. *Mol. Biol. Cell* 18, 2491–2502.
- Widom, J. (1998). Chromatin structure: linking structure to function with histone H1. *Curr. Biol.* 8, R788–R791.
- Wilm, M., Shevchenko, A., Houthaeve, T., Breit, S., Schweigerer, L., Fotsis, T., and Mann, M. (1996). Femtomole sequencing of proteins from polyacrylamide gels by nano-electrospray mass spectrometry. *Nature* 379, 466–469.
- Wiśniewski, J.R., Zougman, A., Nagaraj, N., and Mann, M. (2009). Universal sample preparation method for proteome analysis. *Nat Meth* 6, 359–362.
- Wood, A., Krogan, N.J., Dover, J., Schneider, J., Heidt, J., Boateng, M.A., Dean, K., Golshani, A., Zhang, Y., Greenblatt, J.F., et al. (2003). Bre1, an E3 ubiquitin ligase required for recruitment and substrate selection of Rad6 at a promoter. *Mol. Cell* 11, 267–274.
- Woodcock, C.L., Frado, L.L., and Rattner, J.B. (1984). The higher-order structure of chromatin: evidence for a helical ribbon arrangement. *J. Cell Biol.* 99, 42–52.
- Woodcock, C.L., Safer, J.P., and Stanchfield, J.E. (1976). Structural repeating units in chromatin. I. Evidence for their general occurrence. *Experimental Cell Research* 97, 101–110.
- Worby, C.A., Simonson-Leff, N., and Dixon, J.E. (2001). RNA interference of gene expression (RNAi) in cultured Drosophila cells. *Sci. STKE* 2001, p11.
- Worcel, A., Han, S., and Wong, M.L. (1978). Assembly of newly replicated chromatin. *Cell* 15, 969–977.
- Worcel, A., Strogatz, S., and Riley, D. (1981). Structure of chromatin and the linking number of DNA. *Proc. Natl. Acad. Sci.*

U.S.a. 78, 1461–1465.

Xu, M., Long, C., Chen, X., Huang, C., Chen, S., and Zhu, B. (2010). Partitioning of Histone H3-H4 Tetramers During DNA Replication-Dependent Chromatin Assembly. *Science* 328, 94–98.

Yang, Z., Zhu, Q., Luo, K., and Zhou, Q. (2001). The 7SK small nuclear RNA inhibits the CDK9/cyclin T1 kinase to control transcription. *Nature* 414, 317–322.

Yochum, G.S., and Ayer, D.E. (2002). Role for the mortality factors MORF4, MRGX, and MRG15 in transcriptional repression via associations with Pf1, mSin3A, and Transducin-Like Enhancer of Split. *Mol. Cell. Biol.* 22, 7868–7876.

Zhang, G., Fenyő, D., and Neubert, T.A. (2009). Evaluation of the Variation in Sample Preparation for Comparative Proteomics Using Stable Isotope Labeling by Amino Acids in Cell Culture. *J. Proteome Res.* 8, 1285–1292.

Zhang, H., Li, Y., Yang, J., Tominaga, K., Pereira-Smith, O.M., and Tower, J. (2010). Conditional inactivation of MRG15 gene function limits survival during larval and adult stages of *Drosophila melanogaster*. *Exg* 45, 825–833.

Zhang, Z., Wippo, C.J., Wal, M., Ward, E., Korber, P., and Pugh, B.F. (2011). A Packing Mechanism for Nucleosome Organization Reconstituted Across a Eukaryotic Genome. *Science* 332, 977–980.

Zhao, J., Sun, B.K., Erwin, J.A., Song, J.-J., and Lee, J.T. (2008). Polycomb proteins targeted by a short repeat RNA to the mouse X chromosome. *Science* 322, 750–756.

Zheng, C. (2003). Intra- and Inter-nucleosomal Protein-DNA Interactions of the Core Histone Tail Domains in a Model System. *Journal of Biological Chemistry* 278, 24217–24224.

Zheng, C. (2005). Salt-dependent Intra- and Internucleosomal Interactions of the H3 Tail Domain in a Model Oligonucleosomal Array. *Journal of Biological Chemistry* 280, 33552–33557.

Zhu, Q., Wani, G., Arab, H.H., El-Mahdy, M.A., Ray, A., and Wani, A.A. (2009). Chromatin restoration following nucleotide excision repair involves the incorporation of ubiquitinated H2A at damaged genomic sites. *DNA Repair* 8, 262–273.

Zlatanova, J., Seebart, C., and Tomschik, M. (2007). Nap1: taking a closer look at a juggler protein of extraordinary skills. *Faseb J.* 21, 1294–1310.

REFERENCES

APPENDIX

APPENDIX

List 1: Kinetics of chromatin-binding proteins

Flybase Identifier	Name	Log₂(iBAQ1h/4h)	Flybase Identifier	Name	Log₂(iBAQ1h/4h)
FBpp0077427	Rad1	21.01	FBpp0071252	ric8a	16.26
FBpp0071295	RpS28b	20.54	FBpp0083435	CG17282	16.25
FBpp0078516	Hus1-like	19.90	FBpp0084842	CG1972	16.22
FBpp0070457	eIF2B-beta	19.87	FBpp0072216	CG3511	16.18
FBpp0084573	wdb	19.58	FBpp0086269	RpS15	16.18
FBpp0075700	eIF-2beta	19.16	FBpp0075353	CG7945	16.16
FBpp0080951	CG31673	19.14	FBpp0070862	wuho	16.15
FBpp0073558	CG12096	18.74	FBpp0073283	Vago	16.14
FBpp0077868	CG4858	18.69	FBpp0083802	RpS3	16.09
FBpp0084067	Rpb10	18.65	FBpp0075618	RpS4	16.07
FBpp0084816	Obp99a	18.63	FBpp0085673	Obp56d	16.06
FBpp0290815	CG32438	18.59	FBpp0075348	mrn	16.05
FBpp0081614	RpS29	18.52	FBpp0084342	CG14544	16.03
FBpp0075314	CG7427	18.43	FBpp0082134	Su(fu)	16.00
FBpp0290125	CG18586	18.41	FBpp0085735	cer	15.89
FBpp0088565	eIF-3p66	18.35	FBpp0083195	Nup58	15.89
FBpp0074847	Rad9	18.31	FBpp0083823	CG4408	15.89
FBpp0086397	CG8400	18.20	FBpp0082285	flfl	15.82
FBpp0077235	CG16712	18.17	FBpp0083729	Gclm	15.81
FBpp0087869	pnut	18.14	FBpp0079514	Taf11	15.79
FBpp0289558	CG7656	18.13	FBpp0078144	Ddx1	15.75
FBpp0087901	Vps28	18.12	FBpp0087651	Su(var)2-10	15.74
FBpp0071923	eIF2B-delta	18.08	FBpp0074841	CSN1b	15.71
FBpp0081324	eIF4AIII	18.00	FBpp0076723	CG13298	15.70
FBpp0083740	CG6697	17.97	FBpp0072168	CG3362	15.68
FBpp0086223	Fen1	17.92	FBpp0271847	CG13142	15.65
FBpp0087038	CG8525	17.88	FBpp0074859	Chmp1	15.62
FBpp0079187	Rack1	17.84	FBpp0072056	thoc5	15.56
FBpp0070543	CG10802	17.82	FBpp0271922	dgt3	15.53
FBpp0082042	GstD3	17.78	FBpp0082183	CG7966	15.51
FBpp0082465	RpS5b	17.64	FBpp0071248	Dsor1	15.51
FBpp0099686	RpS8	17.50	FBpp0089262	Adf1	15.51
FBpp0111673	CG34455	17.46	FBpp0083854	CG10214	15.47
FBpp0083057	fray	17.45	FBpp0079899	CG18789	15.46
FBpp0079861	CG14935	17.40	FBpp0290492	Clbn	15.29
FBpp0072955	CG17746	17.40	FBpp0084626	CG4849	15.22
FBpp0075088	TSG101	17.33	FBpp0084786	Cul-5	15.20
FBpp0072072	Adk2	17.32	FBpp0075107	PGRP-SB1	15.19
FBpp0071173	CG12659	17.27	FBpp0073784	Lsd-2	15.13
FBpp0086120	CG6805	17.25	FBpp0074799	CG10419	15.09
FBpp0086701	RpS23	17.24	FBpp0075450	mop	15.07
FBpp0075938	APP-BP1	17.20	FBpp0073330	CG32667	15.05
FBpp0075751	thoc6	17.19	FBpp0074544	Grip84	14.92
FBpp0072021	pita	17.18	FBpp0110242	CG16863	14.92
FBpp0073947	eIF5	17.17	FBpp0087711	Pmm45A	14.87
FBpp0083376	RpS30	17.12	FBpp0112608	Parp	14.71
FBpp0088643	cerv	17.03	FBpp0088381	lola	14.71
FBpp0084927	CG7946	16.97	FBpp0111447	Vml	14.65
FBpp0072614	Rac1	16.85	FBpp0079496	CG5899	14.65
FBpp0083958	CG5524	16.76	FBpp0086998	muskelin	14.64
FBpp0076818	CG5537	16.57	FBpp0080649	Grip71	14.61
FBpp0077979	CG10565	16.46	FBpp0071703	GM130	14.57
FBpp0078645	CG31919	16.45	FBpp0087115	RpS11	14.50
FBpp0072457	MED30	16.40	FBpp0085420	sxc	14.48
FBpp0087063	CG8831	16.39	FBpp0074906	CG7430	14.14
FBpp0083564	Rpl12	16.39	FBpp0110543	CG12547	14.04
FBpp0072425	thoc7	16.36	FBpp0073666	Clic	13.95

Flybase Identifier	Name	Log₂(iBAQ1h/4h)	Flybase Identifier	Name	Log₂(iBAQ1h/4h)
FBpp0073672	I(1)dd4	13.94	FBpp0078150	Aats-ile	2.96
FBpp0085354	CG7843	13.63	FBpp0087757	CG8235	2.91
FBpp0085427	CG10417	13.55	FBpp0086097	eIF3-S9	2.90
FBpp0077236	CG16713	13.53	FBpp0078425	Mms19	2.85
FBpp0291369	CG42616	13.48	FBpp0086010	iclN	2.76
FBpp0087091	CG8378	13.34	FBpp0073965	Aats-arg	2.75
FBpp0075313	AGO2	13.04	FBpp0083800	DNApol-epsilon	2.73
FBpp0080197	CG33090	12.96	FBpp0083769	cdc16	2.72
FBpp0070857	fs(1)M3	12.90	FBpp0084240	Aats-gln	2.71
FBpp0076822	Bre1	12.87	FBpp0072839	CG1240	2.67
FBpp0082387	pr-set7	12.85	FBpp0071301	Aats-lys	2.67
FBpp0084784	yemalpha	12.74	FBpp0087648	tsu	2.66
FBpp0070336	eIF2B-epsilon	12.73	FBpp0079500	sop	2.65
FBpp0073835	CG12608	12.66	FBpp0086705	Tango7	2.64
FBpp0288801	CG14616	12.62	FBpp0078625	DhpD	2.63
FBpp0113081	Taf4	12.59	FBpp0078584	eIF3-S10	2.62
FBpp0071097	CG2175	12.08	FBpp0082137	mbo	2.61
FBpp0083670	CG31156	11.77	FBpp0080890	Arc4	2.61
FBpp0089369	CG17603	11.76	FBpp0080111	p38b	2.58
FBpp0073681	Ndc80	11.45	FBpp0112438	Dbp80	2.58
FBpp0083366	CG17838	11.43	FBpp0073872	CG9281	2.56
FBpp0075122	spd-2	11.28	FBpp0078777	Gpdh	2.55
FBpp0072808	MEP-1	11.26	FBpp0076284	pix	2.55
FBpp0082180	CG7855	10.47	FBpp0076708	Trn	2.54
FBpp0081439	CG11970	10.41	FBpp0079701	Dpy-30L1	2.54
FBpp0076452	RecQ4	9.79	FBpp0290160	CG1801	2.53
FBpp0072043	CG5591	7.94	FBpp0074086	RpS19a	2.52
FBpp0073898	CG8184	6.40	FBpp0076353	CG6831	2.48
FBpp0084048	CG5794	5.66	FBpp0076467	Srp9	2.46
FBpp0078978	CG3430	4.55	FBpp0072693	alphaCop	2.44
FBpp0089153	smid	4.50	FBpp0288780	Cap-G	2.44
FBpp0071049	Ykt6	4.45	FBpp0085156	CG1569	2.42
FBpp0081284	Tom34	4.17	FBpp0086690	SelD	2.42
FBpp0081675	Fmr1	4.17	FBpp0074708	CG9330	2.41
FBpp0071685	Vps35	4.07	FBpp0075833	PCID2	2.41
FBpp0074318	Arp8	4.01	FBpp0082605	CG6045	2.41
FBpp0070883	PpV	3.84	FBpp0081896	CG10535	2.41
FBpp0081124	MAGE	3.73	FBpp0087510	CCS	2.40
FBpp0072142	wibg	3.70	FBpp0074425	CG7322	2.37
FBpp0083238	psidin	3.68	FBpp0070404	Vinc	2.36
FBpp0289479	Rpb4	3.49	FBpp0071969	CG30185	2.35
FBpp0086665	CG8503	3.48	FBpp0083939	CHORD	2.33
FBpp0076867	CG4603	3.47	FBpp0077502	CG7261	2.32
FBpp0087124	CG8877	3.44	FBpp0084828	Obp99b	2.30
FBpp0086812	drk	3.44	FBpp0290145	CG30122	2.28
FBpp0075318	CG12304	3.43	FBpp0075272	Arf72A	2.27
FBpp0080009	CG9934	3.43	FBpp0081255	lds	2.26
FBpp0083551	fit	3.40	FBpp0084780	CG11882	2.25
FBpp0081493	CG11964	3.36	FBpp0074480	Nat1	2.23
FBpp0079804	CENP-meta	3.35	FBpp0079167	poe	2.23
FBpp0075952	Ufd1-like	3.31	FBpp0071144	CG1440	2.22
FBpp0072658	CG12018	3.28	FBpp0071067	Ubc-E2H	2.19
FBpp0071150	Cp36	3.27	FBpp0080880	barr	2.18
FBpp0074418	CG7332	3.20	FBpp0079635	SmB	2.18
FBpp0070347	trr	3.18	FBpp0073003	eIF5B	2.15
FBpp0084818	CAP-D2	3.17	FBpp0070430	CG8636	2.15
FBpp0077307	oho23B	3.10	FBpp0072151	Ssrp	2.14
FBpp0071237	Dip1	3.05	FBpp0087116	CG8858	2.12
FBpp0085809	CG15100	3.05	FBpp0086591	SMC2	2.10
FBpp0072674	CG2021	2.98	FBpp0075399	Msh6	2.10
FBpp0071296	Hex-A	2.97	FBpp0072616	Klp61F	2.10
FBpp0086897	Aats-asp	2.96	FBpp0072041	CG5602	2.09

APPENDIX

Flybase Identifier	Name	Log₂(iBAQ1h/4h)	Flybase Identifier	Name	Log₂(iBAQ1h/4h)
FBpp0083898	Aats-glupro	2.09	FBpp0080905	La	1.68
FBpp0070355	deltaCOP	2.08	FBpp0288398	Dsp1	1.67
FBpp0082177	pic	2.06	FBpp0073235	CG17333	1.67
FBpp0085202	faf	2.05	FBpp0076408	msk	1.67
FBpp0074578	CG12702	2.05	FBpp0071138	CG2263	1.65
FBpp0079417	borr	2.05	FBpp0083245	CG4390	1.65
FBpp0086353	Rho1	2.04	FBpp0070723	Cdk7	1.63
FBpp0082110	CG6359	2.03	FBpp0084452	CG31075	1.63
FBpp0085195	CG1890	2.03	FBpp0077018	Obp19c	1.63
FBpp0099896	zip	2.03	FBpp0080062	Ski6	1.61
FBpp0088428	sw	2.03	FBpp0078465	CG12163	1.61
FBpp0074348	betaCop	2.02	FBpp0079059	ade3	1.61
FBpp0087164	ERp60	2.00	FBpp0076124	UbcD4	1.61
FBpp0074121	CG9099	1.98	FBpp0076693	nudel	1.61
FBpp0085155	gammaCop	1.97	FBpp0070720	Rnp4F	1.60
FBpp0086317	Vha44	1.93	FBpp0083741	CG6726	1.60
FBpp0073552	CG2200	1.93	FBpp0082198	granny-smith	1.60
FBpp0081460	Aats-trp	1.93	FBpp0086373	Aats-cys	1.60
FBpp0079951	Elf	1.93	FBpp0072743	dre4	1.60
FBpp0082987	14-3-3epsilon	1.92	FBpp0077501	GlyP	1.59
FBpp0076433	CG7185	1.92	FBpp0073975	Paf-AHalpha	1.59
FBpp0082849	Det	1.91	FBpp0082298	CG9286	1.58
FBpp0087227	san	1.91	FBpp0075083	CG9705	1.58
FBpp0080489	glu	1.90	FBpp0075073	CG32164	1.58
FBpp0082264	rin	1.90	FBpp0100139	NAT1	1.57
FBpp0072756	CG2034	1.89	FBpp0073966	Chc	1.57
FBpp0089115	groucho	1.88	FBpp0088028	CG30499	1.57
FBpp0071497	mago	1.86	FBpp0082985	CG7998	1.57
FBpp0070320	CG4199	1.85	FBpp0080825	Top2	1.56
FBpp0070279	sta	1.83	FBpp0074918	CG5290	1.56
FBpp0073474	Usp7	1.82	FBpp0081484	CG11985	1.56
FBpp0085254	Cul-2	1.82	FBpp0075100	CG9674	1.55
FBpp0112273	CG30118	1.81	FBpp0076270	Argk	1.55
FBpp0080769	gammaTub37C	1.81	FBpp0071423	ras	1.55
FBpp0082085	CG10038	1.81	FBpp0079648	RnrL	1.55
FBpp0081351	Sgt1	1.80	FBpp0085085	Npc2g	1.54
FBpp0075104	Int6	1.79	FBpp0088040	CG11107	1.54
FBpp0076312	Mcm7	1.79	FBpp0288680	Rrp1	1.53
FBpp0079643	CG5366	1.78	FBpp0087724	sec31	1.53
FBpp0099759	CG10973	1.77	FBpp0083584	CG6028	1.53
FBpp0290194	GS	1.77	FBpp0085850	GstE1	1.53
FBpp0079247	Snx6	1.77	FBpp0070637	CG6133	1.52
FBpp0075683	Klc	1.77	FBpp0070041	Ckllalpha	1.51
FBpp0077424	Drp1	1.76	FBpp0087760	Pgi	1.51
FBpp0082584	Su(var)3-9	1.76	FBpp0072164	spag	1.51
FBpp0082743	CSN5	1.74	FBpp0071503	Xpd	1.50
FBpp0078279	CG1218	1.74	FBpp0078948	CG11329	1.49
FBpp0088899	Tm1	1.74	FBpp0080262	vas	1.49
FBpp0083912	TfIIA-S	1.74	FBpp0080484	Cas	1.49
FBpp0073538	ade5	1.73	FBpp0081767	Fdh	1.48
FBpp0076451	Nmt	1.72	FBpp0081261	Prat	1.48
FBpp0079278	emb	1.72	FBpp0084525	TfIIA-L	1.47
FBpp0075153	Smn	1.72	FBpp0074608	polo	1.47
FBpp0074690	Rab8	1.72	FBpp0077106	CG2976	1.46
FBpp0078463	CG12173	1.71	FBpp0076960	CG1532	1.46
FBpp0084267	CG4673	1.70	FBpp0073297	Dlic	1.46
FBpp0087897	Cul-4	1.70	FBpp0081398	CG8223	1.46
FBpp0072608	msd5	1.70	FBpp0070041	Ckllalpha	1.51
FBpp0078342	Rheb	1.69	FBpp0087760	Pgi	1.51
FBpp0085467	CG9436	1.69	FBpp0072164	spag	1.51
FBpp0078359	sec23	1.69	FBpp0071503	Xpd	1.50
FBpp0081862	Ranbp9	1.68	FBpp0078948	CG11329	1.49

APPENDIX

Flybase Identifier	Name	Log₂(iBAQ1h/4h)	Flybase Identifier	Name	Log₂(iBAQ1h/4h)
FBpp0080262	vas	1.49	FBpp0071213	Moe	1.32
FBpp0080484	Cas	1.49	FBpp0073600	CG1640	1.32
FBpp0081767	Fdh	1.48	FBpp0084367	Ald	1.31
FBpp0081261	Prat	1.48	FBpp0072144	eIF6	1.31
FBpp0084525	TfIIA-L	1.47	FBpp0073551	lic	1.31
FBpp0074608	polo	1.47	FBpp0078850	ade2	1.31
FBpp0077106	CG2976	1.46	FBpp0083036	CG12321	1.30
FBpp0076960	CG1532	1.46	FBpp0288532	CG3523	1.30
FBpp0073297	Dlic	1.46	FBpp0075989	CG8003	1.30
FBpp0081398	CG8223	1.46	FBpp0071470	CG10527	1.30
FBpp0086847	Aats-val	1.46	FBpp0085915	pAbp	1.30
FBpp0080494	VhaSFD	1.45	FBpp0081628	Art4	1.29
FBpp0112333	CG32068	1.45	FBpp0077716	RpLP1	1.29
FBpp0078317	CG2046	1.44	FBpp0088055	dpa	1.29
FBpp0085258	CG1416	1.44	FBpp0070425	mit(1)15	1.29
FBpp0086845	CG33138	1.44	FBpp0085950	CG5721	1.29
FBpp0070118	skpA	1.44	FBpp0073847	Ahcy13	1.29
FBpp0079565	me31B	1.44	FBpp0088069	p47	1.29
FBpp0085529	ubl	1.43	FBpp0079992	CG5525	1.29
FBpp0079462	und	1.42	FBpp0074800	CG10424	1.29
FBpp0073445	Hsc70-3	1.42	FBpp0076937	CG1753	1.29
FBpp0078327	CG2091	1.42	FBpp0291066	CG30410	1.29
FBpp0289825	ATPCL	1.41	FBpp0087140	Mtor	1.29
FBpp0087398	trsn	1.41	FBpp0086328	Khc	1.28
FBpp0082496	CG6904	1.40	FBpp0076819	mad2	1.28
FBpp0073444	CG1578	1.40	FBpp0082998	CG7671	1.28
FBpp0073215	Dhc64C	1.39	FBpp0085585	RpS18	1.28
FBpp0078664	Rpn11	1.39	FBpp0070969	CG4593	1.28
FBpp0088438	Aprt	1.39	FBpp0078278	Rpn5	1.27
FBpp0077351	CG17259	1.39	FBpp0083371	RpS20	1.27
FBpp0081317	Mcm2	1.39	FBpp0085891	Atg7	1.27
FBpp0076359	RpL14	1.38	FBpp0083440	r-l	1.26
FBpp0075111	zetaCOP	1.38	FBpp0084242	RpS27	1.25
FBpp0073554	CG15717	1.38	FBpp0081331	DppIII	1.25
FBpp0078086	Rpb8	1.38	FBpp0080733	Nedd8	1.24
FBpp0088035	Incenp	1.38	FBpp0072932	PHGPx	1.24
FBpp0081736	lrp-1B	1.37	FBpp0079999	Vha68-2	1.23
FBpp0083683	T-cp1	1.37	FBpp0085374	CG17337	1.23
FBpp0085889	Eip55E	1.37	FBpp0074386	CG6617	1.23
FBpp0083851	Nup98	1.37	FBpp0070913	Mcm6	1.23
FBpp0075498	Gl	1.37	FBpp0076215	eIF-4E	1.23
FBpp0111371	CG34261	1.36	FBpp0072583	Psa	1.23
FBpp0075277	DNApol-delta	1.36	FBpp0080705	Aats-asn	1.22
FBpp0075834	CG18815	1.35	FBpp0079399	Cks30A	1.22
FBpp0078009	CG7519	1.35	FBpp0079577	CG4968	1.22
FBpp0081800	Sodh-2	1.35	FBpp0073292	Rpt3	1.22
FBpp0081756	Mcm5	1.35	FBpp0072419	Tudor-SN	1.22
FBpp0086072	CG4802	1.35	FBpp0099885	UGP	1.22
FBpp0084849	CG7789	1.35	FBpp0087774	Vps25	1.21
FBpp0084754	Rpn2	1.35	FBpp0071822	CycB	1.21
FBpp0073173	Rpd3	1.35	FBpp0079914	Aats-thr	1.21
FBpp0077741	lwr	1.35	FBpp0075282	CG5931	1.21
FBpp0110179	CG34132	1.34	FBpp0087367	CG17765	1.21
FBpp0083647	CG7054	1.34	FBpp0078561	growl	1.20
FBpp0074715	asf1	1.34	FBpp0083859	CG10225	1.20
FBpp0088252	Rfabg	1.34	FBpp0078667	eIF-3p40	1.20
FBpp0291025	Alg-2	1.33	FBpp0083860	Rpn9	1.20
FBpp0077143	Gs1l	1.33	FBpp0070953	CG3226	1.20
FBpp0086887	TpplI	1.33	FBpp0085265	Ef2b	1.20
FBpp0082065	Aos1	1.32	FBpp0076376	CG6662	1.20
FBpp0110481	CG40045	1.32	FBpp0083687	Rpn7	1.19

APPENDIX

Flybase Identifier	Name	Log₂(iBAQ1h/4h)	Flybase Identifier	Name	Log₂(iBAQ1h/4h)
FBpp0085619	mus209	1.19	FBpp0100079	Prx5	1.08
FBpp0083872	CG10184	1.19	FBpp0086877	CG4646	1.08
FBpp0077487	CG10882	1.19	FBpp0074502	CG14207	1.07
FBpp0086895	bic	1.19	FBpp0075754	CG5642	1.07
FBpp0074366	Aats-his	1.19	FBpp0079640	CG5362	1.07
FBpp0099974	Pp2A-29B	1.19	FBpp0083413	Rab11	1.07
FBpp0083434	slmb	1.19	FBpp0290556	bur	1.07
FBpp0289426	nbs	1.19	FBpp0085724	Elongin-C	1.07
FBpp0087660	CG11784	1.18	FBpp0079809	CG6287	1.07
FBpp0082240	poly	1.18	FBpp0078500	Karybeta3	1.06
FBpp0079303	lmg	1.18	FBpp0088362	CG10638	1.06
FBpp0087935	CSN4	1.18	FBpp0080121	Rpll33	1.06
FBpp0074069	Pp2B-14D	1.17	FBpp0070368	Pgd	1.06
FBpp0110305	chn	1.17	FBpp0075386	Aats-gly	1.06
FBpp0070729	Mcm3	1.17	FBpp0088021	Rpt1	1.06
FBpp0070484	CG3939	1.17	FBpp0081401	Tcp-1eta	1.06
FBpp0078357	CG12171	1.17	FBpp0078754	Hel25E	1.06
FBpp0084087	CG11089	1.17	FBpp0079468	FKBP59	1.06
FBpp0074558	Bap	1.17	FBpp0076258	Dhpr	1.05
FBpp0084150	vig2	1.17	FBpp0072197	Mov34	1.05
FBpp0099859	CG6664	1.16	FBpp0071386	PPP4R2r	1.05
FBpp0073438	CG2025	1.16	FBpp0076145	CG6767	1.05
FBpp0087764	CG8258	1.16	FBpp0083906	Pros26.4	1.05
FBpp0081370	CG8036	1.16	FBpp0084591	btz	1.05
FBpp0110460	CG17493	1.16	FBpp0075513	Hsc70Cb	1.05
FBpp0082139	Vha55	1.16	FBpp0077831	eRF1	1.05
FBpp0088085	CG1707	1.15	FBpp0072083	RpL12	1.05
FBpp0081374	bel	1.15	FBpp0080509	ApepP	1.05
FBpp0099808	Mi-2	1.15	FBpp0079490	Apf	1.05
FBpp0071218	CG2004	1.15	FBpp0086057	CG30105	1.05
FBpp0070792	CG3011	1.15	FBpp0075247	Pgm	1.05
FBpp0088256	Arf102F	1.15	FBpp0088892	tacc	1.04
FBpp0085876	CG5224	1.14	FBpp0070572	CG2947	1.04
FBpp0078319	CG2051	1.14	FBpp0079637	CG5355	1.04
FBpp0072660	Cdc37	1.14	FBpp0077551	Rrp40	1.04
FBpp0083354	Elongin-B	1.14	FBpp0074151	SmG	1.04
FBpp0073902	Tcp-1zeta	1.14	FBpp0072050	Tal	1.04
FBpp0088004	CanB2	1.14	FBpp0087583	Uba1	1.04
FBpp0075693	CG10688	1.13	FBpp0076890	Pros45	1.04
FBpp0079262	CSN8	1.13	FBpp0079458	Gdi	1.04
FBpp0078684	CG8891	1.13	FBpp0079641	cdc2	1.03
FBpp0074331	Tsf1	1.12	FBpp0075870	CG6084	1.03
FBpp0076727	CG10289	1.11	FBpp0076445	CG7375	1.03
FBpp0110163	CG3689	1.11	FBpp0079326	Aats-ala	1.03
FBpp0074662	Rpn1	1.11	FBpp0077363	Ts	1.03
FBpp0075686	CG10418	1.11	FBpp0082989	14-3-3epsilon	1.02
FBpp0290264	CG31368	1.11	FBpp0075168	Aats-tyr	1.02
FBpp0290694	msps	1.11	FBpp0071184	Sptr	1.01
FBpp0079381	alien	1.11	FBpp0077749	CG11885	1.01
FBpp0099676	CG7215	1.11	FBpp0088368	Inos	1.01
FBpp0082299	Dip-B	1.11	FBpp0087821	CSN7	1.01
FBpp0073327	ran	1.10	FBpp0088454	CG31120	1.01
FBpp0082787	Cctgamma	1.10	FBpp0074500	RpS10b	1.00
FBpp0113083	CG6852	1.10	FBpp0089041	Prosalph7	1.00
FBpp0083986	CG6364	1.10	FBpp0084021	CG5706	1.00
FBpp0087335	Taf5	1.10	FBpp0076894	dod	0.99
FBpp0077790	Hop	1.09	FBpp0084759	CG11899	0.99
FBpp0071226	CG7033	1.09	FBpp0072703	CG13926	0.99
FBpp0081260	CG2846	1.09	FBpp0073331	Klp10A	0.98
FBpp0084995	Fer1HCH	1.09	FBpp0072976	CG12082	0.98
FBpp0288410	wac	1.09	FBpp0075238	PDCD-5	0.98
FBpp0087095	Cct5	1.09	FBpp0075581	flr	0.98

APPENDIX

Flybase Identifier	Name	Log₂(iBAQ1h/4h)	Flybase Identifier	Name	Log₂(iBAQ1h/4h)
FBpp0084824	Pcd	0.98	FBpp0111860	CG13373	0.94
FBpp0076827	CG10576	0.98	FBpp0077516	Uch	0.94
FBpp0080922	Fs(2)Ket	0.98	FBpp0084962	janA	0.94
FBpp0078349	Vha26	0.97	FBpp0087354	Prx2540-2	0.94
FBpp0072341	CG16936	0.97	FBpp0087479	TER94	0.94
FBpp0079746	dUTPase	0.97	FBpp0076460	Arp66B	0.94
FBpp0076600	Cdc27	0.97	FBpp0080048	betaCop	0.93
FBpp0081606	PpD3	0.97	FBpp0083843	Tbp-1	0.93
FBpp0073989	Pros28.1	0.97	FBpp0288790	lqfR	0.93
FBpp0082219	Droj2	0.97	FBpp0071115	Trxr-1	0.93
FBpp0078356	CG31549	0.97	FBpp0088675	rudimentary	0.93
FBpp0077571	Eno	0.96	FBpp0078093	CycH	0.92
FBpp0082816	CG3590	0.96	FBpp0077549	cpb	0.92
FBpp0077419	Pgk	0.96	FBpp0076883	CG10673	0.92
FBpp0080535	Sgt	0.96	FBpp0086971	Nacalphi	0.92
FBpp0071625	HmgD	0.96	FBpp0084810	alph	0.92
FBpp0085035	CG2246	0.95	FBpp0084948	Tpi	0.91
FBpp0083611	PyK	0.95	FBpp0082384	Rpll15	0.91
FBpp0085690	CG11242	0.95	FBpp0071350	CG2990	0.91
FBpp0078806	eIF-4a	0.95	FBpp0071587	CG10306	0.90
FBpp0078024	Pros54	0.95	FBpp0073649	CG11134	0.90
FBpp0087756	FANCI	0.95	FBpp0086732	CG13350	0.90
FBpp0085564	rig	0.95	FBpp0077168	CG3714	0.90
FBpp0078816	CG9135	0.95	FBpp0084497	CG31063	0.90
FBpp0087861	CG2158	0.95	FBpp0070432	Klp3A	0.89
FBpp0290811	shibire	0.94	FBpp0073561	REG	0.89
FBpp0086370	Got1	0.94	FBpp0086156	GstS1	0.89
FBpp0088359	CG10602	0.94	FBpp0086013	eIF3-S8	0.89
FBpp0111860	CG13373	0.94	FBpp0085169	CG11334	0.89
FBpp0077516	Uch	0.94	FBpp0072560	CG9149	0.89
FBpp0084962	janA	0.94	FBpp0079443	hoip	0.89
FBpp0087354	Prx2540-2	0.94	FBpp0076457	Uba2	0.89
FBpp0087479	TER94	0.94	FBpp0070832	CG5941	0.88
FBpp0076460	Arp66B	0.94	FBpp0086400	Prosbeta1	0.88
FBpp0084824	Pcd	0.98	FBpp0077625	CG4764	0.88
FBpp0076827	CG10576	0.98	FBpp0074067	CanA-14F	0.88
FBpp0080922	Fs(2)Ket	0.98	FBpp0074756	rept	0.88
FBpp0078349	Vha26	0.97	FBpp0070842	sqh	0.88
FBpp0072341	CG16936	0.97	FBpp0111817	eIF4G	0.87
FBpp0079746	dUTPase	0.97	FBpp0083673	Dph5	0.87
FBpp0076600	Cdc27	0.97	FBpp0075742	CG4300	0.87
FBpp0081606	PpD3	0.97	FBpp0082121	Arp87C	0.87
FBpp0073989	Pros28.1	0.97	FBpp0078984	smt3	0.87
FBpp0082219	Droj2	0.97	FBpp0078729	CG6907	0.87
FBpp0078356	CG31549	0.97	FBpp0074054	CG4420	0.87
FBpp0077571	Eno	0.96	FBpp0078370	CG1236	0.86
FBpp0082816	CG3590	0.96	FBpp0079650	CG5384	0.86
FBpp0077419	Pgk	0.96	FBpp0112403	eIF-4B	0.86
FBpp0080535	Sgt	0.96	FBpp0081488	Prosbeta3	0.86
FBpp0071625	HmgD	0.96	FBpp0074329	CrebB-17A	0.86
FBpp0085035	CG2246	0.95	FBpp0078827	stai	0.86
FBpp0083611	PyK	0.95	FBpp0087152	RnrS	0.85
FBpp0085690	CG11242	0.95	FBpp0083891	Rab7	0.85
FBpp0078806	eIF-4a	0.95	FBpp0076804	Txl	0.85
FBpp0078024	Pros54	0.95	FBpp0081899	CG14715	0.84
FBpp0087756	FANCI	0.95	FBpp0087704	shrb	0.84
FBpp0085564	rig	0.95	FBpp0074531	e(y)3	0.84
FBpp0078816	CG9135	0.95	FBpp0087722	Dmn	0.84
FBpp0087861	CG2158	0.95	FBpp0072908	CG17737	0.84
FBpp0290811	shibire	0.94	FBpp0084753	Pglym78	0.83
FBpp0086370	Got1	0.94	FBpp0075979	Aps	0.83
FBpp0088359	CG10602	0.94	FBpp0078448	Prosbeta7	0.83

APPENDIX

Flybase Identifier	Name	Log₂(iBAQ1h/4h)	Flybase Identifier	Name	Log₂(iBAQ1h/4h)
FBpp0085869	CG5174	0.83	FBpp0074075	eIF-2alpha	0.71
FBpp0088441	RpS7	0.83	FBpp0080490	CG17331	0.70
FBpp0099726	CG6783	0.83	FBpp0079538	Pros35	0.70
FBpp0076829	DnaJ-1	0.82	FBpp0082601	CG5205	0.70
FBpp0099391	capt	0.82	FBpp0073126	Chd64	0.70
FBpp0288465	CG7546	0.82	FBpp0086190	Ef1beta	0.69
FBpp0086987	CG8771	0.82	FBpp0079436	Trx-2	0.69
FBpp0079527	Pen	0.82	FBpp0078532	CG9769	0.69
FBpp0077645	Plap	0.81	FBpp0088522	UbcD10	0.68
FBpp0087319	Prosbeta5	0.81	FBpp0085250	His3:CG31613	0.68
FBpp0070672	ctp	0.81	FBpp0083503	Rab1	0.68
FBpp0081196	CG1307	0.81	FBpp0072128	Nap1	0.68
FBpp0079979	CG6180	0.81	FBpp0076589	Srp19	0.67
FBpp0084971	CG7911	0.81	FBpp0291495	Rpn3	0.67
FBpp0077016	Pp4-19C	0.81	FBpp0081234	snRNP2	0.67
FBpp0081443	CG11980	0.81	FBpp0082591	Rpb7	0.67
FBpp0078689	Trip1	0.80	FBpp0078393	exba	0.67
FBpp0084767	SP1029	0.80	FBpp0075087	nudC	0.67
FBpp0073452	Amun	0.80	FBpp0085514	vimar	0.66
FBpp0083893	LSm3	0.80	FBpp0076934	Ntf-2	0.65
FBpp0076207	RpS17	0.80	FBpp0082319	sqd	0.65
FBpp0080044	CG6523	0.80	FBpp0080775	RanGap	0.65
FBpp0071600	Rae1	0.80	FBpp0079031	CG13779	0.65
FBpp0073354	CG1749	0.79	FBpp0085855	GstE6	0.64
FBpp0088417	purple	0.79	FBpp0082076	CG10035	0.64
FBpp0083399	Fancd2	0.79	FBpp0087977	Gapdh1	0.64
FBpp0076582	Sh3beta	0.79	FBpp0079256	CG8498	0.63
FBpp0081490	E(var)3-9	0.79	FBpp0083695	Nup133	0.63
FBpp0084281	CG5886	0.79	FBpp0077402	CG2862	0.63
FBpp0077368	Prx6005	0.79	FBpp0083801	sec13	0.63
FBpp0074665	RhoGDI	0.78	FBpp0079221	CG7787	0.62
FBpp0099872	endos	0.78	FBpp0071905	Nup214	0.62
FBpp0073594	Jafrac1	0.78	FBpp0084918	Nlp	0.62
FBpp0084761	Ef1gamma	0.78	FBpp0085075	Sap-r	0.61
FBpp0088818	Bet3	0.78	FBpp0077650	Tfb4	0.61
FBpp0078222	Arf79F	0.78	FBpp0085703	FK506-bp2	0.60
FBpp0082514	Hsc70-4	0.77	FBpp0075068	Rpn12	0.60
FBpp0079710	Nup107	0.77	FBpp0071844	CG2852	0.60
FBpp0082167	CtBP	0.77	FBpp0082746	Dhfr	0.60
FBpp0076393	Idh	0.77	FBpp0082932	pxt	0.60
FBpp0082062	Pros25	0.76	FBpp0087094	SmD3	0.60
FBpp0077359	CG9643	0.76	FBpp0084190	CG11858	0.59
FBpp0072097	tsr	0.76	FBpp0070610	dgt4	0.58
FBpp0073922	Gapdh2	0.76	FBpp0071451	Pros29	0.58
FBpp0084349	Dak1	0.76	FBpp0075170	fax	0.58
FBpp0083514	DNApol-α180	0.76	FBpp0087613	Map60	0.58
FBpp0085065	dj-1beta	0.76	FBpp0080305	UK114	0.58
FBpp0084831	Bub3	0.76	FBpp0079182	CG18591	0.58
FBpp0072250	Nurf-38	0.75	FBpp0086066	Prosalpha5	0.58
FBpp0289797	Arpc3A	0.75	FBpp0083604	sar1	0.57
FBpp0080488	LSm7	0.75	FBpp0070624	mei-9	0.57
FBpp0076377	CG6673	0.75	FBpp0081149	CG1943	0.57
FBpp0073028	CG10863	0.74	FBpp0081244	CG31472	0.57
FBpp0078864	chic	0.74	FBpp0079182	CG18591	0.58
FBpp0086603	Rpn6	0.74	FBpp0086066	Prosalpha5	0.58
FBpp0079148	mts	0.73	FBpp0078831	Arc0	0.56
FBpp0100045	Adh	0.73	FBpp0081820	Tctp	0.56
FBpp0087500	14-3-3zeta	0.72	FBpp0079802	mre11	0.56
FBpp0071050	RpS14a	0.72	FBpp0086533	row	0.55
FBpp0072081	eIF-5A	0.72	FBpp0071277	Zpr1	0.55
FBpp0079542	eEF1delta	0.72	FBpp0070890	Rpt4	0.55
FBpp0290882	rad50	0.72	FBpp0079211	Ssb-c31a	0.54

Flybase Identifier	Name	Log₂(iBAQ1h/4h)	Flybase Identifier	Name	Log₂(iBAQ1h/4h)
FBpp0082682	Akt1	0.54	FBpp0076470	CG8209	0.29
FBpp0074161	CG5010	0.54	FBpp0074017	Cyp1	0.29
FBpp0081845	RpS25	0.54	FBpp0082521	Set	0.29
FBpp0085902	Prp19	0.54	FBpp0110174	FBgn0045035	0.29
FBpp0072421	E(bx)	0.53	FBpp0083214	Vha13	0.29
FBpp0073338	Tim8	0.53	FBpp0075401	Pdi	0.28
FBpp0083867	CG10254	0.52	FBpp0112048	ensconsin	0.28
FBpp0085458	Rab2	0.52	FBpp0083127	P5cr	0.28
FBpp0086474	Vha14	0.52	FBpp0082699	glob1	0.28
FBpp0080268	I(2)35Cc	0.52	FBpp0081725	Rrp46	0.27
FBpp0071406	Gip	0.51	FBpp0087347	CG7637	0.27
FBpp0082078	GstD9	0.51	FBpp0081560	CG16817	0.27
FBpp0070454	sgg	0.50	FBpp0086375	Lis-1	0.26
FBpp0075690	vih	0.50	FBpp0072746	Roughened	0.26
FBpp0071461	cpa	0.49	FBpp0080203	spel1	0.25
FBpp0081664	tws	0.49	FBpp0085235	Map205	0.24
FBpp0084610	ALiX	0.49	FBpp0087502	14-3-3zeta	0.24
FBpp0081704	pont	0.48	FBpp0077378	p16-ARC	0.24
FBpp0077965	CG12975	0.48	FBpp0073572	Bap60	0.24
FBpp0077470	Rab5	0.47	FBpp0080284	I(2)35Bg	0.24
FBpp0082511	Caf1	0.47	FBpp0075508	26-29PA	0.23
FBpp0071293	BCL7-like	0.46	FBpp0075280	brm	0.23
FBpp0088191	Rad23	0.46	FBpp0075958	Sod	0.23
FBpp0084829	Obp99c	0.45	FBpp0271746	CG18190	0.23
FBpp0081430	Cks85A	0.45	FBpp0080943	Pomp	0.23
FBpp0087968	CG30382	0.45	FBpp0082077	GstD1	0.22
FBpp0084188	Nup358	0.45	FBpp0072298	CG3760	0.22
FBpp0081556	Spd5	0.44	FBpp0271716	Fis1	0.22
FBpp0071542	CG9752	0.44	FBpp0073142	CG32251	0.22
FBpp0077277	Ptpa	0.43	FBpp0070607	cib	0.21
FBpp0074663	CG7770	0.43	FBpp0076859	Uev1A	0.21
FBpp0087157	CG8979	0.43	FBpp0075119	Pros26	0.20
FBpp0073034	Ubi3E	0.42	FBpp0074532	CG14222	0.19
FBpp0086736	CG13349	0.42	FBpp0085461	Eb1	0.19
FBpp0291513	WRNexo	0.40	FBpp0085273	Df31	0.18
FBpp0078822	CG13993	0.40	FBpp0081930	Jupiter	0.18
FBpp0086901	CG13319	0.40	FBpp0071553	LSm1	0.17
FBpp0082211	CG32473	0.40	FBpp0074964	CG6259	0.17
FBpp0086996	CG33672	0.40	FBpp0078080	Atox1	0.17
FBpp0078862	lid	0.40	FBpp0071280	His3.3B	0.17
FBpp0074709	Taf6	0.39	FBpp0073648	mus101	0.16
FBpp0076782	Bj1	0.39	FBpp0085223	awd	0.16
FBpp0082477	eff	0.39	FBpp0084848	Ice	0.15
FBpp0086294	Nup62	0.39	FBpp0086252	RpLP2	0.15
FBpp0075612	RpS12	0.39	FBpp0087332	Rpb5	0.15
FBpp0071846	RpS24	0.38	FBpp0081601	rump	0.14
FBpp0076122	alphaTub67C	0.38	FBpp0081843	CG6693	0.13
FBpp0074012	nonA	0.37	FBpp0078490	UbcD6	0.13
FBpp0070999	CG14434	0.37	FBpp0078728	cl	0.13
FBpp0075382	Prosbeta2	0.36	FBpp0071766	RpS16	0.13
FBpp0076200	Uch-L3	0.36	FBpp0085954	Nup75	0.12
FBpp0086115	Bap55	0.35	FBpp0073686	ben	0.12
FBpp0081295	CG33722	0.33	FBpp0075691	tral	0.11
FBpp0070273	CG3740	0.33	FBpp0074128	CG9132	0.11
FBpp0077492	Npc2a	0.32	FBpp0079280	Akap200	0.10
FBpp0070154	CG13364	0.32	FBpp0099893	primo-1	0.10
FBpp0081343	CG9601	0.32	FBpp0072672	alpha-Spec	0.10
FBpp0085204	Acf1	0.32			
FBpp0086468	Vha36	0.31			
FBpp0082692	mor	0.31			
FBpp0071172	Caf1-180	0.30			
FBpp0070666	CG11444	0.30			

APPENDIX

List 2: Chromatin-associated complexes

	Subunit	Log₂(iBAQ1h)	Log₂(iBAQ4h)	StDEV 1 h	StDEV 4h
MCM complex	dpa	22.74	21.41	1.07	0.91
	Mcm2	22.80	21.25	1.30	0.71
	Mcm3	21.98	20.03	1.49	0.54
	Mcm5	21.91	20.84	1.79	1.76
	Mcm6	22.20	20.81	1.43	1.33
	Mcm7	22.65	21.15	1.62	1.50
Nucleosome	His2Av	28.07	28.23	0.67	0.82
	His2A	27.26	27.10	1.20	1.63
	His2B	28.02	27.86	0.75	0.97
	His3.3	28.08	27.84	1.05	1.12
	His4r	28.61	28.64	0.65	0.30
CAF-1	Caf1	26.21	25.72	0.86	0.95
	Caf1-105	21.53	21.75	1.44	1.56
	Caf1-180	22.28	21.80	0.96	0.87
CHRAC	Acf1	23.35	22.76	0.98	1.84
	Iswi	24.53	24.21	0.85	1.38
	Chrac-14	24.26	24.19	0.21	0.75
	Chrac-16	23.94	24.74	1.03	2.21
ORC	Orc1	18.46	21.19	2.09	2.20
	Orc2	18.91	22.01	10.46	1.31
	Orc3	20.93	22.42	2.08	1.63
	Orc4	18.34	21.54	1.66	1.00
	Orc5	19.40	22.00	9.79	0.83
	Orc6	20.86	22.55	1.49	1.20
Brahma	Act42A	20.99	22.71	2.44	2.15
	Bap170	18.95	19.31	3.20	9.30
	Bap55	22.55	22.39	0.59	1.08
	Bap60	20.17	19.89	2.74	3.00
	brm	21.47	21.09	1.40	2.21
	dalao	20.04	20.36	1.98	1.81
	mor	21.87	21.48	0.83	1.34
	polybromo	19.91	20.24	2.03	10.12
	Snr1	20.73	20.95	1.90	10.68

	Subunit	Log₂(iBAQ1h)	Log₂(iBAQ4h)	StDEV1h	StDEV4h
Proteasome - 19S lid	Mov34-PA	26.32	25.07	0.76	0.45
	Rpn7-PA	25.69	24.52	0.70	0.56
	Rpn12-PA	24.98	24.28	0.72	0.58
	Rpn9-PB	25.43	24.23	0.55	0.63
	Rpn6-PA	25.02	24.06	0.82	0.60
	Rpn11-PA	25.25	23.82	0.78	0.73
	Rpn3-PA	24.48	23.46	0.93	0.67
	Rpn5-PA	24.82	23.44	0.75	0.58
	CG13779-PA	21.65	20.80	10.98	0.70
	Pros54-PA	24.92	23.55	0.57	0.72
Proteasome - 19S base	Pros45-PA	25.40	24.31	0.91	0.65
	Rpt3-PA	25.48	24.27	0.96	0.90
	Tbp-1-PA	25.04	24.03	0.67	0.75
	Rpn2-PA	25.07	23.68	0.92	0.78
	Rpn1-PA	24.97	23.64	0.84	0.61
	Pros54-PA	24.92	23.55	0.57	0.72
	Rpt1-PA	24.60	23.30	0.93	1.01
	Pros26-PA	26.05	25.37	0.65	0.37
Proteasome - 20S	Pros28.1-PA	26.22	25.30	0.54	0.63
	Pros29-PA	26.04	25.16	1.13	0.71
	Prosalph7-PA	26.02	25.12	0.31	0.22
	Prosbeta1-PA	25.91	24.95	0.94	0.64
	CG30382-PA	25.61	24.94	0.75	0.42
	Prosbeta7-PA	25.96	24.94	0.73	0.41
	Prosbeta3-PA	25.72	24.83	0.67	0.61
	Prosalph5-PA	25.63	24.80	1.08	0.66
	Pros25-PA	25.56	24.63	0.86	0.71
	CG17331-PA	25.53	24.61	0.85	0.47
	Prosbeta2-PA	25.20	24.43	1.11	0.87
	Prosbeta5-PB	24.23	23.27	0.93	0.80

APPENDIX

List 3: RNA-dependent protein binding

Flybase Identifier	Name	Log₂(-RNase/+RNase)	Flybase Identifier	Name	Log₂ (-RNase/+RNase)
FBpp0080066	CG16972	5.37	FBpp0072298	CG3760	3.87
FBpp0073965	Aats-arg	5.33	FBpp0082514	Hsc70-4	0.71
FBpp0075471	stwl	5.25	FBpp0071359	Yp2	0.70
FBpp0084086	Ela	4.80	FBpp0083860	Rpn9	0.57
FBpp0083610	PyK	4.74	FBpp0071354	Yp1	0.57
FBpp0081467	D1	4.71	FBpp0073652	Yp3	0.48
FBpp0110136	CG34125	4.70	FBpp0072904	Hsp83	0.48
FBpp0077575	Eno	4.70	FBpp0085809	CG15100	0.41
FBpp0075479	CG7768	4.69	FBpp0071301	Aats-lys	0.35
FBpp0099688	Df31	4.68	FBpp0293223	lig	0.34
FBpp0073902	Tcp-1zeta	4.67	FBpp0084761	Ef1gamma	0.32
FBpp0070648	peb	4.64	FBpp0073475	Chrac-16	0.28
FBpp0083355	TFAM	4.61	FBpp0070788	Act5C	0.25
FBpp0071969	CG30185	4.59	FBpp0087947	ACC	0.23
FBpp0076216	eIF-4E	4.59	FBpp0079609	RfC3	0.19
FBpp0073922	Gapdh2	4.59	FBpp0085720	betaTub56D	0.18
FBpp0078806	eIF-4a	4.56	FBpp0080760	CG17549	0.17
FBpp0082849	Det	4.55	FBpp0081710	sle	0.16
FBpp0087764	CG8258	4.54	FBpp0076890	Rpt6	0.16
FBpp0083503	Rab1	4.51	FBpp0087142	Ef1alpha48D	0.15
FBpp0083947	mask	4.49	FBpp0074246	CG8142	0.15
FBpp0076122	alphaTub67C	4.48	FBpp0076782	Rcc1	0.13
FBpp0079280	Akap200	4.48	FBpp0071228	CG7033	0.13
FBpp0271761	Nurf-38	4.43	FBpp0099974	Pp2A-29B	0.11
FBpp0070608	cib	4.43	FBpp0082511	Caf1	0.08
FBpp0075319	CG12304	4.42	FBpp0081861	Irbp	0.08
FBpp0076829	DnaJ-1	4.39	FBpp0073678	Lig4	0.07
FBpp0078664	Rpn11	4.38	FBpp0079527	Pen	0.06
FBpp0084281	CG5886	4.35	FBpp0076182	Hsp27	0.05
FBpp0082219	Droj2	4.35	FBpp0071625	HmgD	0.05
FBpp0081372	CG8036	4.33	FBpp0070894	UbiE	0.05
FBpp0083687	Rpn7	4.32	FBpp0073120	RfC4	0.04
FBpp0072097	tsr	4.32	FBpp0110268	Lsd-2	0.04
FBpp0079436	Trx-2	4.32	FBpp0079812	RfC38	0.03
FBpp0087500	14-3-3zeta	4.29	FBpp0080967	RPA2	0.02
FBpp0077910	CG4365	4.29	FBpp0080322	Ku80	0.02
FBpp0079745	dUTPase	4.28	FBpp0071903	CG3800	0.02
FBpp0082989	14-3-3epsilon	4.27	FBpp0074167	CG5162	0.02
FBpp0076298	Cp18	4.26	FBpp0070616	CG2982	0.01
FBpp0071587	CG10306	4.25	FBpp0100045	Adh	0.00
FBpp0075513	Hsc70Cb	4.22	FBpp0088396	lola	0.00
FBpp0079148	mts	4.22	FBpp0081312	CG2767	0.00
FBpp0074075	eIF-2alpha	4.21	FBpp0080763	fon	0.00
FBpp0073686	ben	4.19	FBpp0076819	mad2	0.00
FBpp0079416	borr	4.18	FBpp0085618	plu	0.00
FBpp0075870	CG6084	4.16	FBpp0082787	Cctgamma	0.00
FBpp0087680	Mad1	4.15	FBpp0087402	Caf1-105	0.00
FBpp0080922	Fs(2)Ket	4.14	FBpp0074331	Tsf1	0.00
FBpp0111819	TER94	4.13	FBpp0083001	CG14309	0.00
FBpp0076859	Uev1A	4.09	FBpp0073380	RPA3	0.00
FBpp0089088	Eb1	4.08	FBpp0079443	hoip	-0.01
FBpp0087583	Uba1	4.07	FBpp0271746	CG18190	-0.02
FBpp0078278	Rpn5	4.05	FBpp0082932	Pxt	-0.04
FBpp0074608	polo	4.05	FBpp0087757	CG8235	-0.05
FBpp0079640	Mdh1	4.05	FBpp0083977	Rox8	-0.05
FBpp0112011	endoB	4.01	FBpp0086897	Aats-asp	-0.05
FBpp0085234	Map205	4.00	FBpp0081356	RpA-70	-0.06
FBpp0071600	Rae1	3.99	FBpp0099655	Chrac-14	-0.07

Flybase Identifier	Name	Log₂(-RNase/+RNase)
FBpp0071099	dec-1	-0.10
FBpp0086190	Ef1beta	-0.11
FBpp0077804	kis	-0.11
FBpp0082729	mtSSB	-0.11
FBpp0074329	CrebB	-0.13
FBpp0288574	CG42232	-0.14
FBpp0083843	Rpt5	-0.15
FBpp0091142	His4:CG33897	-0.18
FBpp0074052	hang	-0.18
FBpp0078869	Vm26Aa	-0.20
FBpp0071501	CG9418	-0.21
FBpp0086429	Mlf	-0.22
FBpp0085250	His3:CG31613	-0.23
FBpp0082076	CG10035	-0.23
FBpp0091129	His2B:CG33884	-0.24
FBpp0084434	His2Av	-0.24
FBpp0087193	tou	-0.25
FBpp0091055	His2A:CG3380	-0.25
FBpp0112210	CG4951	-0.26
FBpp0085863	CG5174	-0.27
FBpp0076224	Hsp26	-0.29
FBpp0080535	Sgt	-0.30
FBpp0077362	Rrp1	-0.31
FBpp0291534	CG5414	-0.35
FBpp0088303	eIF4G	-0.38
FBpp0082428	CG3509	-0.47
FBpp0078250	Osi10	-0.62
FBpp0080825	Top2	-3.78
FBpp0084240	Aats-gln	-4.02
FBpp0079925	CG17218	-4.03
FBpp0088021	Rpt1	-4.04
FBpp0078562	CG14648	-4.17
FBpp0079625	Myo31DF	-4.17
FBpp0080445	Cyt-c-d	-4.21
FBpp0290241	CG31760	-4.34
FBpp0081843	CG6693	-4.56
FBpp0075691	tral	-4.74
FBpp0081845	RpS25	-4.88
FBpp0081234	SmD2	-4.99
FBpp0080837	CG16772	-5.02
FBpp0084256	msi	-5.15
FBpp0073910	mRp530	-5.32

APPENDIX

List 4: Df31 Interactors

Flybase Identifier	Name	iBAQ Average Control	iBAQ Average Df31	Log₂(Df31 IP/control)
FBpp0085273	Df31	0	169386333	27.34
FBpp0087347	CG7637	0	1279567	20.29
FBpp0071295	RpS28b	0	975257	19.90
FBpp0070672	ctp	0	506100	18.95
FBpp0072957	RpL28	0	381267	18.54
FBpp0079484	RpL13	0	318554	18.28
FBpp0080723	RpL30	0	317170	18.27
FBpp0087323	CG6751	0	252761	17.95
FBpp0088658	pnt	0	212963	17.70
FBpp0088542	Nopp140	0	208010	17.67
FBpp0076602	RpL18	0	186543	17.51
FBpp0087498	Jra	0	182090	17.47
FBpp0073098	CG11583	0	171370	17.39
FBpp0085119	CG1542	0	138483	17.08
FBpp0083905	RpS19b	0	126995	16.95
FBpp0084837	CG11470	0	110476	16.75
FBpp0072788	CG9018	0	101840	16.64
FBpp0082996	Dlc90F	0	87180	16.41
FBpp0070749	Mlc-c	0	85300	16.38
FBpp0077524	CG11723	0	85168	16.38
FBpp0075723	l(3)j2D3	0	76977	16.23
FBpp0079635	SmB	0	64755	15.98
FBpp0078354	RpL13A	0	63200	15.95
FBpp0076495	Pdp1	0	59245	15.85
FBpp0070360	Unc-76	0	57420	15.81
FBpp0077081	CG3008	0	54003	15.72
FBpp0082105	Hsp70Bbb	0	53396	15.70
FBpp0082908	AttD	0	52343	15.68
FBpp0075265	elgi	0	52201	15.67
FBpp0110412	RpL38	0	49053	15.58
FBpp0078009	CG7519	0	48053	15.55
FBpp0084617	RpL4	0	47200	15.53
FBpp0072143	ytr	0	44890	15.45
FBpp0075764	RpL10Ab	0	44131	15.43
FBpp0083376	RpS30	0	43873	15.42
FBpp0111619	CG34417	0	39356	15.26
FBpp0072801	RpL8	0	36637	15.16
FBpp0076738	CG32409	0	35775	15.13
FBpp0083884	AP-1sigma	0	35100	15.10
FBpp0086571	BEAF-32	0	34484	15.07
FBpp0074672	Tom20	0	32193	14.97
FBpp0080025	CG16812	0	31056	14.92
FBpp0086252	RpLP2	0	29141	14.83
FBpp0084187	CG11875	0	28337	14.79
FBpp0288504	RhoGAP71E	0	27724	14.76
FBpp0070953	CG3226	0	27449	14.74
FBpp0087663	Prp38	0	27443	14.74
FBpp0085314	RpL21	0	26045	14.67
FBpp0080922	Fs(2)Ket	0	23016	14.49
FBpp0083503	Rab1	0	22614	14.46
FBpp0073266	feo	0	22077	14.43
FBpp0076723	CG13298	0	21703	14.41
FBpp0088165	gw	0	21638	14.40
FBpp0074237	e(y)1	0	21339	14.38
FBpp0084959	RpL32	0	21322	14.38
FBpp0072616	Klp61F	0	20659	14.33
FBpp0078841	WDR79	0	20300	14.31
FBpp0110163	CG3689	0	20173	14.30
FBpp0074709	Taf6	0	18204	14.15
FBpp0074288	Taf8	0	16411	14.00

Flybase Identifier	Name	iBAQ Average Control	iBAQ Average Df31	Log₂(Df31 IP/control)
FBpp0086438	sli	0	16409	14.00
FBpp0087936	Nup44A	0	15711	13.94
FBpp0076095	CG10809	0	15497	13.92
FBpp0070947	CG14440	0	14653	13.84
FBpp0083794	unk	0	13621	13.73
FBpp0076546	Neos	0	13239	13.69
FBpp0086167	CG8963	0	13024	13.67
FBpp0110523	CG17683	0	12950	13.66
FBpp0081445	CG11982	0	12854	13.65
FBpp0070118	skpA	0	12646	13.63
FBpp0113081	Taf4	0	12636	13.63
FBpp0070284	ns3	0	12478	13.61
FBpp0073526	CG4400	0	12477	13.61
FBpp0071084	CG10777	0	12138	13.57
FBpp0080323	wek	0	11647	13.51
FBpp0079625	Myo31DF	0	11432	13.48
FBpp0089083	Ranbp16	0	11342	13.47
FBpp0074650	Kap-alpha1	0	11232	13.46
FBpp0271525	tub	0	11141	13.44
FBpp0082462	CG3817	0	11004	13.43
FBpp0110406	p120ctn	0	10609	13.37
FBpp0074515	CG14215	0	10576	13.37
FBpp0082833	Patr-1	0	10338	13.34
FBpp0078162	Hem	0	10277	13.33
FBpp0074012	nonA	0	10258	13.32
FBpp0080822	CG10189	0	10210	13.32
FBpp0086041	sub	0	10182	13.31
FBpp0074267	CG6769	0	10089	13.30
FBpp0073310	dsh	0	9990	13.29
FBpp0087679	Myd88	0	9630	13.23
FBpp0087631	ced-6	0	9544	13.22
FBpp0072840	Atg2	0	9314	13.19
FBpp0073331	Klp10A	0	9268	13.18
FBpp0073000	ImpE2	0	9262	13.18
FBpp0077759	dbr	0	9234	13.17
FBpp0288651	CG1024	0	9011	13.14
FBpp0087731	CG30349	0	8949	13.13
FBpp0073519	CG4004	0	8888	13.12
FBpp0082682	Akt1	0	8703	13.09
FBpp0082579	MRG15	0	8506	13.05
FBpp0088465	Lmpt	0	8487	13.05
FBpp0086853	Dp	0	8314	13.02
FBpp0082869	CG3995	0	8264	13.01
FBpp0080752	Pax	0	7656	12.90
FBpp0080727	CG10641	0	7502	12.87
FBpp0076725	D19B	0	7388	12.85
FBpp0081260	CG2846	0	7270	12.83
FBpp0088035	Incenp	0	6997	12.77
FBpp0088646	MESK2	0	6996	12.77
FBpp0083947	mask	0	6847	12.74
FBpp0071596	Tbp	0	6812	12.73
FBpp0070216	CG11448	0	6801	12.73
FBpp0288697	yki	0	6733	12.72
FBpp0081225	CG10267	0	6584	12.68
FBpp0072891	pfk	0	6510	12.67
FBpp0075653	CG10984	0	6235	12.61
FBpp0080103	CG9293	0	6224	12.60
FBpp0074970	Edc3	0	6077	12.57
FBpp0074490	CG14200	0	5960	12.54
FBpp0077645	Plap	0	5786	12.50
FBpp0073588	CG1622	0	5718	12.48
FBpp0070610	dgt4	0	5638	12.46

APPENDIX

Flybase Identifier	Name	iBAQ Average Control	iBAQ Average Df31	Log₂(Df31 IP/control)
FBpp0072253	CG4612	0	5576	12.45
FBpp0082897	SF1	0	5439	12.41
FBpp0079817	Reps	0	5433	12.41
FBpp0084543	bigmax	0	5408	12.40
FBpp0288856	tlk	0	5370	12.39
FBpp0076186	Shc	0	5356	12.39
FBpp0084559	raps	0	5116	12.32
FBpp0088657	pnt	0	5011	12.29
FBpp0075501	ssp2	0	4921	12.27
FBpp0079583	GATAd	0	4854	12.25
FBpp0080384	pkaap	0	4815	12.23
FBpp0081087	CG2656	0	4668	12.19
FBpp0078139	CG7139	0	4656	12.19
FBpp0085951	CG5726	0	4269	12.06
FBpp0290582	jar	0	4242	12.05
FBpp0085688	hpo	0	4221	12.04
FBpp0079634	CG5343	0	4086	12.00
FBpp0083575	how	0	3925	11.94
FBpp0079289	fu2	0	3914	11.93
FBpp0074579	CG18809	0	3853	11.91
FBpp0271760	BtbVII	0	3803	11.89
FBpp0087334	cag	0	3680	11.85
FBpp0080402	cact	0	3638	11.83
FBpp0081253	Taf7	0	3632	11.83
FBpp0077697	aru	0	3507	11.78
FBpp0088395	lola	0	3386	11.73
FBpp0078589	CG9853	0	3258	11.67
FBpp0080866	CG10722	0	3206	11.65
FBpp0288749	Yeti	0	3154	11.62
FBpp0074608	polo	0	3131	11.61
FBpp0089003	Nopp140	0	3076	11.59
FBpp0072500	Ckllalpha-i3	0	2917	11.51
FBpp0076997	cactin	0	2722	11.41
FBpp0073371	bif	0	2721	11.41
FBpp0070382	CG3071	0	2720	11.41
FBpp0074562	CG32528	0	2668	11.38
FBpp0078402	CG2931	0	2562	11.32
FBpp0087984	Vps13	0	2235	11.13
FBpp0100055	bbx	0	2136	11.06
FBpp0083133	CG6005	0	2131	11.06
FBpp0081116	CG1227	0	2061	11.01
FBpp0111510	Ect4	0	2036	10.99
FBpp0083872	CG10184	0	2030	10.99
FBpp0072940	YT521-B	0	2019	10.98
FBpp0099495	Lasp	0	2018	10.98
FBpp0086110	CG6522	0	2005	10.97
FBpp0072023	wmd	0	1952	10.93
FBpp0081305	CG9667	0	1892	10.89
FBpp0088375	Rel	0	1877	10.88
FBpp0086119	CG6568	0	1693	10.73
FBpp0075676	CG10754	0	1674	10.71
FBpp0073805	CG32590	0	1461	10.51
FBpp0075725	CG11560	0	1433	10.49
FBpp0081910	mus309	0	1372	10.42
FBpp0078230	jim	0	1270	10.31
FBpp0071303	CG3004	0	1235	10.27
FBpp0074186	CG8949	0	1170	10.19
FBpp0072803	dos	0	1126	10.14
FBpp0074080	TH1	0	1126	10.14
FBpp0086824	cnn	0	1012	9.98
FBpp0081088	Sas-4	0	985	9.95
FBpp0085364	dream	0	842	9.72

Flybase Identifier	Name	iBAQ Average Control	iBAQ Average Df31	Log₂(Df31 IP/control)
FBpp0291145	Cad86C	0	836	9.71
FBpp0085292	CG6448	0	821	9.68
FBpp0089115	CG8384	0	819	9.68
FBpp0083666	loco	0	789	9.63
FBpp0071386	PPP4R2r	0	765	9.58
FBpp0112136	CG3532	0	690	9.43
FBpp0088293	CG32016	0	681	9.41
FBpp0086738	AGO1	0	675	9.40
FBpp0290646	MCPH1	0	646	9.34
FBpp0079628	CG7456	0	624	9.29
FBpp0083799	Rassf	0	535	9.06
FBpp0084783	dgt6	0	487	8.93
FBpp0070462	fs(1)Yb	0	436	8.77
FBpp0076724	D19A	0	418	8.71
FBpp0076359	RpL14	1603	328799	7.68
FBpp0288515	kay	1278	159348	6.96
FBpp0075597	CG10191	341	35193	6.68
FBpp0079788	Nup160	247	20987	6.40
FBpp0078764	CG7236	2583	212432	6.36
FBpp0084924	Sry-delta	4535	344510	6.25
FBpp0085904	imd	1663	94122	5.82
FBpp0076819	mad2	14673	696650	5.57
FBpp0083851	Nup98	675	26392	5.29
FBpp0085187	ttk	2987	71520	4.58
FBpp0099859	CG6664	1838	43120	4.55
FBpp0075724	CG17153	3297	69274	4.39
FBpp0077868	CG4858	38703	764183	4.30
FBpp0087630	CG1888	7379	144163	4.29
FBpp0085281	His2B:CG17949	28706	555993	4.28
FBpp0086767	tum	5129	97930	4.25
FBpp0070150	RpL36	75569	1365382	4.18
FBpp0070761	yu	2852	50977	4.16
FBpp0079500	sop	3930	65414	4.06
FBpp0088445	M(2)21AB	4073	64147	3.98
FBpp0072660	Cdc37	1383	21592	3.96
FBpp0074387	Rip11	1263	19403	3.94
FBpp0289448	CG32506	2136	32670	3.93
FBpp0088899	Tm1	4780	71930	3.91
FBpp0086572	BEAF-32	290680	4282567	3.88
FBpp0076182	Hsp27	47462	662947	3.80
FBpp0073918	CG8578	31518	436527	3.79
FBpp0087861	CG2158	20116	273640	3.77
FBpp0077544	CG14352	13307	180157	3.76
FBpp0085869	CG5174	53884	729210	3.76
FBpp0083695	Nup133	2523	33693	3.74
FBpp0085585	RpS18	35553	463170	3.70
FBpp0099786	cp309	693	8721	3.65

ACKNOWLEDGEMENT

Zuallererst möchte ich mich bei Axel Imhof bedanken für die Möglichkeit meine Botaniker-Laufbahn hinter mir zu lassen und mich einem neuen, spannenden Thema zu widmen. Ich bin dankbar für die Freiheiten, die du mir gelassen hast, deine kontinuierliche Unterstützung und deine stets offene Tür. Dein Optimismus und deine immer neuen Ideen haben dafür gesorgt, dass es nie langweilig wurde.

Prof. Dr. Peter Becker möchte ich danken für das Interesse an meiner Arbeit, die Bereitschaft offizieller Betreuer meiner Doktorarbeit zu sein und für das fantastische wissenschaftliche Umfeld, welches ich in den letzten Jahren genießen durfte.

Prof. Dr. Gernot Längst und Dr. Hakan Sarioglu danke ich für die hilfreichen Diskussionen und Tipps innerhalb meines TACs.

Prof. Dr. Gernot Längst und Dr. Thomas Schubert möchte ich für die tolle und erfolgreiche Zusammenarbeit am Df31 Projekt danken.

Ich danke Simone Vollmer, Gabriele Wagner und Edith Mentele, den treuen Mitgliedern des „Salat-Clubs“, für die vielen schönen Stunden zu Viert und den wechselnden Gastessern, die zu einer entspannten Mittagspause beigetragen haben. Ich werde unsere kulinarischen Experimente und eure nette Gesellschaft vermissen.

I further would like to thank...

...the “Chromatomics” Team, Teresa Barth and Viola Sansoni. I always enjoyed having you two around me, both literally and metaphorically.

...all past and present Imhofs for an enjoyable working atmosphere, good scientific discussions and honest criticism. A special thank you goes to the guys from the ZfP for consulting and data retrieval.

...all members of the Adolf Butenandt Institute for help and advice whenever asked for and for all the nice and unforgettable moments I had in this institute.

Ich möchte mich auch bedanken bei...

...Irene Vetter; von dir habe ich nicht nur viel über gute Laborarbeit gelernt, sondern auch über das Leben an sich - manchmal durchaus detaillierter als ich es wissen wollte...

...Heike Mitlöhner für das Übernehmen aller „unliebsamen“ Fliegenarbeiten.

...Edith Müller und Carolin Brieger für die Unterstützung in allen administrativen Angelegenheiten.

...Gabriele Wagner für das Korrekturlesen dieser Arbeit.

...Christian Albig für die unermüdliche Hilfe beim Formatieren.

Danke an all die Kollegen und Freunde, die mein Leben abseits des Labors bereichert haben!

Meinen Eltern, Beate und Werner Pusch, möchte ich ganz herzlich für ihren steten Rückhalt und die Unterstützung in jeglicher Form und allen Lebenslagen danken. Ich bin unendlich dankbar für alles was ihr bis zu dem heutigen Tag für mich getan habt.

Besonderer Dank gilt meinem Freund Jan Philipp, der meine Entscheidungen auch dann mitgetragen und unterstützt hat, wenn sie für ihn von Nachteil waren. Für dein Vertrauen und die schönen gemeinsamen letzten Jahre möchte ich dir danken.